1. Report No.	2. Government Accession No.	3. Recipient's Catalog No.
TTI-2-8-73-18-3		

4. Title and Subtitle	5. Report Date
Prediction of Thermal Reflection Cracking in West Texas	March, 1976
	6. Performing Organization Code
7. Author(s)	8. Performing Organization Report No.
Hang-Sun Chang, Robert L. Lytton, and Samuel H. Carpenter	Research Report No. 18-3
9. Performing Organization Name and Address	10. Work Unit No.
Texas Transportation Institute Texas A&M University College Station, Texas 77843	11. Contract or Grant No. Study No. 2-8-73-18
	13. Type of Report and Period Covered
12. Sponsoring Agency Name and Address	Interim - September, 1972 March, 1976
Texas State Department of Highways and Public Transportation; Transportation Planning Division P. O. Box 5051 Austin, Texas 78763	14. Sponsoring Agency Code

15. Supplementary Notes

Research performed in cooperation with DOT, FHWA.
Study Title: "Environmental Deterioration of Pavement"

16. Abstract

An economical means of rehabilitating deteriorated pavement is through the use of an overlay. The performance of overlay systems has, however, been far from satisfactory as the performance of any one system has varied widely among different installation sites. This study presents a rational approach for the prediction of overlay life and gives recommendations which are expected to extend the life of overlays.

The predictions are made using linear elastic and viscoelastic stress analysis and viscoelastic fracture mechanics. Initially, a prediction scheme for viscoelastic thermal stresses in the overlay and old asphalt surface is used to predict thermal stresses more accurately than any previous attempt. These stresses are then applied to the crack surface to study the effects of material properties on crack development. The stress intensity factors necessary for this analysis are calculated using the finite element technique with the crack tip elements developed by Pian. Predictions of service life are made using the empirical relationship developed by Paris.

The results show that there are three states of crack growth in an overlay each of which require different layered arrangements of material properties to lower the stress intensity factor and thus retard crack growth. The influence of viscoelasticity properties on reduction of crack growth are presented with the service lives for typical asphaltic concretes.

Computer codes are developed for each calculation step and are fully documented. The analysis performed using these codes represents an initial (continued on back)

17. Key Words	18. Distribution Statement
Thermal reflection cracking, pavement, overlays, prediction of service life.	No Restrictions. This document is available to the public through the National Technical Information Service, Springfield, Virginia 22161.

19. Security Classif. (of this report)	20. Security Classif. (of this page)	21. No. of Pages	22. Price
Unclassified	Unclassified	102	

Form DOT F 1700.7 (8-69)

step in a rational design process to produce overlays resistant to environmental reflection cracking.

PREDICTION OF THERMAL REFLECTION CRACKING IN WEST TEXAS

by

Hang-Sun Chang
Robert L. Lytton
Samuel H. Carpenter

Research Report Number 18-3

Environmental Deterioration of Pavement
Research Project 2-8-73-18

conducted for the
State Department of Highways
and Public Transportation

in cooperation with the
U.S. Department of Transportation
Federal Highway Administration

by the

Texas Transportation Institute
Texas A&M University
College Station, Texas

March, 1976

TABLE OF CONTENTS

TABLE OF FIGURES

TABLE OF FIGURES (continued)

PREFACE

This report details the analytical study of reflection cracking in overlays. The thermal activity of the overlay and original material are studied from a mechanistic viewpoint that gives a theoretical explanation of the observed behavior of some innovative overlay systems. This report is one of a series of reports from the study entitled "Environmental Deterioration of Pavement." The study, sponsored by the State Department of Highways and Public Transportation in cooperation with the Federal Highway Administration is a comprehensive program to verify environmental cracking mechanisms and to recommend maintenance and construction measures to alleviate this pavement cracking problem.

DISCLAIMER

The contents of this report reflect the views of the authors, who are responsible for the facts and accuracy of the data presented herein. The contents do not necessarily reflect the official views or policies of the Federal Highway Administration. This report does not constitute a standard, specification or regulation.

LIST OF REPORTS

Report No. 18-1, "Environmental Factors Relevant to Pavement Cracking in West Texas," by Samuel H. Carpenter, Robert L. Lytton, Jon A. Epps, describes the environment existing in west Texas and relates it to other studies to determine its severity.

Report No. 18-2, "Thermal Activity of Base Course Material Related to Pavement Cracking," by Samuel H. Carpenter and Robert L. Lytton, describes the development of a pavement cracking mechanism emanating from thermal activity of the base course layer in the pavement.

Report No. 18-3, "Prediction of Thermal Reflection Cracking in West Texas." by Hang-Sun Chang, Robert L. Lytton, and Samuel H. Carpenter, describes a rational mechanistic approach to the description of reflection cracking and overlay life through the viscoelastic thermal stress analysis and viscoelastic fracture mechanics.

ABSTRACT

Prediction of Thermal Reflection Cracking in West Texas

An economical means of rehabilitating deteriorated pavement is through the use of an overlay. The performance of overlay systems has, however, been far from satisfactory as the performance of any one system has varied widely among different installation sites. This study presents a rational approach for the prediction of overlay life and gives recommendations which are expected to extend the life of overlays.

The predictions are made using linear elastic and viscoelastic stress analysis and viscoelastic fracture mechanics. Initially, a prediction scheme for viscoelastic thermal stresses in the overlay and old asphalt surface is used to predict thermal stresses more accurately than any previous attempt. These stresses are then applied to the crack surface to study the effects of material properties on crack development. The stress intensity factors necessary for this analysis are calculated using the finite element technique with the crack tip elements developed by Pian. Predictions of service life are made using the empirical relationship developed by Paris.

The results show that there are three states of crack growth in an overlay each of which require different layered arrangements of material properties to lower the stress intensity factor and thus retard crack growth. The influence of viscoelasticity and elasticity properties on reduction of crack growth are presented with the service lives for typical asphaltic concretes.

Computer codes are developed for each calculation step and are fully documented. The analysis performed using these codes represents an initial step in a rational design process to produce overlays resistant to environmental reflection cracking.

IMPLEMENTATION STATEMENT

At present overlays for badly cracked pavements are designed either from the design engineer's experience or from empirical results. These designs have consistently produced an overlay that would perform in one situation but fail miserably in another. A major reason for such poor performance lies in the lack of a rational mechanistic approach to overlay design. Only very recently has the problem of reflection cracking been examined in the light of the relatively new findings available in the field of viscoelastic fracture mechanics.

The data presented in this report represent a significant step forward in the prediction of the service life of an overlay based on its elastic and viscoelastic properties. The relationships, established from a sound theoretical approach, clearly demonstrate the basic principles responsible for the excellent performance of certain overlay systems such as the stress relieving interface. The importance of having a mechanistic description for the behavior is that it will allow a wide variety of materials to be studied without requiring a field installation for each material, which even then only shows the behavior of the overlay under one set of environmental conditions.

The computer codes developed for viscoelastic thermal stress calculations, stress intensity factor calculations, and service life predictions represent the best techniques currently available and are much more efficient and accurate than many numerical techniques currently being used. These techniques will have a wide range of application in the development of a description for environmental behavior of pavement systems.

Based on these calculations, recommended ranges of overlay material properties which are expected to extend the life of overlays considerably are presented and suggestions for long-lasting overlay layered design are given.

CHAPTER I

INTRODUCTION

The most visible form of pavement distress is the appearance of cracks on the asphalt surface. These cracks may be either environmental or traffic induced. In west Texas the predominant cracking pattern is transverse which may be attributed primarily to environmental influences on the pavement. To the driving public cracked pavements are merely uncomfortable and may become an irritation. To the engineer, however, the presence of cracks indicates that severe problems are present in the existing structure and future problems will be accelerated due to the cracking. Loss of load transfer ability, weakening of subgrade strength parameters due to the free access provided for moisture intrusion, debonding, and accelerated rutting are common results seen after cracking is first noticed. Cracking may not initially lower the serviceability of the pavement, thus, the driving public will not complain initially. The effect of such distress, however, severely reduces the long term serviceability resulting in a drastically shortened life for the highway.

When cracking has progressed to a stage where rehabilitation is needed there are two methods available. These are: 1) reconstruction of the entire pavement structure, and 2) use of an overlay to level the riding surface and improve vehicle-surface interaction characteristics (1). When the traffic and environment have not deteriorated the structural properties excessively, the use of an overlay is by far the most economical means of rehabilitation available. Existing methods of overlay design, however, are based primarily on the field experience of the design engineer and empirical results obtained from studies of constructed overlays. As a result the designed overlays have varied widely in their performance. When using an economical design most overlays fall far short of their predicted life when the existing cracks reflect through the new

surface. This action, commonly occurring within the first year for west Texas, lowers the performance of the overlay and produces a pavement in nearly the same condition as existed prior to the overlay. This reflection cracking problem often requires repeated costly maintenance much earlier than planned. Thus, an understanding of the mechanism causing the reflection cracking would allow knowledge of material properties to be used in determining the degree of success to be expected in any rehabilitation project.

The fact that these relatively large amounts of highway cracking could not be directly attributed to traffic loading spurred a growing concern for thermally induced cracking of pavements in the last decade (2). The majority of these studies have been mainly concerned with the fracture susceptibility of asphalt concrete under extremely low temperatures (3, 4). The finding of these studies could not provide results satisfactory enough to explain the same form of cracking found in moderately cold climates. The most common form of low-temperature cracking that is first visible in a pavement is typically the transverse crack. Carpenter, Lytton and Epps (5) have found that transverse cracking in areas similar to west Texas occurs as a result of thermal activity in the base course material. In these climatic areas freeze-thaw cycling predominates as the major climatic variable and typical base course materials commonly used in west Texas are susceptible to cracking due to excessive tensile stresses induced by freeze-thaw cycling. The base course is actually more susceptible than the asphalt to cracking in these areas, and as a consequence could initiate cracks that would then reflect up through the pavement surface due to the accumulating damage of freeze-thaw cycling.

The effect of an overlay would be to insulate the base course from the thermal changes. The effect of the freeze-thaw cycles would be centered mainly in the cracked original asphaltic concrete surface. The facts indicate that

rather than low temperature the effects of thermal cycling are important in the mechanism of reflection cracking of overlays in the west Texas area. There exists a need to further examine the development of crack growth due to repeated cycles of thermal change within the pavement. Such a study should result in predictions of service life to provide field engineers with guidelines for more efficient rehabilitation procedures.

Pavement damage associated with repeated loading is often designated as a fatigue failure. The phenomenologically based Miner's law typically used to describe fatigue damage does not satisfactorily account for the influence of geometry and inhomogenieties, nor does it provide a quantitative measure of the cracking in the pavement. The more complicated mechanism of thermal cycling should not be expected to follow Miner's Law. A more sophisticated approach is necessary to relate thermal activity to the amount of observed cracking.

During recent years the development and application of linear elastic and viscoelastic fracture mechanics concepts have progressed to a point where they now provide a rational design and experimental approach to the problem of crack propagation. Recent experimental work at Ohio State University (6, 7, 8, 9) involved sand asphalt beams and slabs resting on elastic foundations. The results of these experiments verify the applicability of fracture mechanics in predicting fatigue life of asphalt mixtures. The results indicate that the rate of crack propagation in asphalt mixtures can be predicted using the empirical power law relation developed by Paris (10),

$$\frac{dc}{dN} = A(\Delta K)^n \qquad (1\text{-}1)$$

where ΔK = stress intensity factor amplitude,

A, n = fatigue parameters of the material,

dc/dN = rate of crack growth,

c = crack length, and

N = number of stress repetitions

Techniques presently used in the stress analysis of pavement structures have been developed from the general theory of stress and strain and displacement in a layered system as first introduced by Burmister (11) based on the theory of elasticity in a two layered system. A highway pavement is typically composed of three or more layers of various soils with rigid or flexible surface course. The two layer analysis, while providing initial values for stress and strain is only a first approximation.

Improvements have been made and the techniques for stress analysis have been extended to three and more layers. Recently computer codes such as BISTRO and CRALAY (12, 13) have been developed that provide a better understanding of the stress state within the pavement. While these analyses provide descriptions of the stress state, necessary in the fatigue analysis of the pavements life, the use of these analyses to study the life of an overlay is questionable since most pavements requiring overlay are cracked extensively on the surface. The imperfections at the interface of the old and new surface courses cause stress concentrations at the tip of the crack which can result in unexpected failure of the overlay.

The problem of crack initiation and growth has resulted in the rapid development of the theory of fracture mechanics as a separate branch of solid mechanics. The use of fracture mechanics principles has proceeded most rapidly in the study of polymer and solid rocket fuel propellant behavior. This theory proposes that fracture is the process of crack initiation and propagation where the fractures are all progressive, proceeding by crack extension. Through the proper application of fracture mechanics a rational approach is available to predict the conditions under which fracture will occur, thus, allowing a better selection of materials to be made to resist fracture.

Recently these results have been applied to material combinations which could be considered similar to a pavement system (9, 17, 34, 35). The use of

these results has been complicated somewhat by the need for suitable numerical techniques to calculate the stress intensity factor. The more general approach involves use of the technique of finite elements. Special elements modeling the crack tip have been developed and used in finite element computer codes with results being more accurate than previous attempts (48, 49, 50). The newer crack tip elements do not require extremely fine element sizes near the crack tip which greatly reduces computation time.

The remainder of this study will address itself to:

a) the prediction of thermal tensile stresses using the theory of linear viscoelasticity,

b) the application of fracture mechanics principles to an overlay,

c) the development of an efficient and accurate computer code to utilize the thermal stresses to predict stress intensity factors, and

d) the prediction of overlay life as a function of material properties and stress intensity factor. The final result of this study will be to provide a rational procedure by which overlay performance may be evaluated under environmental conditions.

CHAPTER II

THERMAL STRESS ANALYSIS

The Equivalent Viscoelastic Analysis

The rheological characteristics of asphaltic concrete as a function of time and temperature, termed viscoelastic properties, have been defined by various research studies (27, 28, 29). Although nonlinear in behavior the linear viscoelastic analysis provides a very good approximation to the actual behavior of the asphaltic concrete in-situ.

Historically, two different approaches have been used in the development of the application of stress-strain equations within a viscoelastic medium. The first approach utilizes mechanical models consisting of linear springs and dashpots. The second approach has as its basis the hereditary integral and as such covers a broader class of materials and is often easier to apply. In general, the current stress and displacement response in viscoelastic media will depend on the entire history of the applied loads. For a nonaging material the one-dimensional constitutive equation is:

$$\sigma = \int_0^t E\ (t-\tau)\ \frac{d\varepsilon}{d\tau}\ d\tau \qquad (2\text{-}1)$$

The inverse of Eq. (2-1) is of the same general form and represents another useful one-dimensional constitutive equation:

$$\varepsilon = \int_0^t D\ (t-\tau)\ \frac{d\sigma}{d\tau}\ d\tau \qquad (2\text{-}2)$$

where

σ = stress

ε = strain

$E(t)$ = relaxation modulus, stress response due to unit strain applied at t=0

$D(t)$ = creep compliance; strain response due to unit stress applied at t=0

If the relaxation modulus is known, then Eq. (2-1) enables us to calculate

the stress due to general strain histories. In an experiment one usually applies constant strain in a relaxation test or constant stress in a creep test. However, since constant strain relaxation tests are rather difficult to perform with stiff materials, the creep compliance will be the experimental result most often obtained. The creep compliance and relaxation modulus of asphalt concrete normally obey a power law representation. Figure 1 shows the creep compliance derived from Monismith's data (3) which is approximated by the power law

$$D(t) = D_0 + D_1 t^m \tag{2-3}$$

where m is the slope of the straight line region and D_1 is the intercept of straight line with log t = 0. Both m and D_1 are positive constants with $0 \leq m \leq 1$. The product may be expressed as:

$$E(t)D(t) = \frac{\sin(m\pi)}{m\pi} \tag{2-4}$$

and forms the relationship for creep compliance to the power law relaxation modulus in the power law range of behavior (23).

Nonisothermal Behavior of Asphalt Concrete. The mechanical response of viscoelastic materials is normally very sensitive to temperature change. Therefore, nonisothermal behavior is of considerable practical importance. For asphalt concrete, the modulus increases with a decrease in temperature. A common type of temperature dependence, the so called thermorheologically simple behavior, will be assumed to represent the effect of temperature on the relaxation modulus, E(t, T). With this assumption the data at different temperatures can be superimposed to form a single continuous master curve by means of horizontal translation to a reference temperature, T_M. The horizontal distance between a master curve and any one of the curves at temperature T is independent of time and is written as log a_T. Thus, the time and temperature dependence of the rheological characteristics can be sufficiently defined by

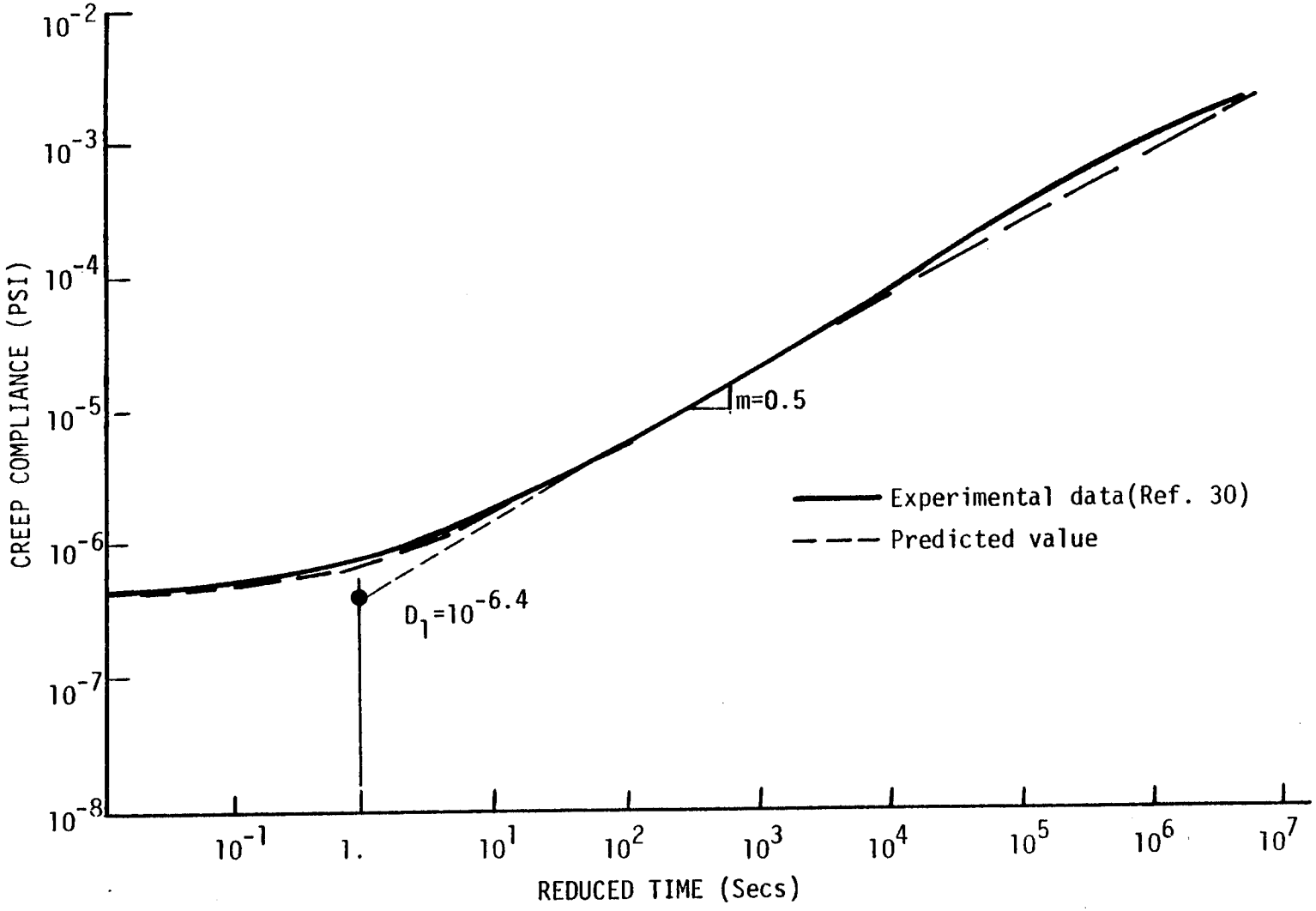

Figure 1. Master Creep Compliance Curve At Reference Temperature of 40°F (After Ref. 30)

the following equations:

$$E(t, T) = E_M(\xi) \tag{2-5}$$

where

$$\xi = \frac{t}{a_T} \tag{2-6}$$

$E_M(\xi)$ is the master curve of relaxation modulus as shown in Figure 2. The quantities ξ and a_T are called the "reduced time" and "horizontal shift factor" respectively. When temperatures are above the glass transition temperature, T_g, of a particular material (i.e., when $T>T_g$), the so called WLF equation normally applies, as shown in Figure 3. The WLF equation is:

$$\log a_T = -F_1(T-T_M)/(F_2+T-T_M) \tag{2-7}$$

where

T = the temperature for which a_T is determined,

T_M = the reference temperature of the master curve, and

F_1 and F_2 are constants and can be calculated by solving the simultaneous equations of two proper points on the curve as follows:

$$\begin{bmatrix} (T_1-T_M) & \log a_{T1} \\ (T_2-T_M) & \log a_{T2} \end{bmatrix} \cdot \begin{bmatrix} F_1 \\ F_2 \end{bmatrix} = - \begin{bmatrix} (T_1-T_M) & \log a_{T1} \\ (T_2-T_M) & \log a_{T2} \end{bmatrix}$$

Estimation of thermal stresses developed within the pavement has been of great concern in areas which suffered a large quantity of transverse temperature cracking. Christison (3) has evaluated several available numerical methods (31, 32) to determine the viscoelastic thermal stress. The main difficulty in applying these techniques is that the predicted stress is often very dependent on the time interval used in the numerical integration. The results calculated may vary up to 50% when using different time increments. Thus, users may have to find the right answer through several unnecessary trials.

A slightly modified form of the existing theory is described and recommended in the JANNAF handbook (33). This approach, which is more accurate

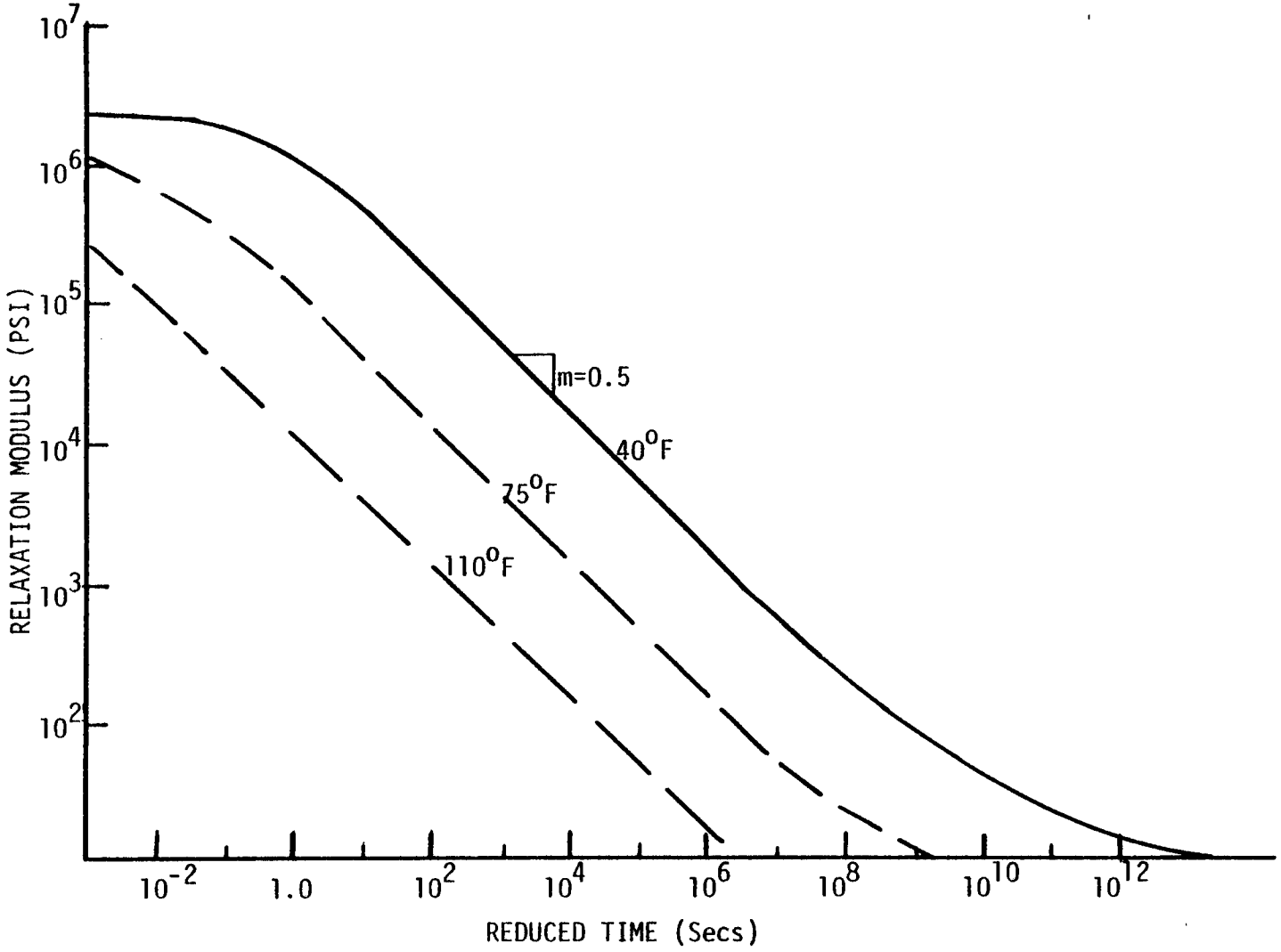

Figure 2. Relaxation Modulus Curves at Various Temperatures with Master Curve (After Ref. 30)

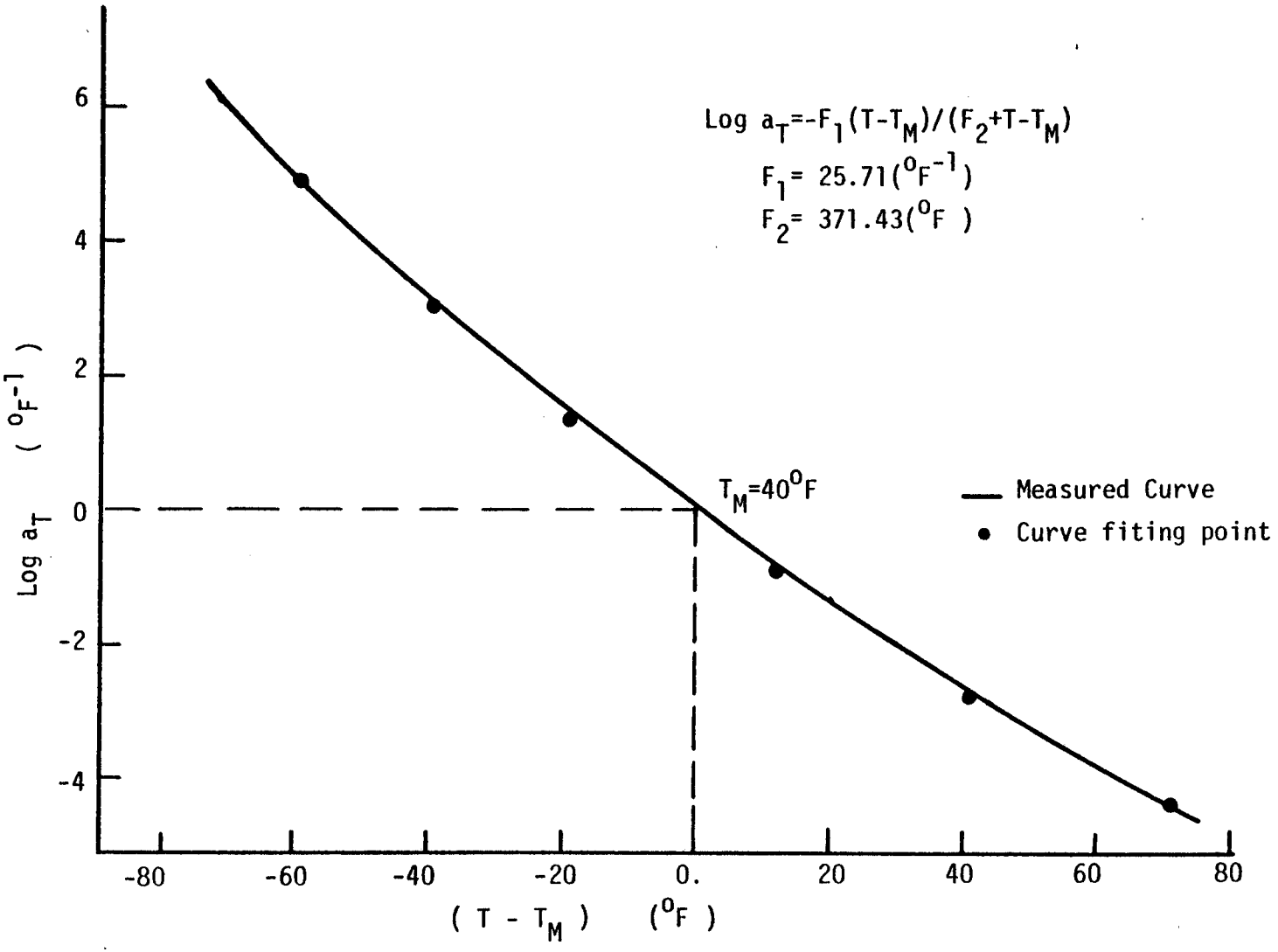

Figure 3. Comparison of Measured and Curve Fit WLF Shift Factor

and efficient, is discussed here.

The uniaxial stress σ due to an axial strain ε and temperature change, $\Delta T = T - To$, is

$$\sigma = E_e(\varepsilon - \alpha\Delta T) + a_F \int_o^t \Delta E(\xi - \xi') \frac{d(\varepsilon - \alpha\Delta T)}{d\tau} d\tau \qquad (2\text{-}8)$$

where

T_o = temperature at stress free state

α = thermal expansion coefficient

E_e = long-time equilibrium modulus; $E_e \simeq 0$ for asphalt

$\Delta E(\xi)$ = the transient component of the relaxation modulus;

$\Delta E(\xi) = E(\xi) - E_e$

a_F = temperature dependent coefficient arising from the free energy change; $a_F = 1$ for thermorheologically simple materials.

Also ξ and ξ' are integrated forms of reduced time,

$$\xi = \int_o^t \frac{dt'}{a_T} \;,\; \xi' = \int_o^\tau \frac{dt'}{a_T} \qquad (2\text{-}9)$$

where a_T, the horizontal shift factor, is a function of temperature. Note that for a perfectly constrained pavement, $\varepsilon = 0$.

If we assume a constant thermal expansion coefficient α and constant rate of straining and cooling (or heating) starting at time $t = 0$, then

$\varepsilon = Rt$ (R = constant rate of strain)

$\Delta T = T - To = R_T t$ (R_T = constant rate of temperature change) and Eq. (2-8) becomes

$$\sigma = (\varepsilon - \alpha\Delta T)E_{ef} = \varepsilon_T E_{ef} \qquad (2\text{-}10)$$

where

t = time for loading

ε_T = strain due to stress

E_{ef} = effective modulus; $E_{ef} = E_e + \frac{a_F}{t} \int_o^t \Delta E(\xi - \xi')dt'$ (2-11)

ΔE and a_T can be expressed as the following power laws.

$$\Delta E(\xi) = E_1 \xi^{-m} \tag{2-12a}$$

$$a_T = \left(\frac{T_M - T_a}{T - T_a}\right)^{\beta} \tag{2-12b}$$

where T_M is the reference temperature for the master curve and E_1 is the intercept of a straight line region with log (ξ) = 0. Both E_1, m, and β are positive constants and T_a may be a positive or negative constant. The temperature T_a is approximately 10 to 20°F below the glass-transition temperature. With these two power laws, Eq. (2-11) may be analytically integrated. Appendix A and Figure 4 illustrate the determination of constants β and T_a. The effective modulus then becomes

$$E_{ef} = E_e + I_T (E_s - E_e) \tag{2-12}$$

where

E_s = isothermal constant strain rate secant modulus at temperature T;

$$= E_e + \frac{a_F E_1}{1-m} \left(\frac{t}{a_T}\right)^{-m} \tag{2-13}$$

For cooling ($T \leq To$):

$$I_T = \frac{1-m}{(\beta+1)^{1-m}} \left(-1 - \frac{1}{\Delta T_n}\right)^{1-m} \int_1^{(\Delta T_n+1)^{\beta+1}} (1-X)^{-m} (X)^{\left(\frac{\beta}{\beta+1} + m-2\right)} dX \tag{2-14a}$$

For heating ($T \geq To$):

$$I_T = \frac{1-m}{(\beta+1)^{1-m}} \left(1 + \frac{1}{\Delta T_n}\right)^{1-m} \int_1^{(\Delta T_n+1)^{\beta+1}} (X-1)^{-m} (X)^{\left(\frac{\beta}{\beta+1} + m-2\right)} dX \tag{2-14b}$$

These results are expressed in terms of the normalized temperature change, ΔT_n, defined as:

$$\Delta T_n = \frac{T - To}{To - T_a} \tag{2-15}$$

Calculation of Viscoelastic Thermal Stresses

To efficiently use the theoretical relationships just developed a computer code

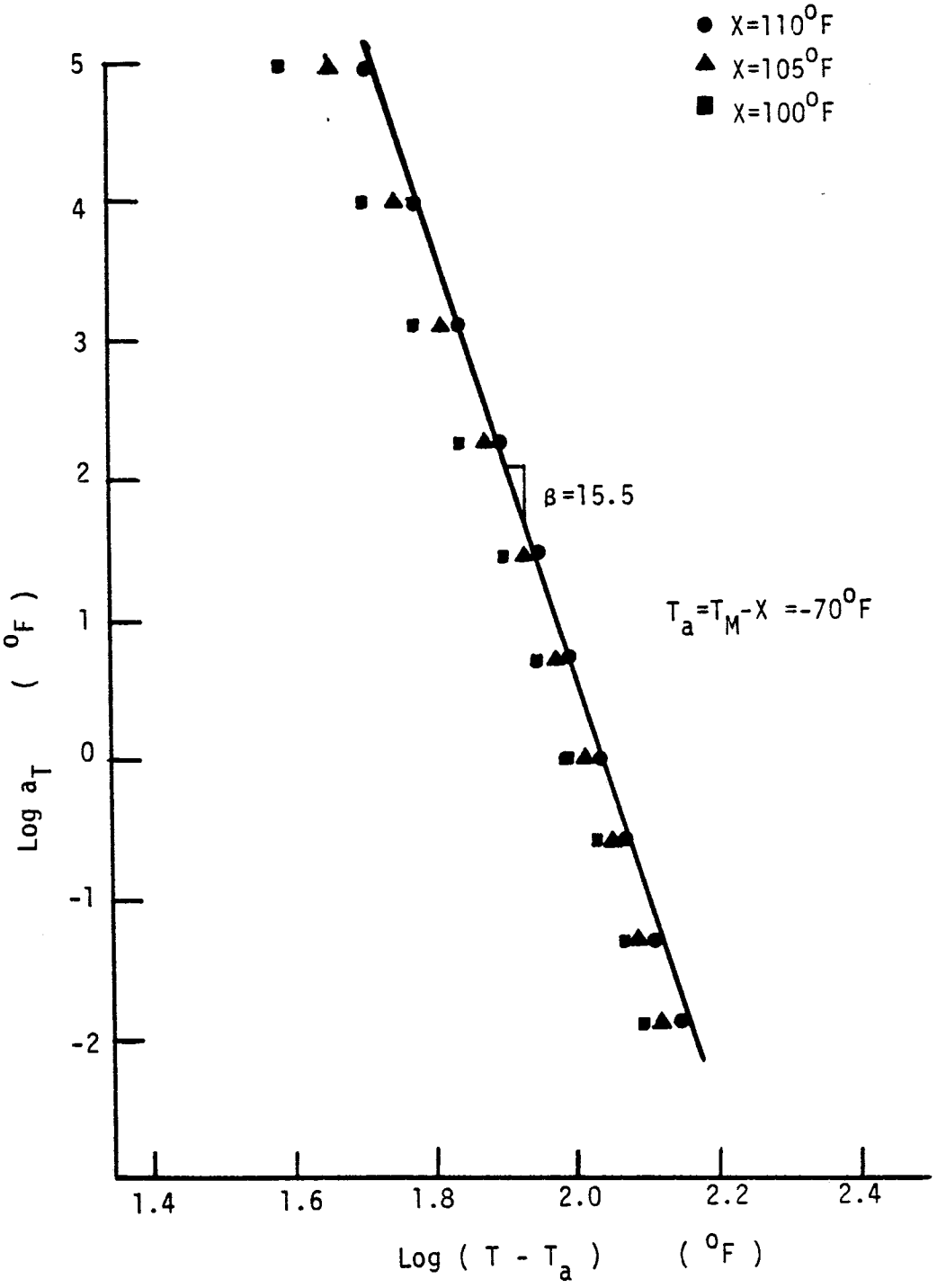

Figure 4. Example of the Method for Graphical Determination of Power Law Constants β and T_a

has been written which can calculate the viscoelastic thermal stresses due to expansion or contraction. The code is explained in Appendix B. It is to be noted that each of the integrals for the factor I_T (Eq. 2-14) have a singularity at either the upper or lower limits. To improve the convergence rate of the numerical integration these two equations can be reformulated as follows:

(i) For the cooling process, the integral can be written as,

$$I_H = \int_H^1 X^a (1-X)^b dX \quad (0 \leq H \leq 1) \tag{2-16}$$

where

$$H = (\Delta T_n + 1)^{\beta+1}$$

$$a = \frac{\beta}{(\beta+1)} + m - 2$$

$$b = -m$$

which have been defined in Eq. 2-12b. If we let A = a + 1 and B = b + 1, the equation becomes

$$I_H = \int_H^1 X^{A-1}(1-X)^{B-1} dx$$

$$= \int_0^1 X^{A-1}(1-X)^{B-1} dx - \int_0^H X^{A-1}(1-X)^{B-1} dx \tag{2-17}$$

or

$$I_H = G(A, B) - G_H(A, B)$$

$$= G(A, B)\,[(1-P(H))] \tag{2-18}$$

where G(A, B) and $G_H(A, B)$ are complete and incomplete Beta functions respectively (38). P(H) is the probability that the random variables follow the Beta function with the degree of freedom of A and B; and further: $P(H) = G_H(A, B)/G(A, B)$. P(H) may be solved using an IMSL scientific subroutine MEBETA (39) which is called directly from the IBM 360/65 computer's local library.

(ii) For the heating process the integral is written as follows:

$$I_H = \int_1^H X^a (X-1)^b dX \quad (H \geq 1) \tag{2-19}$$

Since b is a negative constant, the recurrence formula (40) is used to avoid the singularity at the lower limit. The equation then becomes

$$I_H = \frac{1}{(b+1)} \left[X^{a+1}(X-1)^{b+1} - (a+b+2)\int_1^H X^a (X-1)^{b+1} dX \right] \quad (2\text{-}20)$$

The above integral is calculated by the trapezoidal integration rule. Since the upper limit, H, is increased exponentially, a step by step integration is used to achieve accuracy with an acceptable convergence rate. It can be shown that:

$$I_{H_i} = \int_1^{H_i} X^a(X-1)^{b+1}dX = \sum_{i=0}^{n} \int_{H_i}^{H_i+1} X^a(X-1)^{b+1}dX \quad (n=1, 2, \ldots, 10) \quad (2\text{-}21)$$

where

$$H_i = (\Delta T_{ni}+1)^{\beta+1}; \ (\Delta T_{ni} = 0.1(i), \ i=0, 10) \quad (2\text{-}22)$$

Once the values of I_H have been obtained for each increment of T, a curve, as shown in Figure 5, representing the modulus ratio derived from the test data given in Figures 1, 2, 3, and 4 is incorporated into the computer code for calculating thermal stresses. For any intermediate value of T, a straight line interpolation between the calculated points is performed to obtain I_T.

A comparison with experimental data for viscoelastic thermal stress, shown in Figure 6, demonstrates that this newly developed computer code is capable of predicting tensile stresses much more accurately than existing codes (30, 41). A comparison of the computer codes on an individual basis would show that the proposed method is much more straightforward and efficient.

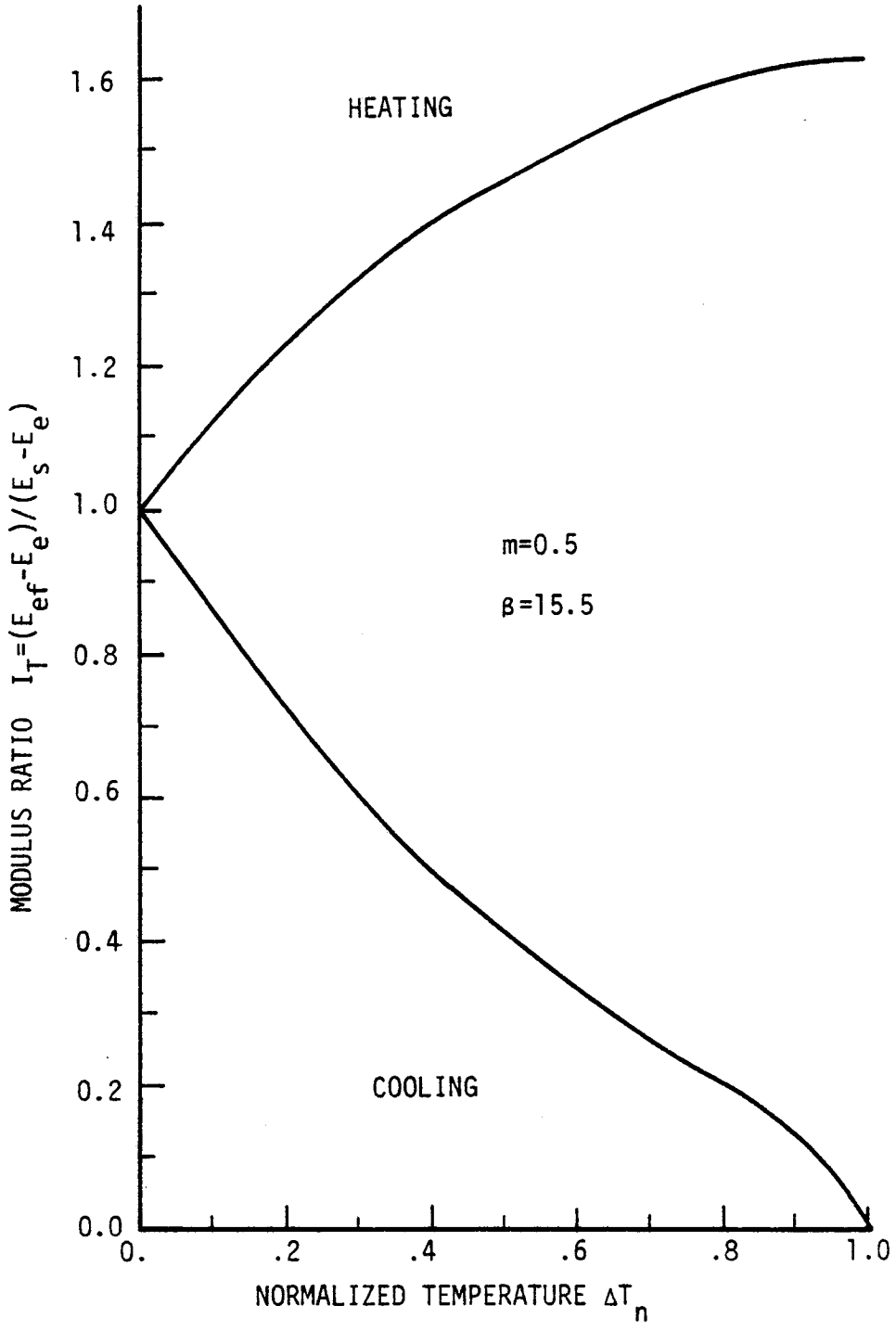

Figure 5. Modulus Ratio for Simultaneous Cooling (or Heating) and Straining

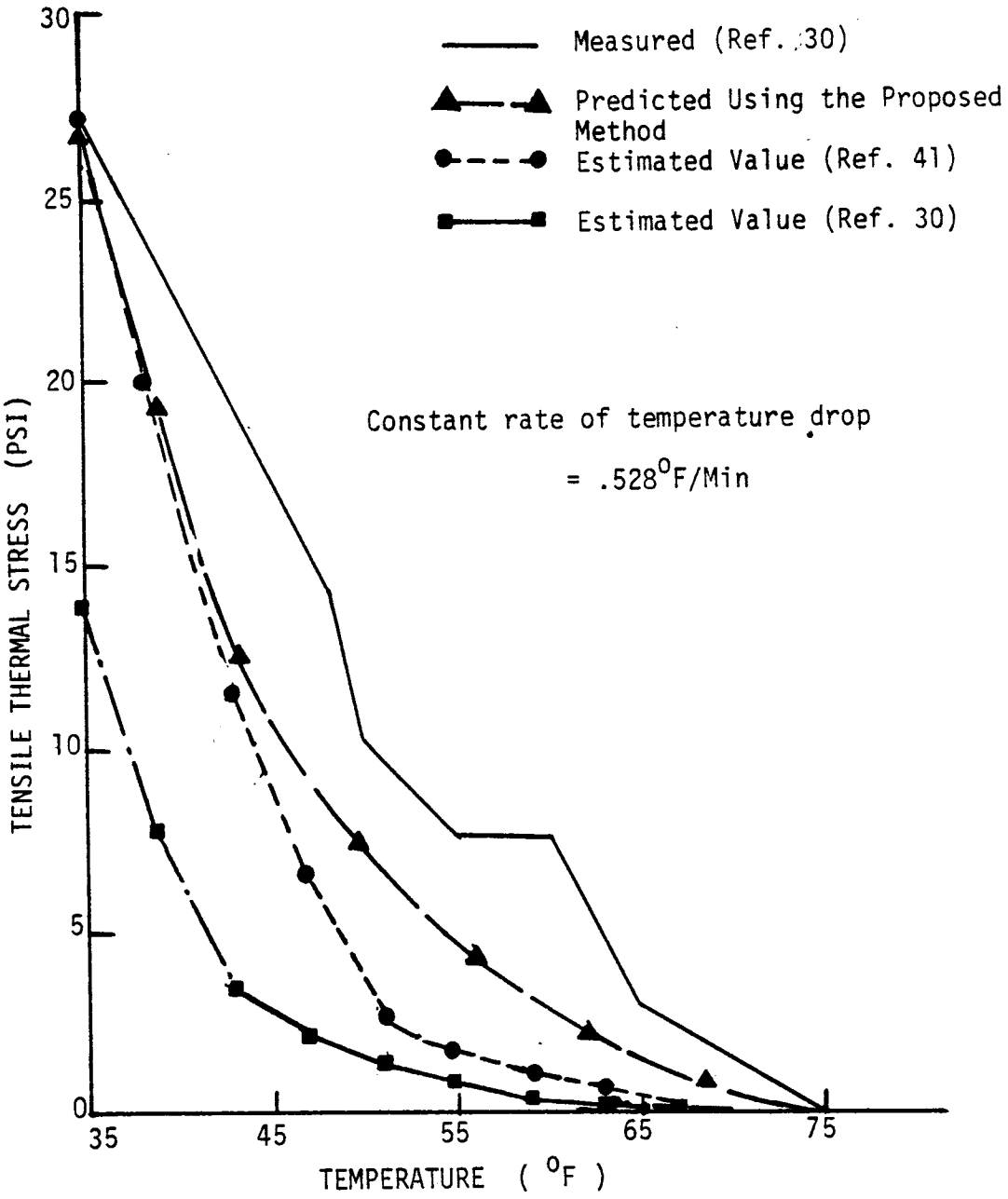

Figure 6. Comparison Between Measured and Predicted Tensile Thermal Stress for Various Predictive Techniques

CHAPTER III

MECHANISTIC APPROACH TO REFLECTION CRACKING IN PAVEMENTS

Fracture Mechanics Concepts

In 1920, Griffith (14) first developed these concepts by assuming the existence of a flaw in a thin elastic plate and described the energy terms controlling the growth of cracks. This elastic body may contain two kinds of potential energy: (1) surface energy (γ) and, (2) elastic strain energy (Ue). The system would become unstable and the crack would increase in size if the difference in strain energy released with crack extension is greater than the energy required to form the new free surface. This criterion leads directly to the expression for the critical stress, σ_{cr},

$$\sigma_{cr} = (2E\gamma/\pi C_{cr})^{\frac{1}{2}} \qquad (3\text{-}1)$$

where E = modulus of elasticity,

C_{cr} = critical half crack size, and

σ_{cr} = critical tensile stress, or the tensile strength of the specimen.

This equation provides a relation between the tensile strength of the specimen and the size of flaw.

Irwin (15) extended Griffith's theory to include the situation of general interest. In this extension the surface energy term, γ, was replaced by an experimentally determined quantity, the so-called crack extension force, G. This is the quantity of stored elastic energy released in a cracking specimen as the result of the virtual extension of an advancing crack. When this quantity reaches a critical value, G_c, the crack will propagate rapidly. For a crack length of 2C in an infinitely wide plate under uniaxial tension the critical stress becomes:

$$\sigma_{cr} = (EG_c/\pi\ C_{cr})^{\frac{1}{2}} \qquad (3\text{-}2)$$

Utilizing linear elasticity theory, researchers have only recently approached the problem of developing mathematical formulations to make practical application of fracture mechanics. Attention has been focused on the intensity of the stress field near the crack tip. This stress field possesses a singularity of the form $\{1/\sqrt{r}\}$ for both linear elastic and viscoelastic materials. The strength or amplitude of this field is referred to as the "Stress Intensity Factor", K. Three fundamental modes of relative crack surface displacements (16) are shown in Figure 7. Any particular problem may be treated as a combination of any of these displacement modes. For example, in the immediate vicinity of the crack tip the stress and displacement for a mode I crack, opening mode, using the coordinate system as defined in Figure 8, may be expressed by the following equations:

$$\sigma_x = K_I(2\pi r)^{\frac{1}{2}} \cos\left(\frac{\theta}{2}\right)\left(1-\sin\frac{\theta}{2}\sin\frac{\theta}{2}\right)$$

$$\sigma_y = K_I(2\pi r)^{\frac{1}{2}} \cos\left(\frac{\theta}{2}\right)\left(1+\sin\frac{\theta}{2}\sin\frac{\theta}{2}\right)$$

$$\tau_{xy} = K_I(2\pi r)^{\frac{1}{2}} \sin\left(\frac{\theta}{2}\right)\cos\left(\frac{\theta}{2}\right)\cos\left(\frac{3\theta}{2}\right) \qquad (3\text{-}3)$$

$$U = \frac{K_I}{2\mu}\left(\frac{r}{2\pi}\right)^{\frac{1}{2}} \cos\left(\frac{\theta}{2}\right)\left(R - 1 + 2\sin^2\left(\frac{\theta}{2}\right)\right)$$

$$V = \frac{K_I}{2\mu}\left(\frac{r}{2\pi}\right)^{\frac{1}{2}} \sin\left(\frac{\theta}{2}\right)\left(R + 1 - 2\cos^2\left(\frac{\theta}{2}\right)\right)$$

$$\tau_{xz} = \tau_{yz} = 0$$

where U and V = horizontal and vertical displacements respectively,

K_I = mode I stress intensity factor,

r = distance from crack tip,

μ = shear modulus, $\mu = E/2\,(1 + \nu)$,

ν = poisson's ratio,

$R = 3 - 4\nu$ for plane strain, and

$R = (3 - \nu)/(1 + \nu)$ for plane stress.

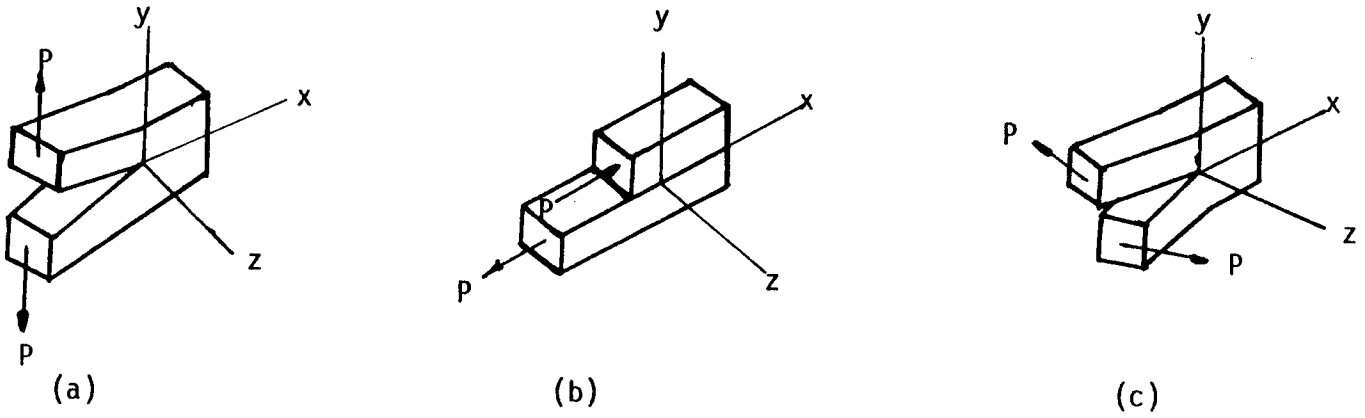

Figure 7. Three Modes of Crack Opening Displacement (a) Mode I - opening mode, (b) Mode II - shearing mode, (c) Mode III - tearing mode

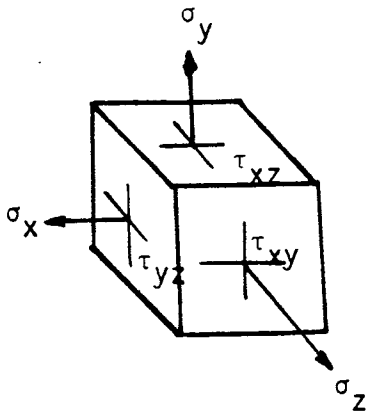

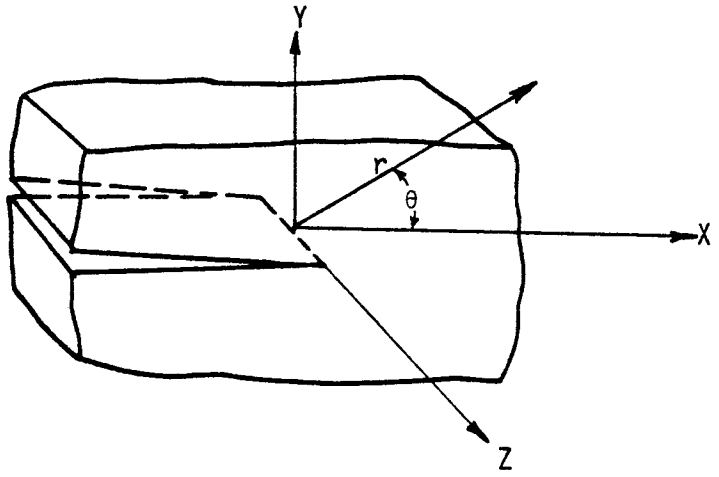

Figure 8. Stress Components on Element of Material and Coordinate System with Crack Front Along Z-axis

Note that for $\theta = 0^0$ the major stresses become equal, namely:

$$\sigma_x = \sigma_y = K_I(2\pi r)^{-\frac{1}{2}} \tag{3-4}$$

and for $\theta = \pi$ the opening or vertical displacement becomes simply:

$$V = C_e K_I \left(\frac{r}{2\pi}\right)^{\frac{1}{2}} \tag{3-5}$$

where $C_e = 4/E$ for plane stress and

$C_e = 4(1-\nu^2)/E$ for plane strain.

The crack propagation in an elastic body will become unstable when the stress intensity factor reaches the so called critical stress intensity factor, K_{IC}, i.e., failure occurs. The quantity, K_{IC}, is a material constant related to the free surface energy, γ, by the following relationship:

$$K_{IC} = (8\gamma/C_e)^{\frac{1}{2}} \tag{3-6}$$

Due primarily to the straight forwardness of the assumptions involved in the stress intensity factor approach and the ability to ignore the little understood surface energy and plastic work phenomena which accompany fracture development, the use of the stress intensity factor is now preferred over use of the free surface energy (17).

Fatigue Crack Growth Law

According to the A.S.T.M. definition, fatigue describes the behavior of materials under repeated cycles of stress or strain which causes deterioration of the materials and results in a progressive fracture (18). Fatigue behavior may be distinguished by three main features: 1) loss of strength, 2) loss of ductility and 3) an increased uncertainty in both strength and service life. All these consequences stem from the inhomogeneity of real materials.

Deterioration resulting from fatigue manifests itself primarily in the formation of cracks in the material. Most cracks responsible for fatigue

failures start at visible discontinuities which act as stress raisers. The subsequent development of cracks due to fatigue in engineering materials can be divided into three phases: (1) crack initiation (2) stable crack growth (3) castastropic fracture. The material of interest, asphalt concrete, behaves as a non-crosslinked polymer. It has been demonstrated that crack initiation occupies only a small portion of time when compared to the total fatigue life (24). Thus the prediction of service life can be obtained by knowing the number of loading cycles required for a crack to grow to a critical size.

Various factors that affect the fatigue behavior that must be considered are the environment, stress state, load history and flaw type of the materials. Paris (19, 20) first suggested that for fatigue crack propagation in metal the crack growth rate was almost exclusively dependent on the change in the stress intensity factor during each cycle (ΔK); and only secondarily dependent on mean stress and frequency. He proposed the following equation based on these assumptions, to describe the crack growth rate:

$$\frac{dc}{dN} = A(\Delta K)^n \qquad (3\text{-}7)$$

where

c = crack length,

N = number of cycles,

ΔK = stress intensity amplitude, $\Delta K = K_{max} - K_{min}$, and

A,n = material constants obtained from experimental tests.

Experimental data collected by Ohio State University (6, 7, 8) from tests on sand asphalt beams and slabs resting on elastic foundations indicate that the crack propagation process in an asphalt mixture can be predicted using this power law relation. The prediction of total fatigue life N_f can then be obtained by integrating expression (3-7) to obtain the number of cycles to failure:

$$N_f = \int_{C_o}^{C_f} \frac{1}{A(\Delta K)^n} dc \qquad (3\text{-}8)$$

where C_o and C_f are, respectively, the initial and final crack size within the overlay. Once the material constants A, n and K_{IC} have been found a prediction of fatigue crack propagation can be determined if the history of the stress intensity factor, K, is known for a particular loading sequence, crack length, and set of boundary conditions.

In addition to elastic fracture mechanics, theories also exist for predicting fracture initiation time and crack growth in viscoelastic media (21, 22). Recently Schapery (23, 24, 25) has developed a general theory of crack growth in viscoelastic media. This theory of fatigue crack propagation in asphaltic concrete was derived from the power law relation (2-7), upon integrating:

$$\frac{dc}{dN} = B_t(\Delta K)^{2(1+1/m)} \tag{3-9}$$

where

$$B_t = \frac{(1-\nu^2)D_1\lambda_m\pi^m}{2^{m+1}} \left[\int_t^{t+tp} \frac{W^{2(1+1/m)}}{\gamma^{1/m}\ \sigma_m^{2}\ I_1^{2}}\, dt\right]^{\frac{1}{m}}$$

m = slope of the straight line region of the creep compliance curve,

D_1 = intercept of straight line with log t = 0 in the creep compliance curve (See Fig. 3)

$$\lambda_m = \frac{3(\pi)^{\frac{1}{2}}\Gamma(m+1)}{4(m+\frac{3}{2})\Gamma(m+\frac{3}{2})} \quad ; \ \Gamma = \text{Gamma function}$$

W = W(t) which defines the wave shape of the stress intensity factor,

γ = fracture energy density (lb/in per unit area),

σ_m = maximum stress a material can sustain,

I_1 = a dimensionless integral, $0 < I_1 \leq 2$ and

t_p = time of loading for a given stress pulse.

Obviously, equality of the empirical Eq. (3-7) and the theoretical Eq. (3-9) requires that

$$A = B_t \qquad \text{and} \qquad n = 2(1+1/m) \tag{3-10}$$

under the conditions for which the extended correspondence principle established by Graham (26) is applicable. This result enables us to predict the response in a viscoelastic media using the results of elastic solutions and to relate the fatigue constants to material properties.

CHAPTER IV

STRESS INTENSITY FACTORS

Stages of Crack Propagation Within the Pavement Structure

Linear fracture mechanics was mainly developed for homogeneous and isotropic materials. It is only recently that the structural design of composite material has brought the attention of engineers to fracture at the bond between dissimilar materials such as an asphaltic concrete. For practical applications to pavement design, the crack growth within a pavement overlay system may be categorized into three stages: (1) when the crack tip is within the old layer growing toward the interface between the old pavement and the new overlay, (2) when the crack tip is resting on the interface, and (3) when the crack is within the new overlay. Each stage produces a different stress intensity factor for the crack tip that gives a new rational insight into material selection.

Stage 1 - Crack Tip Within Old Pavement Layer

Williams (34, 35) first discussed the stress state around a crack in dissimilar media and found that the stresses at the crack tip were of the form

$$\sigma \sim r^{\lambda} \qquad (\lambda = -\tfrac{1}{2} \pm iB) \tag{4-1}$$

where λ is a complex number for the solution of bi-material problems and B is zero if the crack is in a homogeneous medium. The numerical approach by Leverenz (36) studied the problem of a bi-material plate as shown in Figure 9 subject to uniform displacement, containing a crack perpendicular to the interface. He concluded that if a plate containing a crack is bonded to a second material with a higher elastic modulus, the value of the stress intensity factor will be smaller when compared with that of only one material. The reverse effect is also true.

Cook and Erdogan (37) solved the problem of two bonded elastic half planes containing a finite crack fully embedded in one of the half planes. Similar

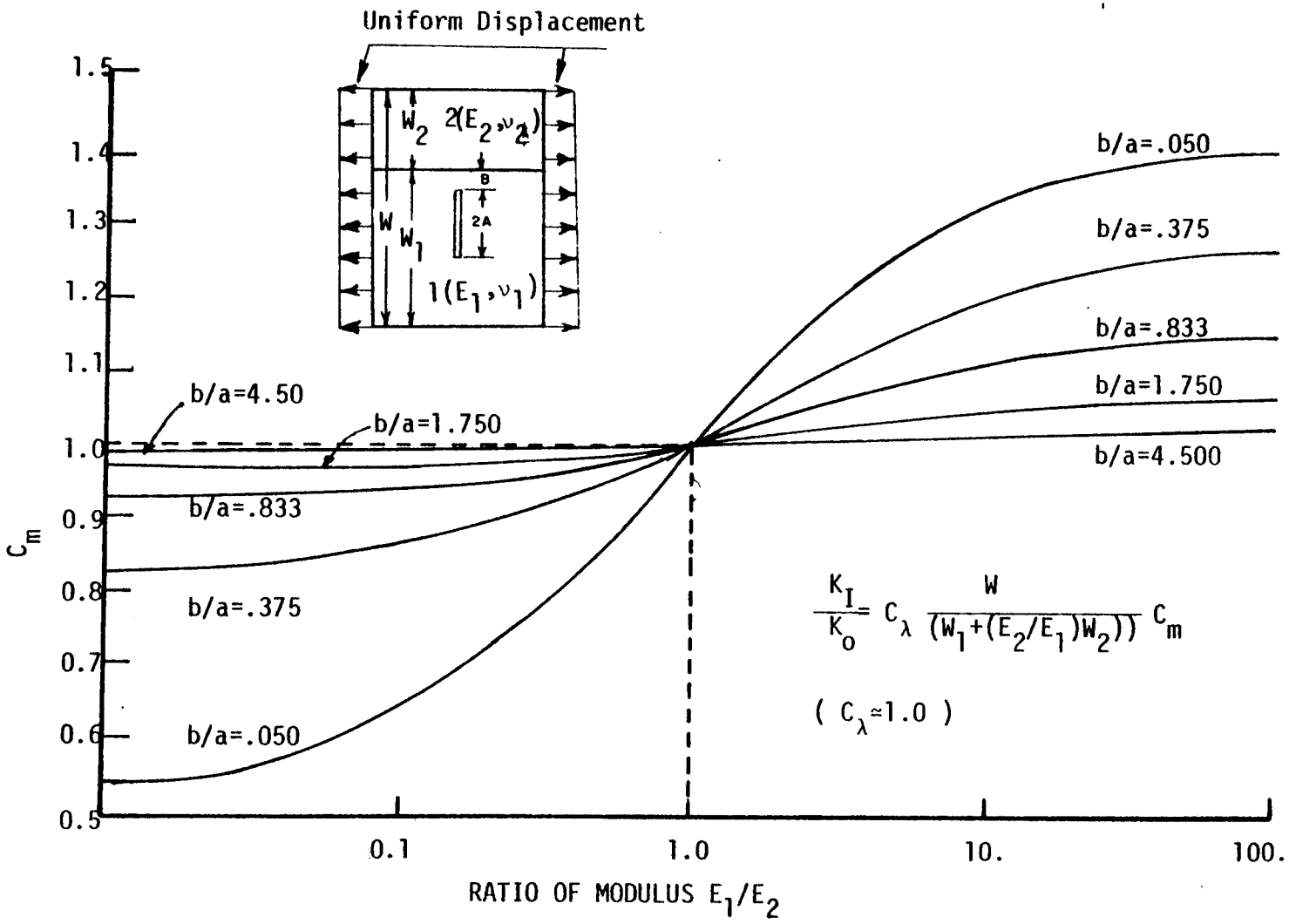

Figure 9. Ratio of Stress Intensity Factor in a Bi-material Plate (After Ref. 36)

effects for the modulus of the second material on the stress intensity factor as shown in Figure 9 were found. In this case, the stress singularity at the crack tip is in the form of

$$\sigma \sim r^{1-\lambda} \tag{4-2}$$

When the crack is perpendicular to the interface, λ is real and is the solution of the following characteristic equation:

$$2a_1 \cos\pi\lambda - (a_2\lambda^2 + a_3) = 0 \tag{4-3}$$

where $a_1 = (m + R_2)\ (1 + mR_1)$,

$a_2 = -4(m + R_2)\ (1 - m)$,

$a_3 = (1 - m)\ (m + R_2) + (1 + mR_1)\ (m + R_2) - m(1 + R_1)\ (1 + mR_1)$,

$m = \mu_2/\mu_1$ as defined in Figure 10

μ is the shear modulus and $R=3-4\nu$ for plane strain, $R=(3-\nu)/(1+\nu)$ for plane stress conditions

Stage 2 - Crack Touching the Interface

For the special case when a semi-infinite crack is touching the interface, the stress intensity factor is dependent on the bi-material constants, and:

$$K_I = (2)^{\frac{1}{2}} P r_o^{-\lambda_1} \left[\frac{m(1+R_1)[(1-2\lambda_1)(m+R_2) + (1+2\lambda_1)(1+mR_1)]}{2\pi a_1 \sin\pi\lambda_1 + 2a_2\lambda_1} \right] \tag{4-4}$$

where λ_1 is the root of Eq. (4-3). Figure 10 also shows the calculated values of K_I for various material combinations. The same trend for stress intensity factor under distributed loads has been found to be similar (37). In the case of a homogeneous medium, $\lambda_1 = \frac{1}{2}$, and Eq. (4-4) reduces to the following known result.

$$K_o = \frac{P}{\pi} \left(\frac{2}{r_o}\right)^{\frac{1}{2}} \tag{4-5}$$

It is important to note that Figure 9 and Figure 10 show the opposite effect on stress intensity factor given the same combination of material

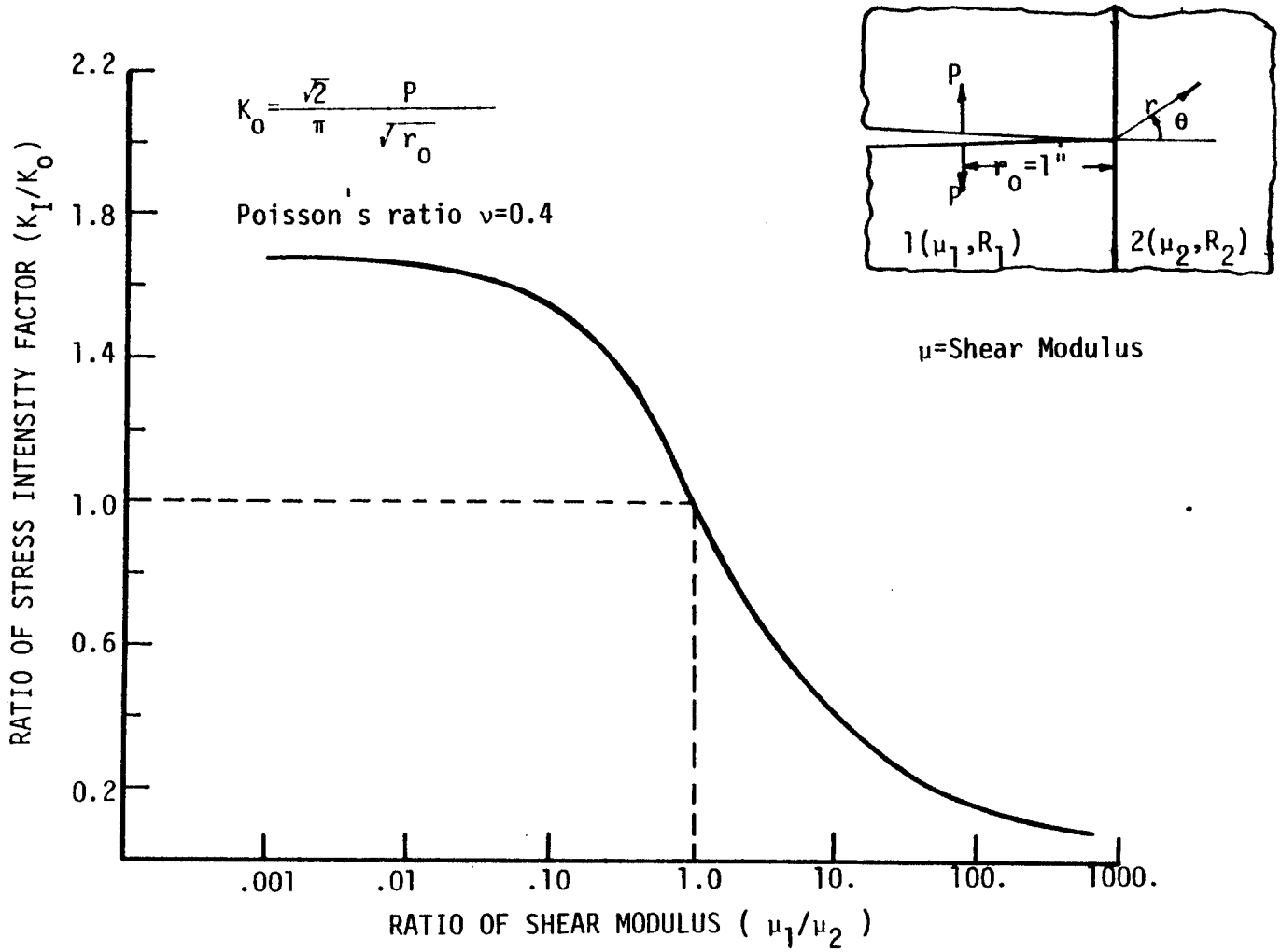

Figure 10. Ratio of Stress Intensity Factor of Semi-infinite Crack Touching an Interface (After Ref. 37)

constants. From this it can be concluded that a higher modulus for the overlay material will reduce the stress intensity factor of those cracks still embedded in the pavement. However, for the crack already touching the interface, a lower modulus layer will serve as a stress relieving medium. The experimental findings of field tests (57, 58, 59) are consistent with the results predicted using these theoretical approaches.

Although some experiments have produced encouraging results, documentaries as to the reasons for success or failure are scarce. Roberts (58) reported that experiments in Iowa showed a substantial difference in reflection cracking between asphalt mixtures made with 80 and with 115 penetration asphalt. It has been found that softer asphalt can reduce reflection cracking approximately 50% over that of the stiffer asphalt (80 penetration). Haas (59) in Canada also reinforced the use of softer material. An NCHRP report (1) recently recommended a stress relieving layer between the overlay and existing pavement. From these findings, it may be surmised that the asphalt stiffness can be a significant factor in the elimination or delay of cracking. The major point however, is that the theory presented in this chapter clearly illustrates the basis for the visual findings of the cited research efforts. They represent perhaps the first theoretical explanation of observed field experience.

Stage 3 - Crack Within the New Overlay

Once the crack tip has reflected through the surface, and the surface has been overlaid, however, the development of the stress intensity factor is the most important factor in predicting the thermal fatigue life of the overlay. The prediction of the stress intensity factor will be discussed in the remainder of this chapter.

Determination of Stress Intensity Factor

The finite element method is generally accepted because of its ability to handle very general geometries, a variety of material properties, and

loading conditions. Early studies on fracture mechanics problems involving the finite element were conducted by Tuba (42) and Kobayashi (43). They attempted a straight-forward application of the technique with no special attention given to the stress singularity at the crack tip. Computational experiments indicated the need for very large degrees of freedom and raised serious questions about the reliability under the given conditions (44, 45). New improvements using the energy method approaches such as the energy release rate method (46) and the J-integral method (47) still require the use of an extremely fine mesh near the crack tip and are restricted to only Mode I analysis (See Figure 2).

Recently Pian and Tong (48) adopted the hybrid-element concept and the complex variable technique to construct a special element for the tip region and combined it with the conventional finite element solution scheme. This technique permits the proper consideration of the stress intensity at the crack tip and also leads to a very efficient program (49, 50). The use of such an element has been shown to be very efficient and highly accurate even when a coarse element mesh is used (50).

A Fortran computer program (Appendix C), which incorporates Desai's (51) constant strain finite element program with Pian's tip element, has been modified into double precision on the IBM 360/65 for the analysis of pavement reflection cracking problems. This program calculates both Mode I and Mode II stress intensity factors and also provides an option which calculates the strain energy of the plane structure for an alternate solution by the energy method.

When dealing with boundary values over an infinite region such as a pavement structure, the problem can be analyzed as the superposition of two problems (52) as shown in Figure 11. The solution for problem (a) is trivial

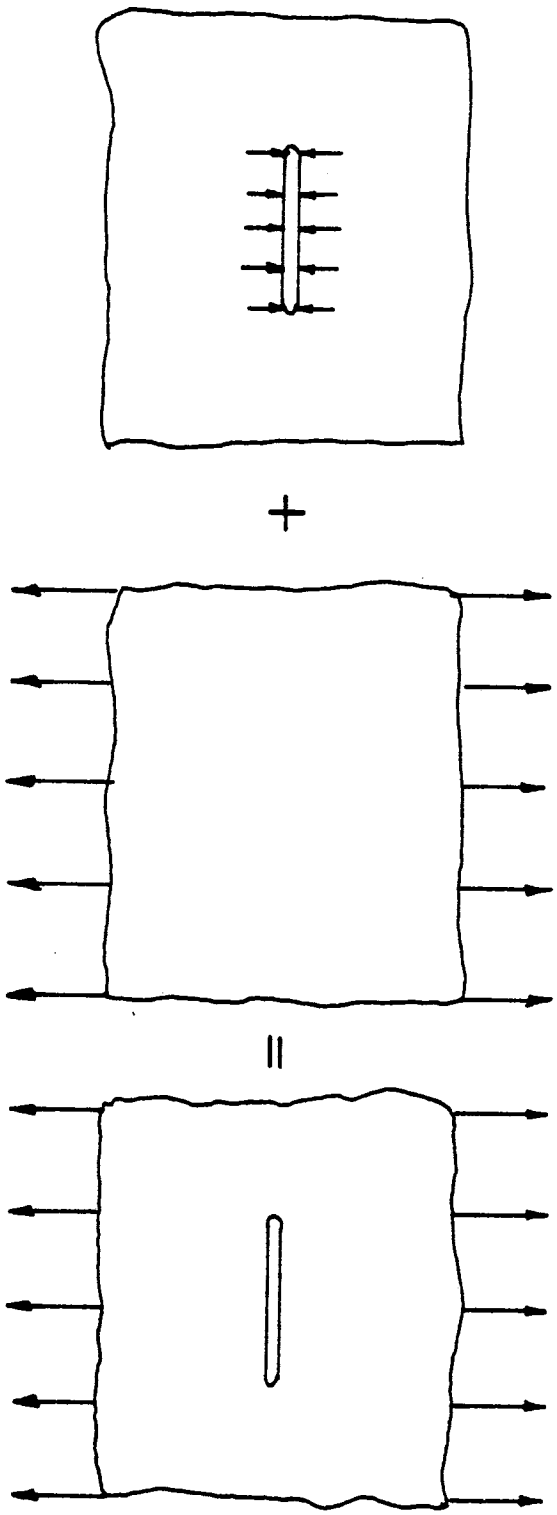

Figure 11. The Superposition Principal of an Infinite Body Containing a Crack

as the stress is the same everywhere. The magnitude of the stress intensity factor for problem (b) is the same as for the overall problem. Thus the analytical approach can be simplified by applying the tensile forces as compression forces over the finite region of the crack surface.

Figure 12 shows the finite element representation of a pavement structure and two types of tip elements. The cracks, assumed to be propagating upward, were studied in incremental lengths. Since the crack is assumed perpendicular to the interface, only the mode I stress intensity factor will be considered in this study. Thus the five node crack tip elements are used because of the nature of symmetry. As a rule of thumb, the size of the tip element is chosen as $r < c/10$ where c is the half crack length. The distances of the crack from the remote boundaries are determined such that the solutions will not be affected by the presence of the boundaries.

A proper choice of the crack tip length, z, where the forces cannot be applied directly is a major consideration. In this region, a solution for the stress intensity correction factor, C_K, following Barenblatt (53) is used, in which:

$$C_K = (2)^{\frac{1}{2}} \int_0^z \frac{\sigma_e(\xi)d\xi}{\sqrt{\xi}} \qquad (4\text{-}6)$$

where ξ is the distance away from crack tip and $\sigma_e(\xi)$ is the surface stress inside the crack tip element, i.e., $-\sigma_e$ is the thermal stress at the depth near the tip region.

If z is sufficiently small, $\sigma_e(\xi)$ can be assumed as a constant, $\sigma_e(\xi) = \sigma_e$. The correction factor C_K, for this case then becomes

$$C_K = (\frac{8}{\pi})^{\frac{1}{2}} \cdot \sigma_e \cdot (Z)^{\frac{1}{2}} \qquad (4\text{-}7)$$

and the resultant mode I stress intensity factor will be:

$$K_I = K + C_K \qquad (4\text{-}8)$$

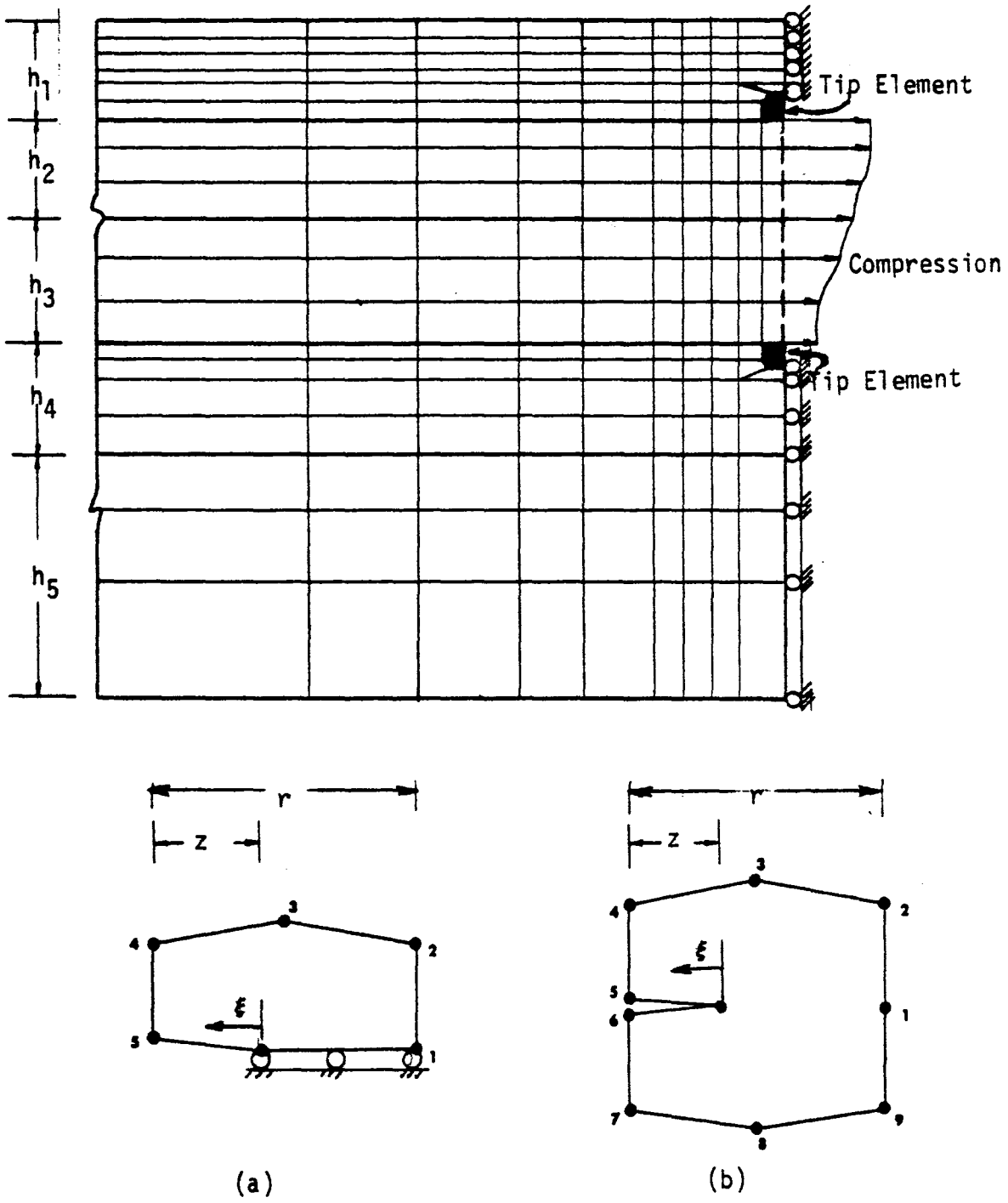

Figure 12. Finite Element Representation of Pavement Structure, (a) Five-node Tip Element for Symmetric Case, (b) Nine-node Tip Element for Non-symmetric Case

where K is the computed solution obtained when forces are applied at the crack surface.

Figure 13 is a schematic diagram of pavement temperature, thermal stresses, stiffness and stress intensity factor history during a single cycle. As can be seen from the figure, the stiffness and thermal stress of the pavement material will increase as its temperature decreases. At the same time the stress intensity factor, which depends upon both the stress and the stiffness, increases to a maximum when the temperature reaches its minimum value. In the computer program written to predict crack growth, it is assumed that the instantaneously stable crack growth occurs when the pavement reaches its minimum temperature. Consequently, the calculated maximum stress intensity factor K_{max}, is used for the prediction of fatigue life which is done in the following Chapter.

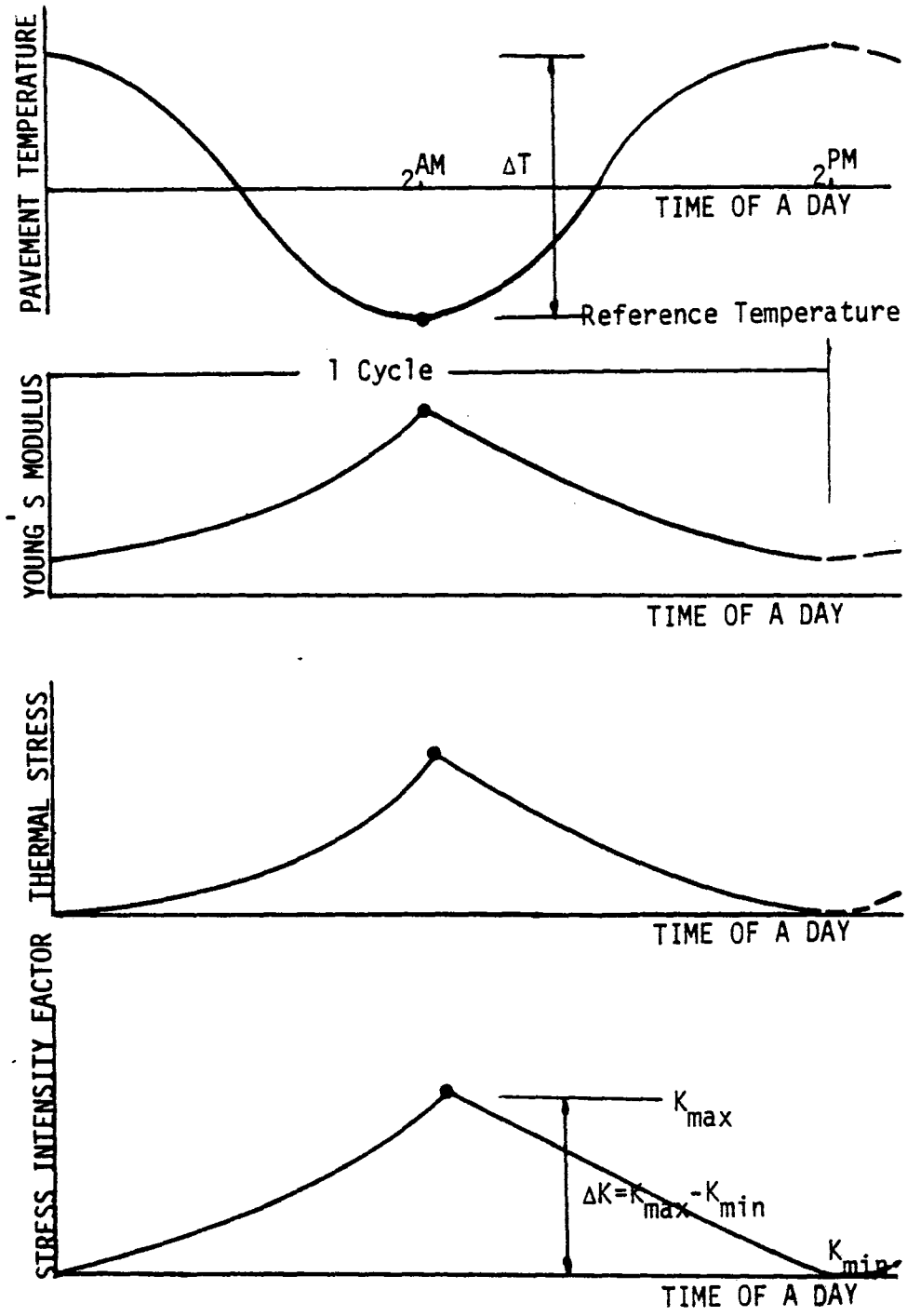

Figure 13. A Schematic Diagram Showing the Assumed Behavior of Pavement Temperature, and the Consequent Asphalt Pavement Stiffness, Thermal Stress and Stress Intensity Factor During a Day

CHAPTER V

PREDICTION OF OVERLAY LIFE

Prediction Scheme

The problem to be analyzed is a four layer flexible pavement which is overlaid by a relatively thin asphalt concrete surface. A crack is assumed to be existing in the base course and old surface layer as shown in Figure 14. Each layer is characterized by an elastic modulus and Poisson's ratio, which are reported elsewhere (11, 54, 55). A plane strain condition is assumed for the pavement structure.

Pavement temperature profiles calculated from West Texas climatic variables were calculated by Carpenter (56) using Dempsey's heat-transfer computer program (57). A preliminary thermal stress analysis was performed for the asphalt concrete specified in the previous chapter using the viscoelastic thermal stress computer code. The results, shown in Figure 15, indicate that due to the viscoelastic nature of the asphalt, thermal stresses may be negligible when pavement temperatures are above the freezing temperature ($32^{o}F$). Therefore it seems reasonable to assume that cracks will propagate during the more severe weather conditions present in winter.

Figure 16 shows a typical temperature profile when pavement temperatures are below freezing. Thermal stresses were computed by assuming the maximum temperature of each layer to be the stress free state temperature. Since the viscoelastic properties of the base course layer are not known at this time, only the elastic thermal stress (i.e., $\sigma = \alpha \cdot E \cdot (\Delta T)$) is calculated for the base course. The resultant thermal stresses versus depth are shown in Figure 17. The type of thermal stresses exhibited are rather unusual. Because of the different thermal activity possessed by each layer, however, and the creep effect of the asphalt concrete, these data are realistic.

For the prediction of service life, the important factors to be considered

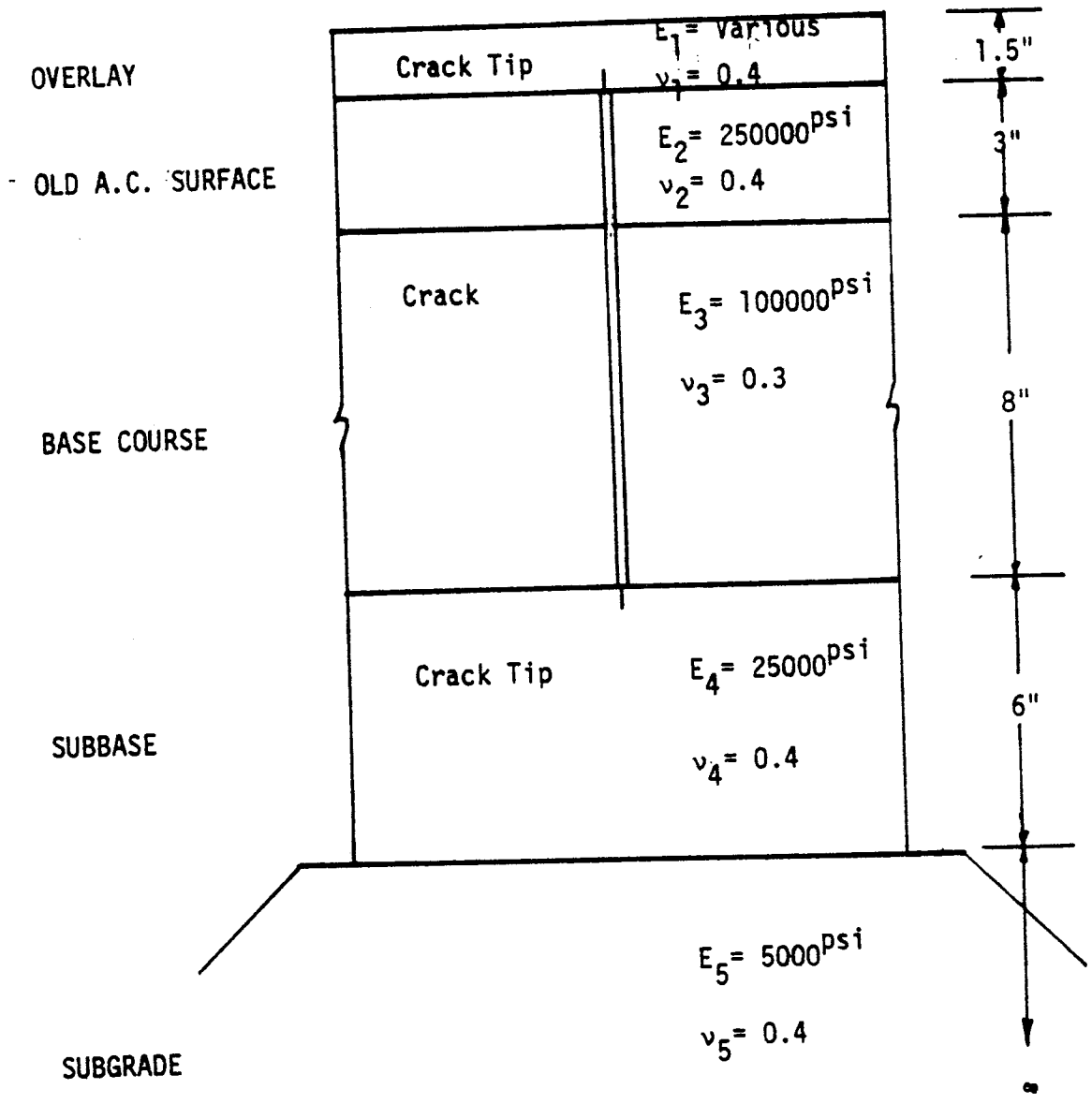

Figure 14. Cracked Pavement Model

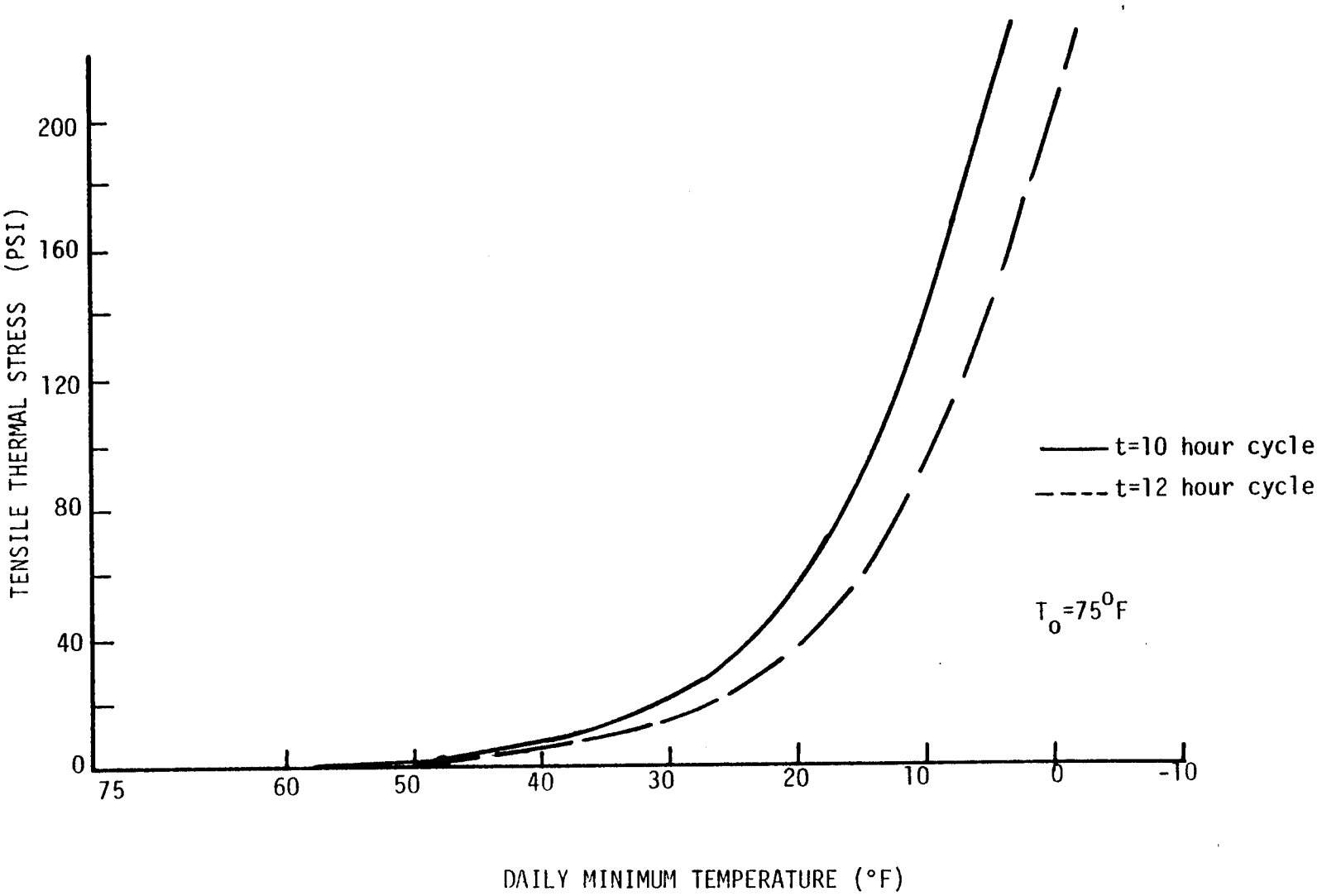

Figure 15. Maximum Thermal Stress Induced By Different Daily Minimum Temperatures

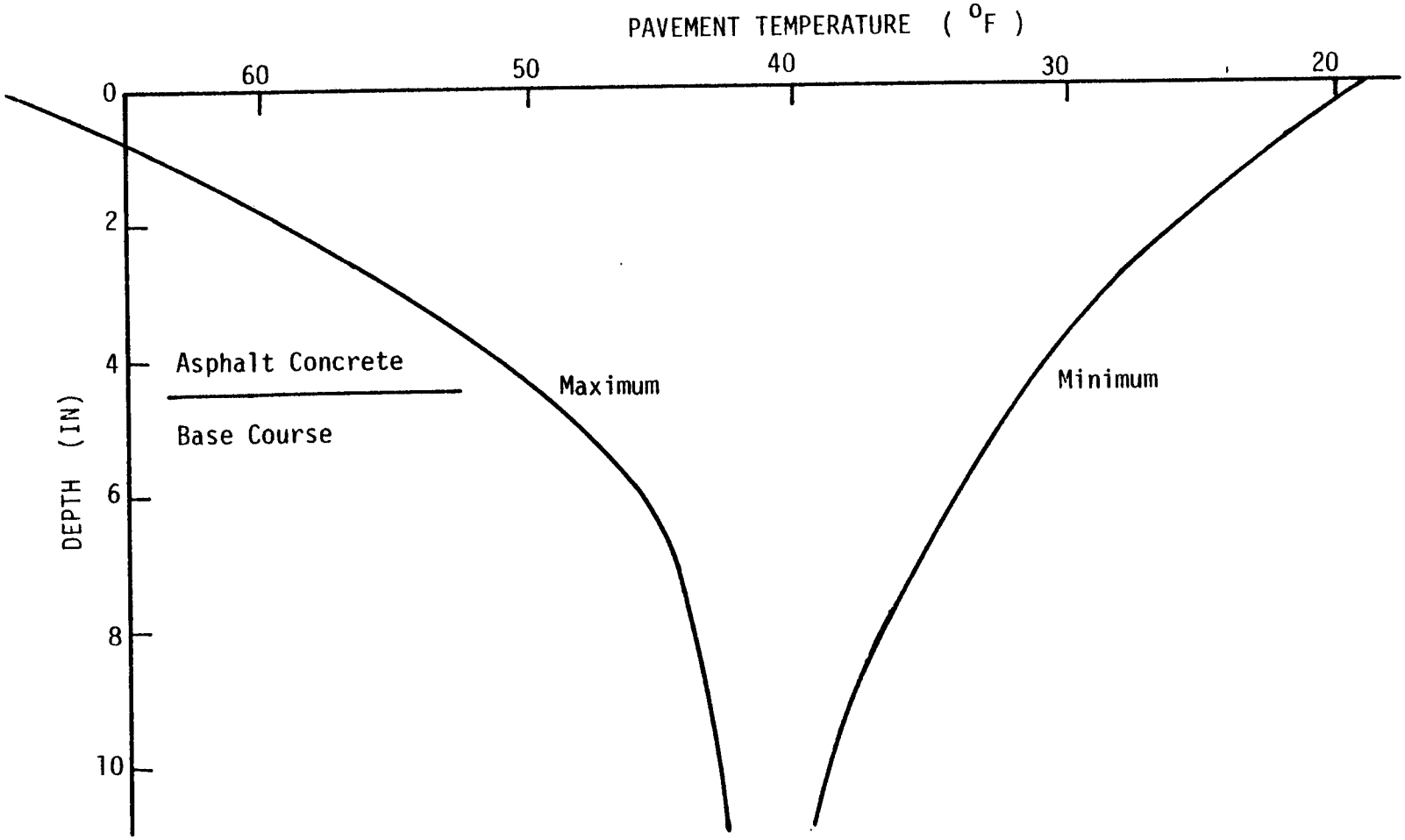

Figure 16. Maximum and Minimum Pavement Temperature Profile During Freeze in West Texas (Winter, 1966)

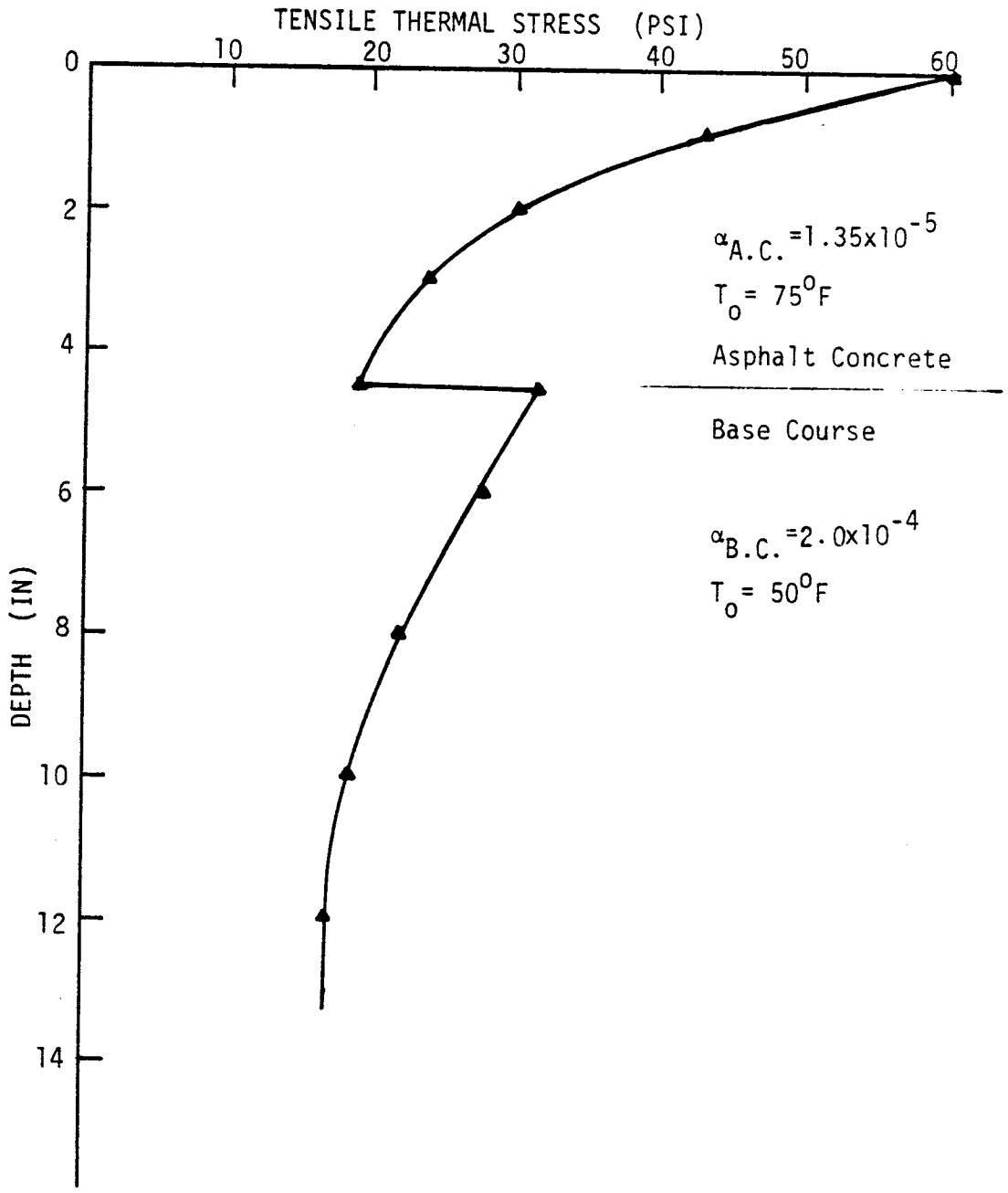

Figure 17. Calculated Maximum Thermal Stresses Within Pavement

are as follows:

1. The stress intensity factor history during the stable crack growth (e.g. $K_I = K_I(C)$), where C is the crack length within the overlay.
2. The fatigue parameters A and n.
3. The critical stress intensity factor K_{IC}.

Using the finite element method with the crack tip elements previously discussed, stress intensity factors were calculated by increasing the crack length within the overlay. Figure 18 shows that the stress intensity factor increases with increasing crack length. Figure 18 also shows that an increase in the overlay modulus will decrease the stress intensity factor. It is to be noted that the basic assumptions of the fracture mechanics computer code are only valid for the crack tip nearly $h_1/15$ away from either boundary (i.e., either the interface or the pavement surface). Therefore extrapolation was used to extend those values to the boundary.

The Fortran computer code developed for the estimation of service life is shown in Appendix D. A second order polynominal developed within the program is used to fit the function $K_K = K_I(C)$, shown in Figure 18. Integration was performed using Simpson's rule. The criterion for overlay failure is defined as the time when either, (1) the stress intensity factor reaches the critical level for a specified material or, (2) the crack tip reaches the surface plane of an overlay.

As discussed previously n is related to the viscoelastic property m, the slope of the creep compliance curve, as given by Equation (3-10).

$$n = 2(1 + \frac{1}{m}) \qquad (3\text{-}10)$$

Normally m varies as $0.5 \leq m \leq 1$ for the asphalt concrete, therefore a variation of n, $4 \leq n \leq 6$ can be anticipated. A value of m=1 indicates a soft asphalt. The experimental results have also shown that for beams and plates resting on

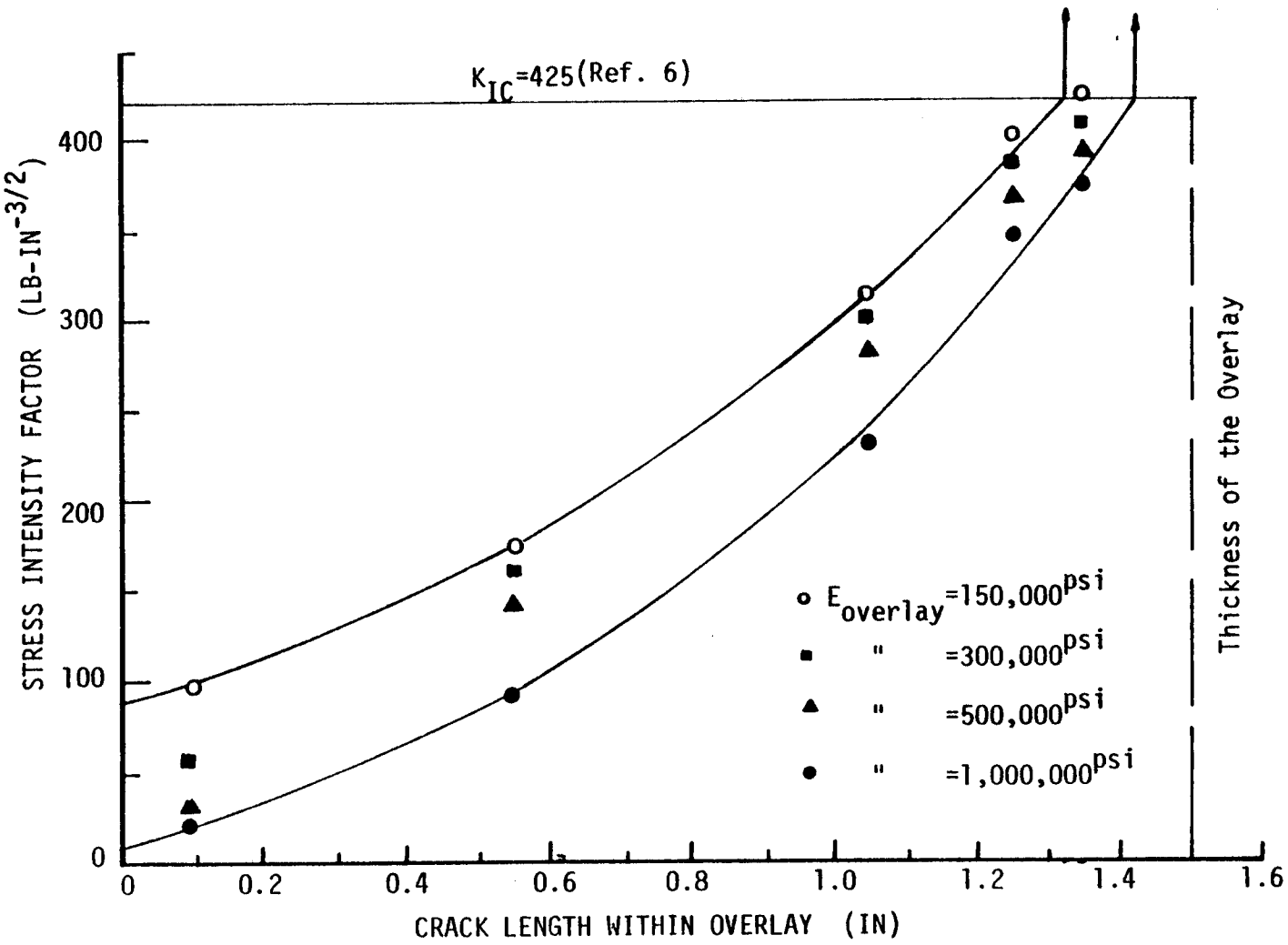

Figure 18. Stress Intensity Factor Verses Crack Length Within Overlay

foundations with sufficient rigidity, a typical value of n will be 4 at 77°F. Probably due to strain effects (e.g. crack tip blunting), values of n somewhat less than 4 have been reported for the unsupported specimens (7, 8). Also, it is noted that n increases with decreasing temperature (6).

It is important to recall from the viscoelastic fracture mechanics approach that A can be related to B_t as was shown in equations (3-9) and (3-10). Values of A are direct function of D_1 and an inverse function of the fracture properties (γ, σ_m). A decrease of D_1 indicates a higher modulus and a lower value for A. Also, an increase of either γ, the fracture energy, or σ_m, the maximum stress a material can sustain, will result in a decrease in A which results in a decrease in the rate of crack growth.

It is important to note that an increase in the overlay modulus will have two major effects on the crack growth equation. These are:

a. It will decrease A, thus decreasing the rate of crack growth, and

b. It will decrease K for a fixed stress level.

In order to examine the net effects of the variation of these material properties on the service life of the overlay, the following typical range or of the fatigue parameters for asphalt concrete was utilized in the computer code developed in Appendix D.

1. $10^{-14} \leq A \leq 10^{-10}$

2. $3 \leq n \leq 6$

The results, shown in Figure 19, demonstrate the wide range of calculated service life for the wide range of material properties.

The calculations for service life show that changes in the modulus of the overlay had a small effect on the stress intensity factor. This result provides a basis for use of equation (3-8) to predict service life.

$$N_f = \int \frac{1}{A(\Delta K)^n} \, dc \qquad (3\text{-}8)$$

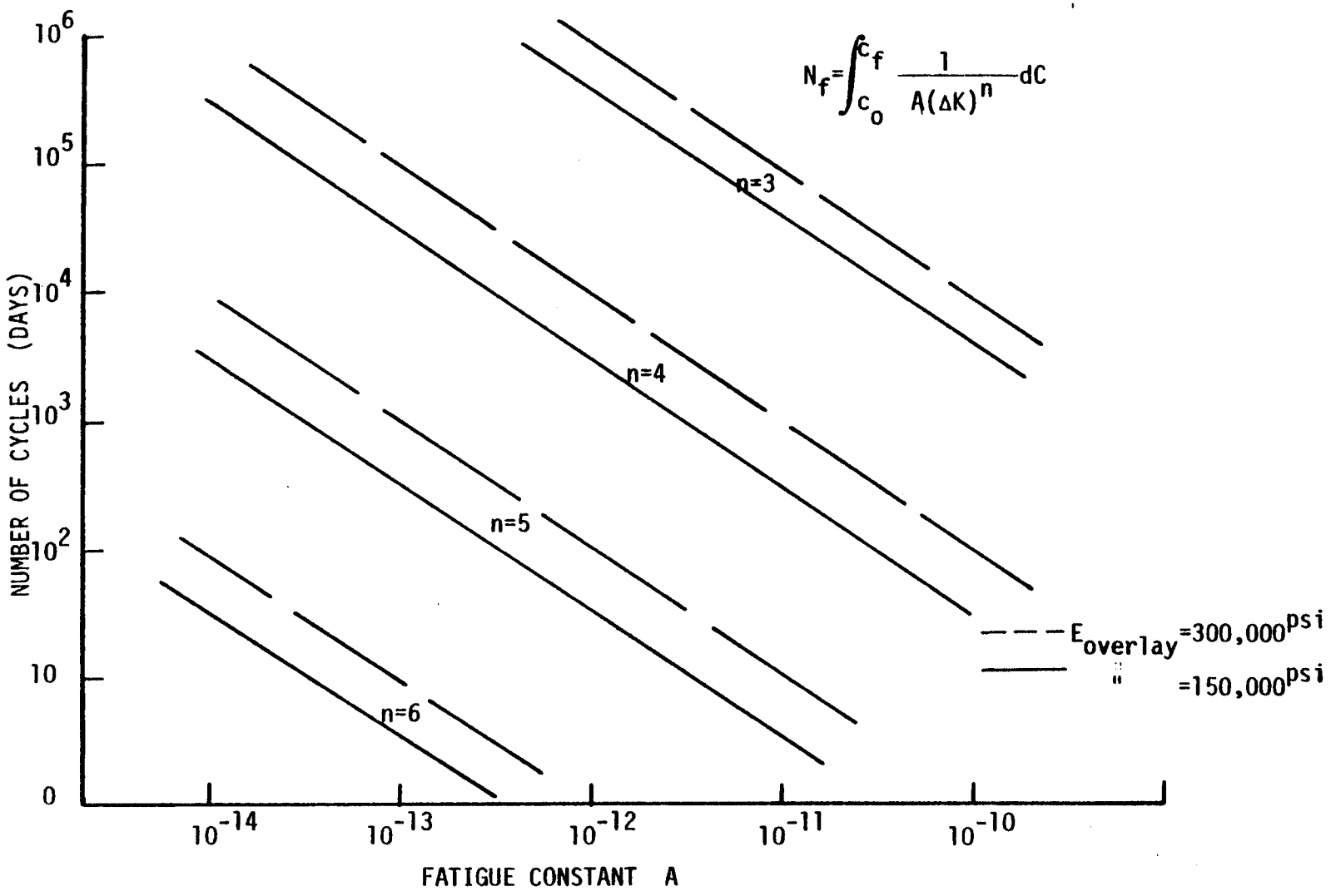

Figure 19. The Effect of Material Constants on The Overlay Service Life

The stress intensity factors being used are the result of calculations which assume that pavement moduli fall within a fairly broad range of values.

Common Values of A and n

The values for A and n necessary for this study are not reported together frequently in the literature. Christison reported stiffness modulus data which converted to an n value of 5.0 with a standard deviation of 0.24 for seven asphalts in Canada (3). Shahin and McCullough (41) report that for the stiffest asphalt concrete mixture an A value of $8x10^{-13}$ would be approximately correct. These values are not for the same material; therefore they cannot be used together to predict a service life of 1000 cycles. This is not an unreasonable life span, however.

Monismith (30) reports an n value of 5.1 for the asphaltic concrete used in his study, however no value of A is given as the fatigue problem was not addressed. Ramsamooj, et al. (7) gave values for A and n for sand asphalt slabs in various configurations. They reported data for unbonded slabs, top surface slabs, beams on an elastic solid and slabs. The values for n were all 4.0. The values for A varied from $3.5x10^{-12}$ to $5x10^{-12}$. It becomes apparent that asphaltic concrete may possess a rather narrow range of material properties, however, a variation in these properties changes the results appreciably.

CHAPTER VI

CONCLUSIONS AND DISCUSSION

Conclusions

The design of pavement overlays to resist reflection cracking involves many complex and interrelated variables. In this study, the principles and concepts of linear elastic and viscoelastic fracture mechanics were used to study the crack propagation in flexible pavement due to thermal contraction and expansion.

A successful overlay should eliminate or at least delay the reflection cracking. Many experiments have been done on reducing the reflection cracking, however, most of the efforts have only been empirical field trials. Treatments that worked in one area failed in another (58). This study has examined the effects of mechanical properties on the service life expectancy of an overlay and has proposed a rational approach to estimate the service life of the overlay. The procedure is quite general and permits evaluation of general temperature effects on the growth of pavement cracking.

The crack propagation law for the asphalt concrete $dc/dN = A(\Delta K)^n$, which was verified by the experiments at Ohio State University, was used as the basis of the mechanistic approach. Viscoelastic fracture mechanics was used to relate the fracture phenomena to the material properties.

It was shown in Figures 18 and 19 that an overlay with a higher modulus tends to reduce the stress intensity factor within the pavement. The fatigue parameter, A, which is a function of the elastic modulus, can be controlled by the asphalt content, aggregate gradation and fracture properties of the mixture. The other parameter, n, is related to the asphalt penetration or hardness. These two parameters are the significant factors in determining the service life expectancy. Therefore, Figure 19 provides a valuable guide for choosing the appropriate overlay material which may increase its service life.

The following conclusions may be drawn from this study:

1. The best overlay design to reduce the appearance of cracking is, as shown in Figure 20, namely:

   a) a thin layer with soft asphalt (low n) and low modulus of elasticity to serve as a stress relieving medium overlaid by,

   b) a layer with soft asphalt (low n) and a high modulus of elasticity.

Although this arrangement will hasten the propagation of unseen cracks through the surface of the old pavement, it will slow them down considerably when they reach the surface and contact the underside of the stress-relieving layer.

2. The use of the finite element analysis in conjunction with the crack tip element is an accurate and simple method for the determination of stress intensity factors.
3. The stress intensity factor is a measure of crack opening force and is proportional to the applied stresses. Therefore the reduction of the pavement thermal activity i.e., the value of thermal expansion coefficient, α, would reduce the reflection cracking substantially.
4. The fatigue parameter A can be related to, and is some function of material properties such as elastic modulus ($\frac{1}{E_1}$ or D_1) and fracture properties (γ, σ_m). The other fatigue parameter, the exponent, n, is inversely related to the slope, m, of the creep compliance curve. These parameters can be controlled by the choice of asphalt content and mixture properties.
5. A pavement overlay with soft asphalt (low n) and higher asphalt concrete modulus tends to reduce the stress intensity factor. However, a stress relieving layer is needed for those cracks touching the interface.
6. Both A and n play an important role in determining the expected service life. Smaller values of A and n will extend the expected life.

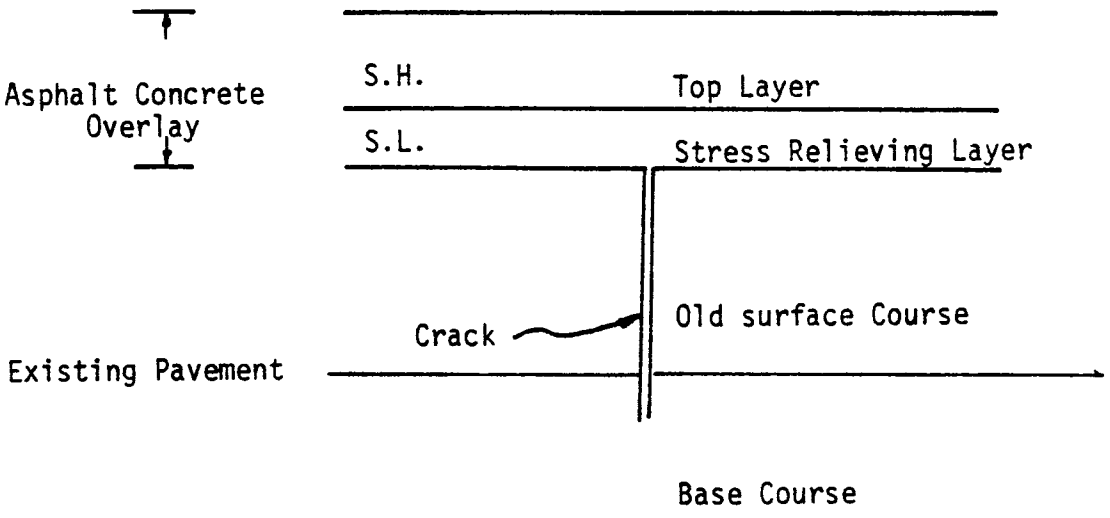

Figure 20. A Recommended Overlay Design Concept for a Cracked Flexible Pavement

Discussion

Although this report clearly shows that a rational design procedure for overlays is obtainable there are several areas that require further work before the process could be considered a complete procedure.

First, the thermal stresses predicted from the viscoelastic approach are more accurate than those predicted by previous viscoelastic techniques. Equations (3-9) and (3-10) however, assumed a linear change in the pavement temperature from maximum to minimum during the daily cycle. Further development of the theory and laboratory testing will be necessary before the non-linear temperature change and its effect on the residual modulus can be accounted for accurately. The shift produced by this consideration will move predicted stresses closer to measured values.

Secondly, the study of traffic induced cracking conducted at Ohio State University should be combined with the results of this study. This would produce a general prediction scheme that would combine traffic and environmental influences into a system that would logically analyze overlay systems and predict service life.

Finally, this study examined only one overlay thickness in developing the prediction scheme. This thickness, 1½ inches, is typical of the most commonly used overlay, but the effect of thickness on the behavior and service life of the overlay should be studied. This would be merely an extension of the work presented in this study.

This study is an analytical study that applies concepts which have been developed and validated in other industries, namely the polymer and solid rocket fuel industries. The application of these concepts is logically done and initial research, as cited, clearly shows that these concepts are proper for the study of asphalt concrete. The results developed in this study will be verified by laboratory testing in an overlay testing device currently under construction as

an integral part of this research study. This verification of the performance of actual overlay systems in the laboratory, coupled with a proven analytical technique to predict performance will provide the basis for a comprehensive study of reflection cracking due to environmental effects and later even allow the inclusion of traffic effects to formulate a complete design system for overlays.

REFERENCES

1. NCHRP Synthesis of Highway Practice 9, Pavement Rehabilitation - Materials and Techniques, 1969.

2. AAPT, Non-Traffic Load Associated Cracking of Asphalt Pavement Symposium, Vol. 35, 1966.

3. Christison, L.T., The Response of Asphalt Concrete Pavements to Low Temperatures, Ph.D. Dissertation, University of Alberta, pp. 59-60, 1972.

4. Hajek, J.J., and Haas, R.C.G., Predicting Low-Temperature Cracking Frequency of Asphalt Concrete Pavements, Highway Research Board Record No. 407, pp. 39-54, 1972.

5. Carpenter, S.H., Lytton, R.L. and Epps, J.A., Pavement Cracking in West Texas Due to Freeze-Thaw Cycling, Transportation Research Board, Record No. 532, pp. 1-14, 1975.

6. Majidzadeh, K., Kauffmann, E.M., and Chang, C.W., Verification of Fracture Mechanics Concepts to Predict Cracking of Flexible Pavements, Report No. FHWA RD-73-91, June 1973, Final Report.

7. Ramsamooj, D.V., Majidzadeh, K., and Kauffmann, E.M., The Analysis and Design of Flexibility of Pavement, Proc. Third International Conference on the Structure Design of Asphalt Pavements, 1, University of Michigan, 1972, pp. 692-704.

8. Majidzadeh, K., Ramsamooj, D.V., and Fletcher, T.A., Analysis of Fatigue of Sand-Asphalt Mixture, Proc. of the AAPT, Vol. 38, 1969.

9. Majidzadeh, K., Kauffmann, E.M., and Ramsamooj, D.V., Application of Fracture Mechanics in the Analysis of Pavement Fatigue, Proc. of AAPT Vol. 40, 1971.

10. Paris, C.P., and Erodogan, F.J., A Critical Analysis of Crack Propagation Laws, Journal of Basic Engineering, Transaction ASME, Series D, Vol. 85, 1963, pp. 528-553.

11. Burmister, D.M., The General Theory of Stresses and Displacements in Layered Systems and Applications to the Design of Airport Runways. HRB Proc., Vol. 23, 1943, pp. 126-148.

12. Peutz, M.G.F., Van Kempen, H.P.M. and Jones, A., Layered Systems Under Normal Surface Loads, HRB Proc. Vol. 228, 1968.

13. Gerrard, C.M., Theoretical and Experimental Investigations of Model Pavement Structures, Departmental Report No. 18, Department of Civil Engineering, University of Melbourne, 1969.

14. Griffith, A.A., The Phenomenon of Rupture and Flow in Solids - Philosophical Transactions of the Royal Society of London, Series A, Vol. 221, 1920, pp. 163-198.

15. Irwin, G.R. and Kies, J.A., Fracturing and Fracture Dynamics, Welding Journal, Vol. 31, Research Supplement, February 1952, pp. 955-1005.

16. Irwin, G.R., Fracture Mechanics, Proc., First Symposium on Naval Structures Mechanics, MacMillan Press, 1958.

17. Coten, H.T., Fracture Mechanics of Composites, Fracture, An Advanced Treatise edited by H. Librowitz Vol. 7, Academic Press, 1972.

18. Manual on Fatigue Testing, ASTM Special Technical Publication No. 21, American Society for Testing Materials, Philadelphia, 1949.

19. Paris, C.P., The Fracture Mechanics Approach to Fatigue. Fatigue, An Interdisciplinary Approach, Syracuse University Press, 1964.

20. Paris, C.P., Gomes, M.P., and Anderson, W.E., A Rational Analytic Theory of Fatigue, Trend in Engineering , (University of Washington), Seattle, Washington, Vol. 13, No. 1, 1961.

21. Williams, M.L., Initiation and Growth of Viscoelastic Fracture, Int. J. Fracture Mechanics, Vol. 1, 1965, pp. 292-310.

22. Wunk, M.P. and Knauss, W.G., Delayed Fracture in Viscoelastic - Plastic Solids, Int. J. Solids Structures, Vol. 6, 1970, pp. 7-20.

23. Schapery, R.A., Viscoelastic Behavior and Analysis of Composite Materials, Texas A&M University, Rpt. MM 72-3, August 1972.

24. Schapery, R.A., Theory of Crack Initiation and Growth in Viscoelastic Media, Int. J. of Fracture, Vol. 11, No. 1, February 1975, pp. 141-159.

25. Schapery, R.A., A Theory of Crack Growth in Viscoelastic Media, Texas A&M University, Rpt. MM 2764-73-1, March 1973.

26. Graham, G.A.C., The Correspondence Principle of Linear Viscoelasticity Theory for Mixed Boundary Value Problems Involving Time-Dependent Boundary Regions, Q. Applied Math., Vol. 26, 1968, pp. 67-174.

27. Secor. D.E. and Monismith, C.L., Analysis and Interrelation of Stress - Strain - Time Data for Asphalt Concrete, Transactions of the Society of Rheology, 1964, pp. 19-32.

28. Krokosky, E.M., Tons, E. and Andrews, R.D., Rhoelogical Properties of Asphalt-Aggregate Composites, Paper presented at 66th Annual Meeting, ASTM, Atlantic City, N.J., June 1963, pp. 1263-1286.

29. Saal, R.N.J. and Labout, J.W.A., Rheological Properties of Asphalt, Rheology - Theory and Applications, Vol. 2, Academic Press, Inc., N.Y., 1958.

30. Monismith, C.L., Secor, G.A. and Secor, K.E., Temperature Induced Stress and Deformations in Asphalt Concrete, Proc., Association of Asphalt Paving Technologists, Vol. 34, February 1965, pp. 248-279.

31. Humphreys, J.S. and Martin, C.T., Determination of Transient Thermal Stress in a Slab with Temperature Dependent Viscoelastic Properties, Transactions of the Society of Rheology, Vol. VII, 1963, pp. 155-170.

32. Fromm, H.J. and Phang, W.A., Temperature - Susceptibility Control in Asphalt Cement Specifications, HRB No. 350, 1971, pp. 30-38.

33. JANNF Solid Propellant Structure Integrity Handbook, September 1972, CPIA Publication 230, UTEC CE 72-160, Chemical Propulsion Information Agency, pp. 107-136.

34. Williams, M.L., The Stresses Around a Fault or Crack in Dissimilar Media, Bulletin of the Seismological Society of America, Vol. 49, April 1959, pp. 199-204.

35. Zak, A.R. and Williams, M.L., Crack Point Stress Singularities at a Bi-material Interface, Journal of Applied Mechanics, March 1963, pp. 142-143.

36. Leverenz, R.K., A Finite Element Stress Analysis of a Crack in a Bi-material Plate, International Journal of Fracture Mechanics, Vol. 8, No. 3, September 1972, pp. 311-324.

37. Cook, T.S. and Erdogan, F., Stress in Bonded Materials with a Crack Perpendicular to the Interface, Int. J. Eng. Sci. , Vol. 10, 1972,pp. 677-697.

38. Abramowitz, M. and Stegun, I.A., Handbook of Mathematical Functions with Formulas, Graphs, and Mathematical Tables, Dover Publications, Inc., N.Y. 1964, pp. 262-944.

39. The IMSL library, Vol. 2, International Mathematical and Statistical Libraries, Inc., P. MDBETA-1, 1973.

40. CRC Standard Mathematical Tables, The Chemical Rubber Co. 18th Edition, 1962.

41. Shahin, M.Y. and McClullough, B.F., Prediction of Low-Temperature and Thermal-Fatigue Cracking in Flexible Pavements - Research Report 123-14, Texas Highway Department, Center of Highway Research and Texas Transportation Institute, August 1972.

42. Chan. S.K., Tuba, I.S. and Wilson, W.K., On the Finite Element Method in Linear Fracture Mechanics, A paper presented at the 2nd National Symposium on Fracture Mechanics, Lehigh University, June 17-19, 1968.

43. Kobayashi, A.S., Mainden, D.E., Simon, B.J. and Iida, S., Application of the Method of Finite Element Analysis of Two-Dimensional Problems in Fracture Mechanics, Office of Naval Research NR064-478, Technical Report 5, October 1968.

44. William, W.K., On Combined Mode Fracture Mechanics, University of Pittsburgh, Ph.D. Dissertation 1969.

45. Oglesby, J.J. and Lamacky, O., An Evaluation of Finite Element Methods for the computation of the Elastic Stress Intensity Factors, NSRDS, Report No. 3751, 1972.

46. Anderson, G.P., Ruggles, V.L. and Stibor, G.S., Use of Finite Element Computer Program in Fracture Mechanics, Int. J. of Fracture Mechanics, Vol. 7, No.1, March 1971, pp. 63-76.

47. Paris, P.C. and Sih, G.C., Stress Analysis of Cracks, ASTM Special Technical Publication, No. 381, June 1964.

48. Tong, P., New Displacement - Element Approach to Crack Problems in Plane Elasticity, Int. J. of Numerical Method in Engr. Vol. 7, 1973, pp. 297-308.

49. Luk, C.H., Assumed Stress Hybrid Finite Element Mehtod for Fracture Mechanics and Elastic-Plastic Analysis, Ph.D. Thesis M.I.T., Department of Aeronaut and Astronaut, Mass:, 1973.

50. Tong, P., Pian, T.H.H. and Lasry, S.J., A Hybrid-Element Approach to Crack Problems in Plane Elasticity, Int. J. for Numerical Method in Engineering, Vol. 7, 1973, pp. 297-308.

51. Desai, C.S. and Abel, J.F., Introduction to the Finite Element Method, Van Nostrand Reinhold Company, 1972.

52. Hilton, D.D. and Sih, G.C., Application of the Finite Element Method to the Calculation of Stress Intensity Factors, Mechanics of Fracture I, edited by G.C. Sih, Noordhoff International Publishing,1973.

53. Barenblatt, G. I., The Mathematical Theory of Equilibrium Cracks in Brittle Fracture, Advances in Applied Mechanics, Vol. VII, Academic Press, 1962, pp. 55-129.

54. Monismith, C.L. Seed, H.B., Mitry, F.G. and Chan, C.K., Prediction of Pavement Deflections from Laboratory Tests, Second International Conference on the Structure Design of Asphalt Pavements, Proceedings, 1967, pp. 109-140.

55. Barenberg, E.J., A Structural Design Classification of Pavements Based on an Analysis of Pavement Behavior, Material Properties and Mode of Failure, Civil Engineering Publication, University of Illinois, 1965.

56. Unpublished data, to be published as a Technical Report through Texas Transportation Institute at a later date.

57. Sherman, G.B., Reflection Cracking, Paper Prepared for the FHWA-HRB Workshop on Pavement Rehabilitation in San Francisco, September 19-22, 1973.

58. Roberts, S.E., Cracks in Asphalt Resurfacing Affected by Cracks in Rigid Bases, Proc. HRB, Vol. 33, 1954, pp. 341-345.

59. Haas, R.C.G., Low Temperature Pavement Cracking in Canada - The Problem and its Treatment, Canadian Good Roads Assn. Proc., 1970, pp. 69-96.

APPENDIX A

Determination of Constants β and Ta in Eq. 2-12b

The determination of constants β and Ta in Eq. (2-12b) can be accomplished from experimental data as follows:

1. Estimate a value of $Ta = T_M - x$, and substitute it into Eq. (2-12b), then plot the data in the form log a_T vs log (T-Ta).
2. If the points fall approximately on a straight line, the estimate of Ta is the correct value and β is the slope of the log-log curve. If not, estimate another value of Ta and repeat the process.

The following computer program was developed by assuming that F_1 and F_2 in Eq. (2-7) are known. The subroutine Plot 1 provides a graph, as shown in the example print out, which could narrow the range of searching values of x.

Guide for Data Input

Card 1 (F10.0)

cc 1-10 TM Reference temperature for master curve

Card 2 (F10.0) (See Eq. 2-12b and Figure 5)

cc 1-10 F1 A WLF shifting factor

11-20 F2 A WLF shifting factor

Card 3 (F10.0) (A set of cards)

cc 1-10 X Trial value for $Ta = T_M - x$

Card 4 (blank) One blank card allows normal termination of the computer program

```
      DIMENSION AT(100),TLOG(100)
      READ(5,1) TM
      READ(5,1) F1,F2
  100 READ(5,1,END=99) X
    1 FORMAT(8F10.0)
      J= 1
      TA=TM - X
      WRITE(6,31)
   31 FORMAT('1',5X,'T',10X,'T-TA',5X,'AT',7X,'TLOG')
      T = -40.
      N = 15
      DO 10 I=1,N
      T = T + 10.
      TMTA = T - TA
      AT(I) = -F1*(T-TM)/(F2+T-TM)
      TLOG(I) = ALOG10(TMTA)
      WRITE(6,32) T,TMTA,AT(I),TLOG(I)
   32 FORMAT(4G12.4)
   10 CONTINUE
      CALL PLOT1(J,AT,TLOG,N)
      WRITE(6,21) X
   21 FORMAT('-',5X,'X = ',F13.3)
      WRITE(6,22) TA,TM
   22 FORMAT('-',5X,'TA= ',F13.3,'TM= ',F13.3)
      J=J+1
      GO TO 100
   99 CONTINUE
      WRITE(6,20)
   20 FORMAT('1')
      STOP
      END

      SUBROUTINE PLOT1(NO,X,Y,N)
      DIMENSION X(100),Y(100),A(55)
      DATA DOT,PLUS,BLANK/'-','+',' '/
    1 FORMAT('0',1X,'CHART NO.',I5//7X,'X',13X,'Y',9X,
     1 'Y(MIN) = ',1P1E11.4,10X,'Y(MAX) = ',1P1E11.4)
    2 FORMAT(1P2E14.4,3X,55A1)
      YMIN=Y(1)
      YMAX=Y(1)
      DO 10 I=2,N
      IF(YMIN.GT.Y(I)) YMIN=Y(I)
      IF(YMAX.LT.Y(I)) YMAX=Y(I)
   10 CONTINUE
      YSCALE =(YMAX-YMIN)/50.
      WRITE(6,1) NO,YMIN,YMAX
      DO 40 I=1,N
      LL=(Y(I)-YMIN)/YSCALE
      L =LL+2
      DO 20 J=1,L
   20 A(J)=DOT
      A(L+1)=PLUS
      L2=L+2
      DO 30 J=L2,55
   30 A(J)=BLANK
      WRITE(6,2) X(I),Y(I),A
   40 CONTINUE
      RETURN
      END
```

```
     T          T-TA     AT       TLOG              X =          111.000
  -30.00      41.00      5.971      1.613
  -20.00      51.00      4.953      1.708           TA=          -71.000TM=          40.000
  -10.00      61.00      3.999      1.785
  0.0         71.00      3.103      1.851
   10.00      81.00      2.259      1.908
   20.00      91.00      1.463      1.959
   30.00      101.0      0.7113     2.004
   40.00      111.0      0.0        2.045
   50.00      121.0     -0.6740     2.083
   60.00      131.0     -1.314      2.117
   70.00      141.0     -1.921      2.149
   80.00      151.0     -2.500      2.179
   90.00      161.0     -3.059      2.207
   100.0      171.0     -3.576      2.233
   110.0      181.0     -4.077      2.258
```

```
      X              Y         Y(MIN) =  1.6128E 00          Y(MAX) =  2.2577E 00
  5.9765E 00     1.6128E 00    --+
  4.9533E 00     1.7076E 00    ---------+
  3.9993E 00     1.7853E 00    ---------------+
  3.1029E 00     1.8513E 00    --------------------+
  2.2593E 00     1.9085E 00    ------------------------+
  1.4632E 00     1.9590E 00    ----------------------------+
  7.1134E-01     2.0043E 00    --------------------------------+
  0.0            2.0453E 00    -----------------------------------+
 -6.7404E-01     2.0828E 00    --------------------------------------+
 -1.3136E 00     2.1173E 00    -----------------------------------------+
 -1.9214E 00     2.1492E 00    -------------------------------------------+
 -2.4996E 00     2.1790E 00    ---------------------------------------------+
 -3.0503E 00     2.2068E 00    ------------------------------------------------+
 -3.5756E 00     2.2339E 00    --------------------------------------------------+
 -4.0770E 00     2.2577E 00    ----------------------------------------------------+
```

APPENDIX B

Computer Program for Prediction of Viscoelastic Thermal Stress

This appendix contains a computer program for calculating thermal stress of a restrained bar subject to a linear temperature change with time between maximum and minimum temperature.

The program consists of a main program and five subroutines:

MAIN - Calls the subroutines and calculates modulus ratio and resultant thermal stress. A flow chart of the main program is shown in Figure B-1.

DATAIN - Reads in parameters required for the numerical computations of the viscoelastic stress equation. These parameters will be defined in the input data guide.

INTGRT - Provides numerical integrations using the trapezoidal rule. This subroutine is called by subroutine HEAT.

CURVE - Establishes the modulus ratio curve within this program.

COOL - Calculates the cooling process.

HEAT - Calculates the heating process.

MDBETA - Calculates incomplete Beta function. This subroutine is provided by the IBM IMSL local computer program library.

Input Data Guide

Card 1 (10A8) Title of the problem

Card 2 (I5, 5X, 2F10.0) (See Figure 3 and Figure 4)

cc 1-5 INDEX 0= data read from master creep compliance curve
1= data read from master relaxation curve.

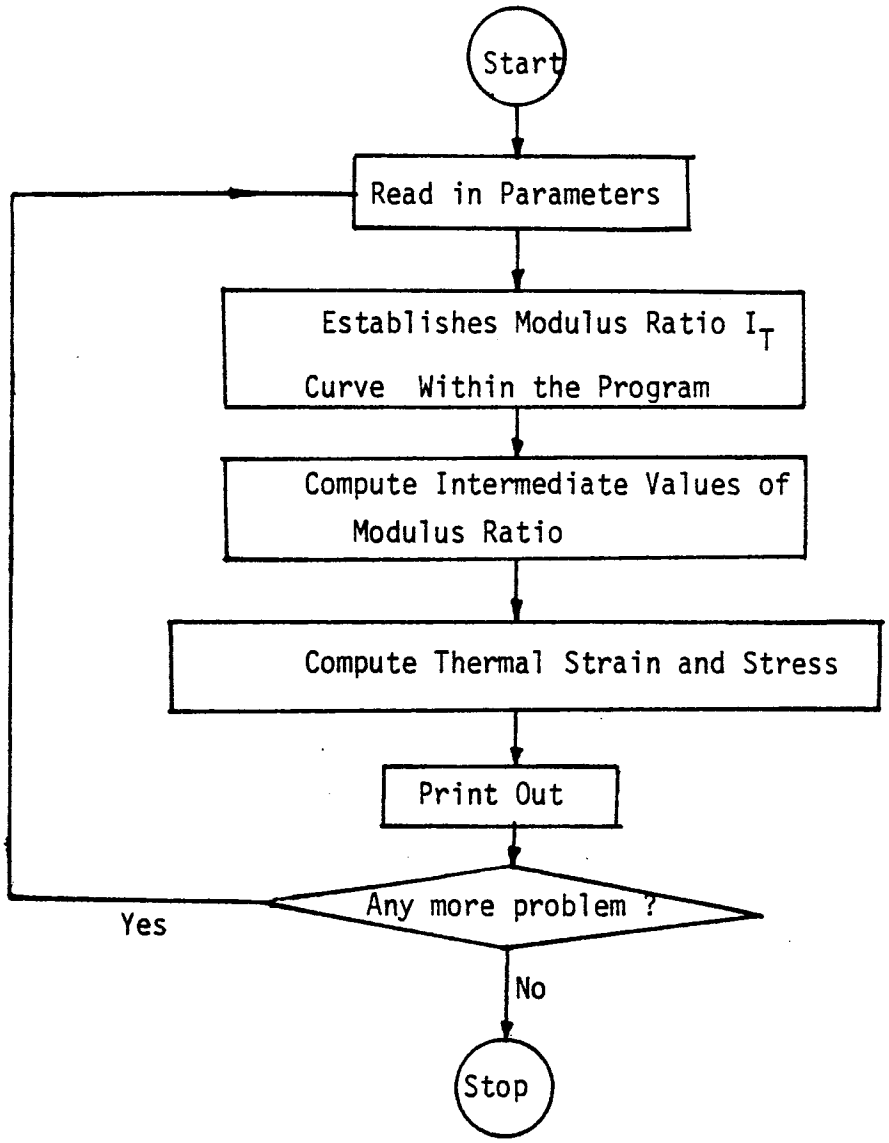

Fig. B-1. Flow Chart for Viscoelastic Thermal Stress Analysis Computer Program

cc 11-20 D1 Value of interception with log t=0.

cc 21-30 DF Initial value of creep curve.

Card 3 (8F10.0)

cc 1-10 CN Slope of creep compliance curve

cc 11-20 CM Slope of power law curve for shift factor (Figure 6 and Appendix A)

cc 21-30 ALPHA Thermal expansion coefficient, α

cc 31-40 TM Reference temperature of master curve

cc 41-50 TR Stress free state temperature

cc 51-60 TA Power law constant for shift factor (Figure 6)

cc 61-70 F1 Constants for WLF shift factor (Figure 5)

cc 71-80 F2 Constants for WLF shift factor (Figure 5)

Card 4 (15)

cc 1-5 NPR Number of problems

Card 5 (15, 5X, 4F10.0) A set of NPR cards

cc 1-5 IX 0= Plane stress

1= plane strain

cc 11-20 TMIN Minimum (for cooling) or maximum (for heating) temperature

cc 21-30 PERIOD Total thermal loading time (hours)

cc 31-40 STEP The intermediate time step (hours)

cc 41-50 UNU Poisson's ratio

```
C
C
C     VISCOPLASTIC THERMAL STRESS ANALYSIS FOR CONSTANT RATE COOLING OR
C     HEATING IN A RESTRAINED BEAM OR SLAB
C
C
      IMPLICIT REAL*8 (A-H,O-Z)
      DIMENSION TH(11),TC(11)
      COMMON/IN/CN,CM,ALPHA,TM,TR,TA,F1,F2,E1,EE
      DIMENSION HC(3)
      DATA HC/'COOLING ','HEATING ','ISOTHERM'/
      CALL DATAIN
      CALL CURVE(TH,TC)
      READ(5,1) NPR
    1 FORMAT(I5)
      DO 2 I=1,NPR
      READ(5,3) IX,TMIN,PERIOD,STEP,UNU
    3 FORMAT(I5,5X,4F10.0)
C     IX = 0  --PLANE STRESS
C     IX = 1  --PLANE STRAIN
      DELT = TMIN - TR
      HOUR = 0.D0
      WRITE(6,200)
  200 FORMAT('1',4X,'PROCESS',5X,'TEMP.',2X,'(AT)',2X,'NORMALIZED',4X,
     1  'MODULUS',5X,'SECANT',6X,'EFFECTIVE',4X,'STRAIN',6X,'STRESS',
     2  6X,'TIME',8X,              /,' ',22X,'LOG.',1X,'TEMP. CHANGE',
     3  4X,'RATIO',6X,'MODULUS',5X,'MODULUS')
 1000 CONTINUE
      HOUR = HOUR + STEP
      IF(HOUR.GT.PERIOD) HOUR = PERIOD
      RR = DELT/PERIOD
      DT = RR*HOUR
      TIME = HOUR*3600.
      TTN = TIME **(-CN)
      T = TR + DT
      AT1 = -F1*(T-TM)/(F2+T-TM)
      AT = 10.D0** AT1
      ATN = AT** CN
      DTN = DT/(TR-TA)
      DTR = DABS(DTN*10.)
      NN = IDINT(DTR)
      DIF = DTR - NN
      N = NN + 1
      IF (DELT)90,100,110
   90 RATIO = (TC(N+1)-TC(N))*DIF +TC(N)
      J = 1
      GO TO 120
  100 RATIO = 1.D0
      J = 3
      GO TO 120
  110 RATIO = (TH(N+1)-TH(N))*DIF + TH(N)
      J = 2
  120 CONTINUE
      ESS = ATN*E1*TTN/(1.D0 -CN)
      EEF = EE + RATIO*(ESS - EE)
      STRAIN = ALPHA * DT
      GI = DFLOAT(IX)/(1.- UNU)
      IF(IX.EQ.0) GI = 1.
      STRESS = GI * STRAIN * EEF
      WRITE(6,150) I,HC(J),T ,     AT1,DTN,RATIO,ESS,EEF,STRAIN,
     1  STRESS,HOUR
  150 FORMAT('0',I3,A8,3F8.2,2X,F12.2,2X,4G12.4,F8.2,2(1X,G11.4))
      IF(HOUR.LT.PERIOD) GO TO 1000
    2 CONTINUE
      WRITE(6,140)
  140 FORMAT('1')
      STOP
      END
```

```
C
      SUBROUTINE DATAIN
      IMPLICIT REAL*8 (A-H,O-Z)
      COMMON/IN/CN,CM,ALPHA,TM,TR,TA,F1,F2,E1,EE
      DIMENSION TITLE(10)
      READ(5,11)TITLE
      READ(5,12) INDEX,D1,DF
      DF = 10.D0**DF
      D1 = 10.D0** D1
      READ(5,13) CN,CM,ALPHA,TM,TR,TA,F1,F2
   11 FORMAT(10A8)
   12 FORMAT(I5,5X,2F10.0)
   13 FORMAT(8F10.0)
      WRITE(6,14) TITLE
   14 FORMAT('1',10X,'* * * ',10A8,' * * *')
      IF(INDEX.EQ.1) GO TO 17
      PI = 3.1415926
      PIN = PI * CN
      E1 = 1.00/D1 *(DSIN(PIN)/PIN)
      IF(DF.EQ.1.) GO TO 15
      EE = 1.00/DF
      GO TO 18
   15 EE = 0.D0
      GO TO 18
   17 E1 = D1
      EE = DF
   18 CONTINUE
      WRITE(6,41) TP
      WRITE(6,42) TR
      WRITE(6,43) ALPHA
      WRITE(6,19) E1,EE,CN,CM
   41 FORMAT('0',5X,'REFERENCE TEMP. FOR MASTER CURVE.',T48,G13.4)
   42 FORMAT('0',5X,'REFERENCE TEMP. FOR ZERO STRESS STATE.',T48,G13.4)
   43 FORMAT('0',5X,'COEFF. OF THERMAL EXPANSION .',T48,G13.4,//)
   19 FORMAT('0',5X,'* * * E1= ',G13.4,2X,'EE= ',G13.4,/,
     1  5X,'* * * CN=',G13.4,2X,'CM=',G13.4,/)
      WRITE(6,100)
  100 FORMAT('0',2X,'CURVE FOR EFFECTIVE MODULUS RATIO')
      RETURN
      END
```

```
C
C
C
      SUBROUTINE HEAT(A,B,H,INT,F,AREA,HS)
      IMPLICIT REAL*8(A-H,O-Z)
      DIMENSION F(INT)
      COMMON HH(11),ZZ
      COMMON/KK/ I
      DA = H**(A+1.)*(-1.+H)**(B+1.)/(B+1.)
      DB = -(A+B+2.)/(B+1.)
      DO 10 J=1,INT
      XX = HH(I) + HS*(J-1)
   10 F(J) = XX**A*(-1.+XX)**(B+1.)
      CALL INTGRT(INT,F,HS,AR)
      ZZ = ZZ + AR
      AREA = DA + ZZ*DB
      RETURN
      END

      SUBROUTINE COOL(A,B,H,AREA)
      IMPLICIT REAL *8(A-H,O-Z)
      REAL*4 SH,SA1,SB2,SP
      COMMON/GT/ GAB1
      A1 = A + 1.D0
      B1 = B + 1.D0
      P = 0.
      SH = SNGL(H)
      SA1 = SNGL(A1)
      SB2 = SNGL(B1)
      SP = SNGL(P)
      CALL MDBETA(SH,SA1,SB2,SP,IER)
      IF(IER.EQ.0) GO TO 10
      WRITE(6,20) IER,SP,SH,SA1,SB2
   20 FORMAT('-',50X,' * * ERROR IER',6X,'P',10X,'H',10X,'A',10X,'B',
     1  /,'0', 58X,I5,4G12.4)
   10 CONTINUE
      P = DBLE(SP)
      H = DBLE(SH)
      A1 = DBLE(SA1)
      B2 = DBLE(SB2)
      AREA = GAB1 * (1.DO - P)
      RETURN
      END
```

```
      SUBROUTINE  CURVE(TH,TC)
      IMPLICIT REAL*8 (A-H,O-Z)
      DIMENSION TH(11),TC(11)
      COMMON/IN/CN,CM,ALPHA,TM,TR,TA,F1,F2,E1,EE
      DIMENSION HC(2)
      DATA HC/'COOLING ','HEATING '/
      COMMON/GT/ GAB1
      DIMENSION F(50)
      COMMON HH(11),ZZ
      COMMON/KK/ I
  100 CONTINUE
      INT = 40
      A = CM/(CM+1.) + CN - 2.
      B = -CN
      DM = (1.-CN)/(CM + 1.)**(1.-CN)
      WRITE(6,12)
   12 FORMAT('-',13X,'DTN',10X,'CONS',10X,'AREA',10X,'RATIO')
      GA = DGAMMA(A+1.)
      GB1 = DGAMMA(B+1)
      GAB1 = GA*GB1/ DGAMMA(A+B+2.DO)
      TH(1) = 1.DO
      TC(1) = 1.DO
      TC(11) = 0.DO
      DO 40 INDEX =1,2
      WRITE(6,14)
   14 FORMAT(' ')
      HH(1) = 1.
      AREA = 0.
      ZZ = 0.
      DTN = 0.
      DO 10 I=1,10
      DTN = DTN + 0.1
      DTR = DABS(DTN)
      IF(INDEX.EQ.1) GO TO 21
C
C     * * * FOR HEATING PROCESS  * * *
C
      H = (DTN+1.)**(CM+1.)
      HH(I+1) = H
      HS = (HH(I+1)-HH(I))/(INT-1)
      CALL HEAT(A,B,H,INT,F,AREA,HS)
      CONS = DM*(1.+1./DTN)**(1.-CN)
      TII = CONS * AREA
      TH(I+1) = TII
      GO TO 25
C
C     * * * FOR COOLING PROCESS  * * *
C
   21 CONTINUE
      IF(I.EQ.10) GO TO 10
      RR = -DTR
      H = (1.+RR )**(CM+1.)
      HH(I+1) = H
      HS = (HH(I) - HH(I+1))/(INT-1)
      CALL COOL(A,B,H,AREA)
      CONS = DM*(-1.-1./RR )**(1.-CN)
      TII = CONS * AREA
      TC(I+1) = TII
   25 CONTINUE
      WRITE(6,30)HC(INDEX),DTN,CONS,AREA,TII
   30 FORMAT('0',2X,A8,4G12.4)
   10 CONTINUE
   40 CONTINUE
      RETURN
      END



      SUBROUTINE INTGRT(N,F,H,AREA)
      IMPLICIT REAL*8(A-H,O-Z)
      DIMENSION F(N)
      AREA = 0.
      S = 0.5* H
      DO 10 I=2,N
      AREA = AREA + S*(F(I-1)+ F(I))
   10 CONTINUE
      RETURN
      END
```

* * * VISCOELASTIC THERMAL STRESS ANALYSIS

REFERENCE TEMP. FOR MASTER CURVE. 40.00

REFERENCE TEMP. FOR ZERO STRESS STATE. 75.00

COEFF. OF THERMAL EXPANSION . -0.13500-04

* * * E1= 0.1599D 07 EE= 0.0
* * * CN= 0.5000 CM= 15.50

CURVE FOR EFFECTIVE MODULUS RATIO

	DTN	CONS	AREA	RATIO
COOLING	0.1000D 00	0.3693	2.349	0.8673
COOLING	0.2000	0.2462	2.987	0.7352
COOLING	0.3000	0.1888	3.268	0.6145
COOLING	0.4000	0.1508	3.384	0.5101
COOLING	0.5000	0.1231	3.425	0.4216
COOLING	0.6000	0.1005	3.437	0.3454
COOLING	0.7000	0.8058D-01	3.439	0.2771
COOLING	0.8000	0.6155D-01	3.440	0.2117
COOLING	0.9000	0.4103D-01	3.440	0.1411
HEATING	0.1000D 00	0.4082	2.762	1.127
HEATING	0.2000	0.3815	4.089	1.233
HEATING	0.3000	0.2562	5.162	1.323
HEATING	0.4000	0.2303	6.070	1.398
HEATING	0.5000	0.2132	6.854	1.461
HEATING	0.6000	0.2018	7.533	1.514
HEATING	0.7000	0.1918	8.122	1.558
HEATING	0.8000	0.1846	8.626	1.593
HEATING	0.9000	0.1788	9.036	1.616
HEATING	1.000	0.1741	9.334	1.625

PROESS	TEMP.	(AT) LOG.	NORMALIZED TEMP. CHANGE	MODULUS RATIO	SECANT MODULUS	EFFECTIVE MODULUS	STRAIN	STRESS	TIME
ICOOLING	68.67	-1.84	-0.04	0.94	0.1436D 05	0.1347D 05	0.8550D-04	1.151	0.20
ICOOLING	62.33	-1.46	-0.09	0.88	0.1573D 05	0.1390D 05	0.1710D-03	2.377	0.40
ICOOLING	56.00	-1.06	-0.13	0.83	0.2027D 05	0.1675D 05	0.2565D-03	4.296	0.60
ICOOLING	49.67	-0.65	-0.17	0.77	0.2813D 05	0.2162D 05	0.3422D-03	7.394	0.80
ICOOLING	43.33	-0.23	-0.22	0.71	0.4097D 05	0.2921D 05	0.4275D-03	12.49	1.00
ICOOLING	37.00	0.21	-0.26	0.66	0.6192D 05	0.4089D 05	0.5130D-03	21.97	1.20

APPENDIX C

Finite Element Computer Program with Crack Tip Element

This plane stress/strain finite element computer code is written in FORTRAN IV language with double precision on IBM 360/65. The elements used are 4-CST quadrilaterals and/or constant strain triangles with optional crack tip element. The code has sufficient storage for 300 nodes, 250 elements and 10 different materials. It requires the machine with a core storage of 430K and five additional temporary disk spaces. The maximum semi-bandwidth of the stiffness matrix is 64. It is possible to change the capacity by modifying the COMMON, DIMENSION and DATA statements.

The present code contains a number of checks of input data. When errors are located they are described and execution is stopped. However, the checks in the code do not cover all possibilities. One method of checking input is to compare with the original drawing.

Most of the computational steps are carried out in the various subroutines of the code. Following is a list of subroutines with an explanation of their functions:

DATAIN — Reads and echo prints all input data. Performs checks for data.

ASEMBL — Initializes and assembles overall stiffness matrix and load vector. Introduces geometric boundary condtitions.

QUAD — Computes stress-strain matrix, stiffness matrix, body force vector, and strain-displacement matrix of either a 4-CST quadrilateral element or a triangular element.

CST	Computes strain-displacement matrix, stiffness matrix, and body force vector of constant strain triangle (CST) element.
CRACK	Reads the input data and prints the stiffness matrix for tip element.
HYBRID	Computes the stiffness matrix, displacement-stress intensity factor vector for the tip element.
LOC	Computes vector subscript for a specific storage mode.
SIFAC	Computes and prints the stress intensity factor.
GEOMBC	Applies prescribed displacement boundary conditions at a single node.
BANSOL	Triangularizes the overall banded stiffness by symmetric Gauss-Doolittle decomposition or solves for displacement vector corresponding to a particular load vector.
STRESS	Computes the strains, stresses, and principal stresses. Prints the stresses and principal stresses at element centroids.

Temporary Disk Track Utilization

Unit 1 - Stores multipliers, pivots, condensed loads, strain, displacement, and stress-strain matrix (to be used to compute strain and stress).

Unit 2 - Stores crack tip element stiffness matrix, displacement-stress intensity factor vector and nodal data.

Unit 3 - Stores element stiffness matrix.

Unit 4 - Stores input node number, node identification and concentrated load or displacement.

Unit 8 - Stores surface traction information.

Guide for Input Data

Identification card (15, 3X, 9A8) One card per problem.

cc 1-5		Problem number
cc 9-80		Title of the problem

Basic parameters (6I5) One card per problem.

cc 1-5	NNP	Number of nodal points
cc 6-10	NEL	Number of elements (for 4-CST only)
cc 11-15	NMAT	Number of different materials
cc 16-20	NSLC	Number of surface tractions
cc 21-25	NOPT	Option for stress state, 1=plain strain, 2=plain stress
cc 26-30	NBODY	Option for body force, 0=no weight, 1=weight in the negative y direction
cc 31-35	NCKEL	Number of crack tip elements.

Material properties (4F10.0) NMAT cards per problem.

cc 1-10	E	Modulus of elasticity
cc 11-20	PR	Poisson's ratio
cc 21-30	RO	Density of material
cc 31-40	TH	Thickness of material

Nodal point data (2I5, 4F10.0) (See Note 3 below)

cc 1-5		Nodal point number
cc 6-10	KODE(I)	Index of displacement and concentrated load conditions at node I
cc 11-20	X	Horizontal coordinate of node I
cc 21-30	Y	Vertical coordinate of node I

cc 31-40 ULX Concentrated load or displacement in X and Y directions at node I

cc 41-50 ULY Concentrated load or displacement in X and Y directions at node I

Element Data (6I5) (See note 5 & 6 below)

cc 1-5 El. No. Element number

cc 6-10 I Index of the first node in quadrilateral

cc 11-15 J Index of the second node in quadrilateral

cc 16-20 K Index of the third node in quadrilateral

cc 21-25 L Index of the forth node in quadrilateral

cc 25-30 MTYP Material type number

Surface tractions (2I5, 4F10.0) (See note 7 below)

cc 1-5 N.P.I

cc 6-10 N.P.J

cc 11-20 SURTRX(I)

cc 21-30 SURTRX(J)

cc 31-40 SURTRY(I)

cc 41-50 SURTRY(J)

Crack tip element data NCKEL cards per problem (see note 8 and Figure C)

Card 1 (2I5, 2F10.0, I5)

cc 1-5 KEY Type of crack tip element, 1=five node case, 2=nine node case

cc 6-10 MATYP Type of material where crack tip is embedded

cc 11-20 XC Horizontal coordinate of crack tip

cc 21-30 YC Vertical coordinate of crack tip

cc 31-35 NCOT Special case of tip element. Only need for the five node case is when nodal data has to be counted clockwise, 1=yes, 0=no.

Card 2 (10I5) (See note 9)

Indices for 5 nodes 1 2 3 4 5 MAXDIF

(or Indices for 9 nodes 1 2 3 4 5 6 7 8 9 MAXDIF)

One blank card allows normal EXIT from computer.

Note on Input Data

1. Data cards must be in proper sequence.

2. Units must be consistent.

3. Usually one card is needed for each node. However, if some nodes fall on a straight line and are equidistant, data for only the first and the last points of this group are needed. Intermediate nodal point data are automatically generated by linear interpolation.

4. Forces and/or displacements prescribed at a node are identified by KODE as explained below:

KODE	Force/Displacement Boundary Condition
0	ULX = Prescribed Load in x direction
	VLY = Prescribed Load in y direction
1	ULX = Prescribed Disp in x direction
	VLY = Prescribed Load in y direction
2	ULX = Prescribed Load in x direction
	VLY = Prescribed Disp in y direction
3	ULX = Prescribed Disp in x direction
	VLY = Prescribed Disp in y direction

The sign of an applied force or displacement follows the sign of the coordinate directions. For instance, a force in the positive x direction is positive, and so on. For the nodes automatically generated as in Note 3, KODE=0, ULX=0 and VLY=0 are assigned for the generated nodes.

5. IE(M,1), IE(M,2), IE(M,3), IE(M,4) denote four corner nodes, I, J, K, L, of a quadrilateral element, M. The program also permits use of triangular elements, which are indicated by repeating the third node; that is, IE(M,3) = IE(M,4), or K=L. For a right-handed coordinate system the nodes must be input counter-clockwise around the element. IE(M,5) denotes the type of material in the element.

The maximum difference between numbers of any two nodes for a given element must be less than MAXBW/2.

6. Usually one card is needed for each element. However, if some elements are on a line in such a way that their corner node indices each increase by one compared to the previous element, only the data for the first element on the line need be input. However, note that data for the last element of the assemblage must be input. The omitted element data is generated internally by the computer. The same material type as the previously input element is assigned to all generated elements.

7. Surface tractions must be specified between two adjacent nodes only. The three possible cases are shown in Figure C-1. For case (a) only SURTRX(I) and (J) are input, and columns 31-50 are left blank. For case (b) only SURTRY (I) and (J) are input and columns

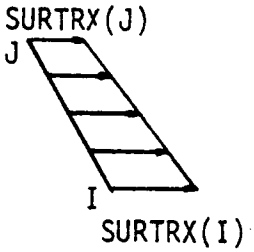

(a) Tractions in x direction

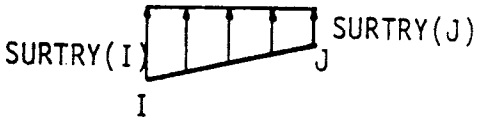

(b) Tractions in y direction

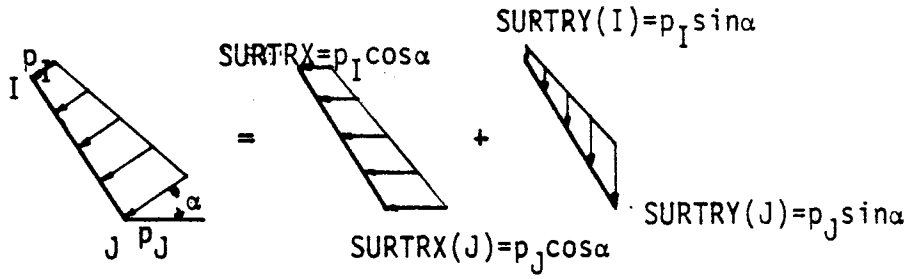

(c) Tractions in both x and y direction

Figure C-1. Three Possible Cases of Surface Tractions on Element Side I-J

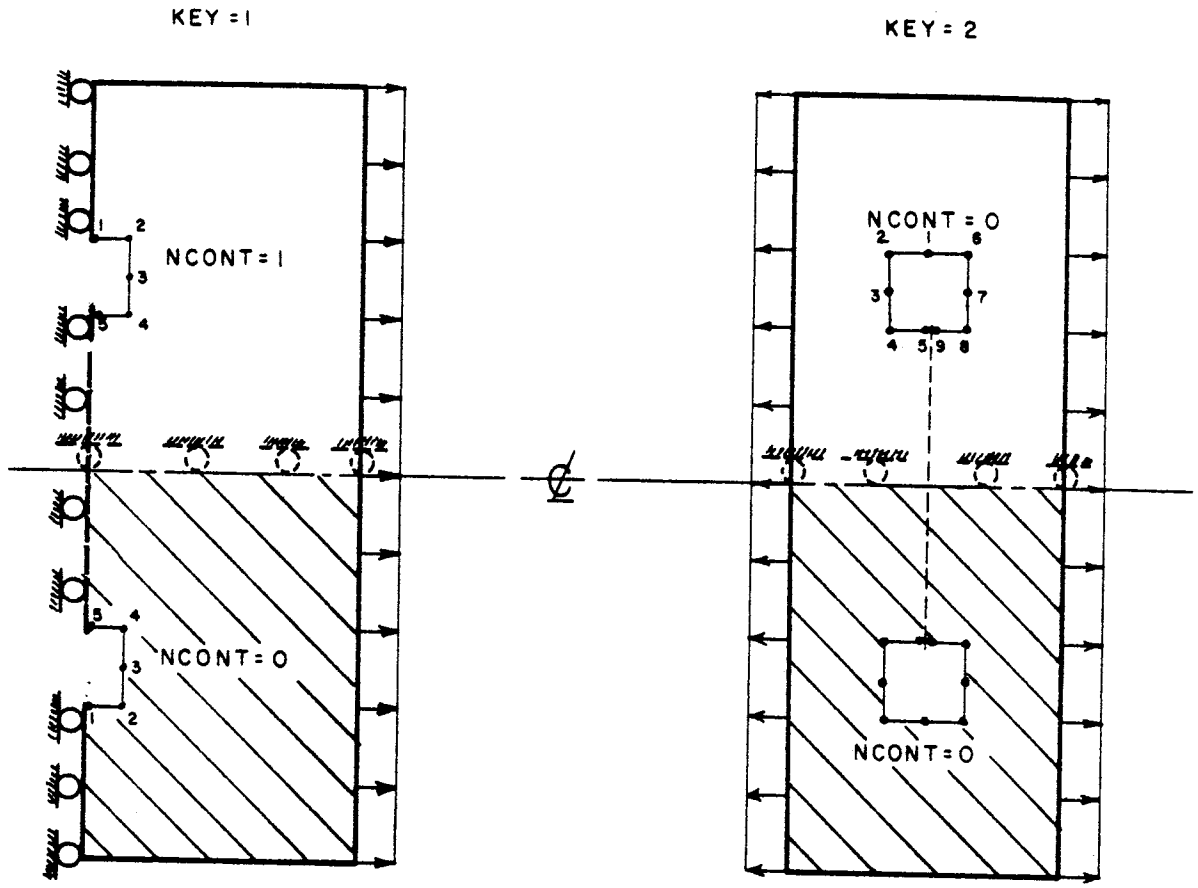

Figure C-2. Possible Cases for Crack Element Nodal Data

11-30 are left blank. For both tractions all columns from 1 to 50 are input. Moreover, the user must multiply all surface intensities by the thickness of the element before the intensities are input in the computer.

The signs of tractions follow the directions of coordinate axes. A traction in the negative y direction is negative, and so on.

8. Two cards are in sequence for each crack element. More than one crack element can be generated. Tip element nodal data are usually counted counterclockwise. Possible cases for the nodal data are shown in Figure C-2.

9. MAXDIF alway follows the last one of node numbers.

10. Omit tip element data if NCKEL=0.

11. One blank card at end of each run allows normal exit from computer.

Additional Note

JCL to execute the Finite Element Computer Program "FINITE" stored in TAMU DPC disk.

```
1  JOB card
2  /*PASSWORD
3  /*CLASS        G
4  //GO EXEC PGM=FINITE, REGION=430K
5  //GO.STEPLIB DD DISP=SHR,DSN=USER.CE.CHANG.JOBLIB
6  //GO.FT01F001 DD UNIT=SYSDA,DISP=(NEW,DELETE),SPACE=(CYL,(1,1))
7  //GO.FT02F001  DD UNIT=SYSDA,DISP=(NEW,DELETE),SPACE=(CYL,(1,1))
8  //GO.FT03F001  DD UNIT=SYSDA,DISP=(NEW,DELETE),SPACE=(CYL,(1,1))
```

```
 9  //GO.FT04F001  DD UNIT=SYSDA,DISP=(NEW,DELETE),SPACE=(CYL,(1,1))
10  //GO.FT08F001  DD UNIT=SYSDA,DISP=(NEW, DELETE),SPACE=(CYL,(1,1))
11  //GO.FT07F001  DD SYSOUT=B
12  //GO.FT06F001  DD SYSOUT=A
13  //GO.FT05F001  DD *

   -- data cards ---
14  /*END
```

```
      IMPLICIT REAL*8 (A-H,O-Z)
      DIMENSION TITLE(9)
      COMMON E(10),PR(10),RO(10),TH(10),X(300),Y(300)
      COMMON/CONS/ NNP,NEL,NMAT,NSLC,NOPT,NBODY,MTYP,NCKEL
      COMMON/ONE/ QK(10,10),Q(10),B(3,10),C(3,3),BT(3,6),XQ(5),YQ(5)
      COMMON/TWO/ IBAND,NEQ,R(600),AK(600,64)
      COMMON/T1/ IE(250,5)
      DATA MAXEL, MAXNP, MAXMAT, MAXBW
     1  /  250,  300,  10,   64 /
C
C PROBLEM  IDENTIFICATION  AND  DESCRIPTION
C
 9999 READ(5,100)NPROB,(TITLE(I),I=1,9)
      IF(NPROB.LE.0) GO TO 999
 1020 WRITE(6,200) NPROB,(TITLE(I),I=1,9)
      CALL DATAIN (MAXEL,MAXNP,MAXMAT,MAXSLC,ISTOP)
      MAXDOF = 2*MAXNP
C
C COMPUTE  MAX, NODAL DIFFERENCE AND SEMI-BANDWIDTH, EQ. (6-1)
      MAXDIF = 0
      DO 1 I=1,NEL
      DO 1 J=1,4
      DO 1 K=1,4
      LL= IABS(IE(I,J)- IE(I,K))
      IF(LL.GT.MAXDIF) MAXDIF = LL
    1 CONTINUE
      IBAND = 2*(MAXDIF + 1)
      NEQ = 2*NNP
      IF(IBAND.GT.MAXBW) GO TO 900
      IF(ISTOP.GT.0) GO TO 999
      CALL ASEMBL(ISTOP)
      IF(ISTOP.GT.0) GO TO 999
C
C  TRIANGULARIZE STIFFNESS MATRIX, EQ, (2-2), KKK=1
C
C  SOLVE FOR DISPLACEMENTS CORRESP, TO LOAD VECTOR R, EQ,(2-3), KKK=2
      CALL BANSOL(AK,R,NEQ,IBAND,MAXDOF,MAXBW)
      WRITE(6,300)(I,R(2*I-1),R(2*I),I=1,NNP)
C
      CALL STRESS(WORK)
C
      WRITE(6,605)
  605 FORMAT('1')
      TOTAL = 0.
      SUM = 0.
      IF(NCKEL.EQ.0) GO TO 645
      REWIND 2
      WRITE(6,37) NCKEL
   37 FORMAT('0',5X,'NCKEL =',I3)
      DO 36 I=1,NCKEL
      CALL SIFAC(I, TOTAL)
      SUM = SUM + TOTAL
   36 CONTINUE
  645 CONTINUE
      ENERGY = SUM + WORK
      WRITE(6,400) ENERGY
  400 FORMAT('-',5X,'. . . TOTAL STRAIN ENERGY = ',G20.8,' . . . ')
          GO TO 9999
  900 WRITE(6,901) IBAND,MAXBW
      GO TO 9999
  100 FORMAT(I5,3X,9A8)
  200 FORMAT(/8H1PROBLEM,I5,3H.. ,9A8/)
  300 FORMAT(37H1OUTPUT TABLE 1.. NODAL DISPLACEMENTS //
     1        13X,4HNODE, 9X, 11HL = X-DISP.,9X,11HV = Y-DISP./
     2       (5X,I12,2E20.8))
  901 FORMAT(///12H BANDWIDTH =,I4,25H EXCEEDS MAX, ALLOWABLE =,I4//
     1 30H GO ON TO NEXT PROBLEM         )
  999 STOP
      END
```

```
      SUBROUTINE DATAIN(MAXEL,MAXNP,MAXMAT,MAXSLC,ISTOP)
      IMPLICIT REAL*8 (A-H,O-Z)
      COMMON/CONS/ NNP,NEL,NMAT,NSLC,NOPT,NBODY,MTYP,NCKEL
      COMMON E(10),PR(10),RO(10),TH(10),X(300),Y(300)
      COMMON/T1/ IE(250,5)
      ISTOP = 0
      REWIND 4
      REWIND 8
      READ(5,1)  NNP,NEL,NMAT,NSLC,NOPT,NBODY,NCKEL
C
      WRITE(6,100) NNP,NEL,NMAT,NSLC,NOPT,NBODY
      WRITE(6,200) NCKEL
C
C CHECKS TO BE SURE INPUT DATA DOES NOT EXCEED STORAGE CAPACITY
           IF(NNP.LE.MAXNP) GO TO 201
                ISTOP = ISTOP + 1
      WRITE(6,251) MAXNP
  201      IF(NEL.LE.MAXEL) GO TO 202
                ISTOP = ISTOP + 1
      WRITE(6,252) MAXEL
  202      IF(NMAT.LE.MAXMAT) GO TO 204
                ISTOP = ISTOP + 1
      WRITE(6,253) MAXMAT
  204      IF(ISTOP.EQ.0) GO TO 205
      WRITE(6,255) ISTOP
      STOP
C
  205 READ(5,2)(E(I),PR(I),RO(I),TH(I),I=1,NMAT)
      WRITE(6,101)
C
C  READ AND PRINT NODAL DATA (REF. 1)
      WRITE(6,51)(I,E(I),PR(I),RO(I), TH(I),  I=1,NMAT)
      WRITE(6,103)
                N=1
    5 READ(5,3) M,KODE    ,X(M),Y(M),ULX    ,VLY
      UULX = ULX
      VVLY = VLY
      KKODE = KODE
           IF(M-N) 4,442,7
    4 WRITE(6,105) M
      WRITE(6,52) M,KODE    , X(M),Y(M),ULX    ,VLY
                ISTOP= ISTOP +1
           GO TO 5
    7           DF = M + 1 - N
                RX=(X(M)-X(N-1))/DF
                RY=(Y(M)-Y(N-1))/DF
    8 KODE = 0
                X(N)=X(N-1)+RX
                Y(N)=Y(N-1)+RY
                ULX = 0.
                VLY = 0.
           GO TO 6
  442 ULX = UULX
      VLY = VVLY
      KODE = KKODE
    6 WRITE(6,52) N,KODE    ,X(N),Y(N),ULX    ,VLY
      WRITE(4) N,KODE,ULX,VLY
                N=N+1
           IF(M-N) 9,442,8
    9      IF(N.LE.NNP) GO TO 5
C
C  READ AND PRINT ELEMENT PROPERTIES, TABLE 6-4
      WRITE(6,106)
   13           L=0
   14 READ(5,15) M,(IE(M,I),I=1,5)
   16           L=L+1
           IF(M-L)117,17,18
  117 WRITE(6,118) M
      WRITE(6,53) M,(IE(M,I), I=1,5)
                ISTOP=ISTOP+1
           GO TO 14
   18           IE(L,1)= IE(L-1,1)+1
                IE(L,2)= IE(L-1,2)+1
                IE(L,3)=IE(L-1,3)+1
                IE(L,4)=IE(L-1,4)+1
                IE(L,5)=IE(L-1,5)
   17 WRITE(6,53) L,(IE(L,I),I=1,5)
           IF(M-L)20,20,16
   20      IF(NEL-L)21,21,14
   21      CONTINUE
C
C READ AND PRINT SURFACE LOADING(TRACTION) CARDS
           IF(NSLC.EQ.0) GO TO 31
   30 WRITE(6,108)
           DO  40 L=1,NSLC
      READ(5,41) ISC,JSC,SURX1,SURX2,SURY1,SURY2
      WRITE(8) ISC,JSC,SURX1,SURX2,SURY1,SURY2
   40 WRITE(6,42)ISC,JSC,SURX1,SURX2,SURY1,SURY2
   31      IF(ISTOP.EQ.0) GO TO 999
      WRITE(6,900) ISTOP
C
    1  FORMAT(7I5)
  100 FORMAT(35HOINPUT TABLE 1.. BASIC PARAMETERS   ///
     1        5X, 40H NUMBER OF NODAL POINTS. . . . . .,I5//
     2        5X, 40H NUMBER OF ELEMENTS. . . . . .,I5//
     3        5X, 40H NUMBER OF DIFFERENT MATERIALS . . . . .,I5//
```

```
     4       5X, 40H NUMBER OF SURFACE LOAD CARDS. . . . . .,I5//
     5       5X, 40H 1 = PLANE STRAIN, 2 = PLANE STRESS. . ..I5//
     6       5X, 40H BODY FORCES(1 = IN -Y DIREC., 0 = NONE),I5,/)
200 FORMAT('0',6X,'NUMBER OF CRACK ELEMENTS . . . . . .' ,I5)
251 FORMAT(////33H TOO MANY NODAL POINTS, MAXIMUM =, I5)
252 FORMAT(////30H TOO MANY ELEMENTS, MAXIMUM = ,I5)
253 FORMAT(////30H TOO MANY MATERIALS, MAXIMUM =,I5)
255 FORMAT(////28H EXECUTION HALTED BECAUSE OF,I5,13H FATAL ERRORS/)
  2  FORMAT(4F10.0)
101 FORMAT(36H0INPUT TABLE 2.. MATERIAL PROPERTIES //
     1       10H  MATERIAL,5X,10HMODULUS OF,6X,9HPOISSON'S,7X,
     28HMATERIAL,7X,  8HMATERIAL /
     34X,6HNUMBER,5X,10HELASTICITY,8X,7H  RATIO,8X,7HDENSITY,6X,
     49HTHICKNESS )
  51 FORMAT(I10,4E15.4)
103 FORMAT(34H1INPUT TABLE 3.. NODAL POINT DATA ///
     1       5X,5HNODAL,48X,7HX-DISP.,8X,7HY-DISP./
     25X,5HPOINT,6X,4HTYPE,14X,1HX,14X,1HY,8X,7HOR LOAC,8X,7HOR LOAD)
  3  FORMAT(2I5,4F10.0)
105 FORMAT(5X,17HERROR IN CARD NO.,I5/)
  52 FORMAT(2I10,4E15.4)
106 FORMAT(34H1INPUT TABLE 4.. ELEMENT DATA     //
     1       11X,31HGLOBAL INDICES OF ELEMENT NODES/3X,7HELEMENT,
     27X,1H1,7X,1H2,7X,1H3,7X,1H4,2X,8HMATERIAL)
118 FORMAT(5X, 25HERROR IN ELEMENT CARD NO.,I5/)
  15 FORMAT(6I5)
  53 FORMAT(I10,4I8,I10)
108 FORMAT(37H1INPUT TABLE 5.. SURFACE LOADING DATA  //
     117X, 33HSURFACE LOAD INTENSITIES AT NODES/
     24X,6HNODE I,4X,6HNODE J,10X,2HXI,10X,2HXJ,10X,2HYI,10X,2HYJ)
  41 FORMAT(2I5,4E10.3)
  42 FORMAT(2I10,4E12.4)
900 FORMAT(///45H ASSEMBLY AND SOLUTION WILL NOT BE PERFORMED.,I5,
     121H  FATAL CARD ERRORS     )
999 RETURN
    END
```

```
      SUBROUTINE  ASEMBL(ISTOP)
      IMPLICIT REAL*8 (A-H,O-Z)
      COMMON/CONS/ NAP,NEL,NMAT,NSLC,NOPT,NBODY,MTYP,NCKEL
      COMMON E(10),PR(10),RC(10),TH(10),X(300),Y(300)
      COMMON/ONE/ QK(10,10),Q(10),B(3,10),C(3,3),BT(3,6),XQ(5),YQ(5)
      COMMON/TL/ IE(250,5)
      COMMON/TWO/ IBAND,NEQ,R(600),AK(600,64)
      DIMENSION LP(8)
C
      REWIND 1
      REWIND 2
      REWIND 3
      REWIND 4
      REWIND 8
C  INITIALIZE
                ISTOP = 0
C  INITIALIZE PARTS OF MATRICES C AND BT
                BT(1,4) = 0.0
                BT(1,5) = 0.0
                BT(1,6) = 0.0
                BT(2,1) = 0.0
                BT(2,2) = 0.0
                BT(2,3) = 0.0
                C(1,3) = 0.0
                C(2,3) = 0.0
                C(3,1) = 0.0
                C(3,2) = 0.0
C
C INITIALIZE OVERALL STIFFNESS MATRIX AK AND OVERALL LOAD VECTOR R
          DO  2 I=1,NEQ
              R(I)=0.0
          DO  2 J =1,IBAND
    2         AK(I,J)=0.0
C
C COMPUTE  ELEMENT  STIFFNESSES AND LOADS ONE BY ONE
C
          DO 10 M=1,NEL
          IF(IE(M,5).GT.0) GO TO 11
              ISTOP = ISTOP + 1
          GO TO 10
   11     CALL QUAD(M,AREA)
          IF(AREA.GT.0.0) GO TO 16
              ISTOP = ISTOP + 1
      WRITE(6,20) M
C
C  STORE ELEMENT STIFFNESS MATRIX TO COMPUTE STORED ENERGY
   16 IF(IE(M,3).EQ.IE(M,4)) GO TO 201
      LIM = 10
```

```
      GO TO 205
  201 LIM = 6
  205 WRITE(3) LIM,((QK(I,J),J=1,LIM),I=1,LIM)
C
C  CONDENSE ELEMENT STIFF, FROM 10X10 TO 8X8, EQ.(5-64), AND ELEMENT
C  LOADS FROM 10X1 TO 8X1, EQ.(5-64D).    (REF.2)
      IF(IE(M,3).EQ.IE(M,4)) GO TO 26
           DO 31 J = 1,2
                IJ= 10-J
                IK= IJ+1
                PIVOT = QK(IK,IK)
           DO 32 K= 1,IJ
                F = QK(IK,K)/PIVOT
                QK(IK,K)=F
           DO 33 I=K,IJ
                QK(I,K)=CK(I,K)- F*QK(I,IK)
   33           QK(K,I) = QK(I,K)
   32           Q(K) =Q(K)-QK(IK,K)*Q(IK)
   31           Q(IK) =Q(IK)/PIVOT
C
C STORE MULTIPLIERS,PIVOTS,CONDENSED LOADS, STRAIN-DISP, AND STRESS-STRAI
C MATRICES ON SCRATCH TAPE NO. 1 (TO BE USED LATER TO COMPUTE STRAINS AND
C STRESSES )
   26 WRITE (1) ((QK(I,J),J=1,10),I=9,10), Q(9), Q(10),
     1((B(I,J),J=1,10),I=1,3),((C(I,J),J=1,3),I=1,3),XQ(5),YQ(5)
C
C  ASSEMBLE STIFF.  AND  LOADS , DIRECT STIFF, METHOD, SEC, 6-5.
C
                LIM=8
           IF(IE(M,3).EQ.IE(M,4)) LIM = 6
           DO 40 I=2,LIM,2
                IJ = I/2
                LP(I-1) = 2*IE(M,IJ) - 1
   40           LP(I) = 2*IE(M,IJ)
           DO 50 LL=1,LIM
                I = LP(LL)
                R(I) = R(I) + Q(LL)
           DO 50 MM=1,LIM
                J = LP(MM) - I + 1
           IF(J.LE.0) GO TO  50
                AK(I,J)= AK(I,J)+ QK(LL,MM)
   50      CONTINUE
   10      CONTINUE
      IF(NCKEL.EQ.0) GO TO 35
      DO 14 I=1,NCKEL
   14 CALL CRACK
   35 CONTINUE
C
C ADD EXTERNALLY APPL, CONC, NODAL LOADS TO R
           DO 55 N=1,NNP
      READ(4) M,KODE,ULX,VLY
           IF(KODE    .EQ.3) GO TO 55
                K=2*N
           IF( KODE    .EQ.1) GO TO 57
                R(K-1) = R(K-1) + ULX
           IF(KODE    .NE.0) GO TO 55
   57           R(K) = R(K) + VLY
   55      CONTINUE
C
C  CONVERT LINEARLY VARYING SURFACE TRACTIONS TO STATIC EQUIVALENTS,
C  AND ADD TO OVERALL LOAD VECTOR  R, EQ.(5-61A).
           IF(NSLC.EQ.0) GO TO 60
           DO 61 L = 1,NSLC
      READ(8) ISC,JSC,SURX1,SURX2,SURY1,SURY2
                I = ISC
                J = JSC
                II=2*I
                JJ=2*J
                DX = X(J) - X(I)
                DY = Y(J) - Y(I)
                EL = DSQRT(DX*DX+DY*DY)
                PXI = SURX1 * EL
                PXJ = SURX2 * EL
                PYI = SURY1 * EL
                PYJ = SURY2 * EL
                R(II-1)=R(II-1)+PXI/3.0 + PXJ/6.0
                R(JJ-1)=R(JJ-1)+ PXI/6.0 + PXJ/3.0
                R(II)=R(II)+ PYI/3.0 + PYJ/6.0
                R(JJ)= R(JJ) + PYI/6.0 + PYJ/3.0
   61      CONTINUE
C
C INTRODUCE KINEMATIC CONSTRAINTS (GEOMETRIC BOUNDARY CONDITIONS),
C  EQ.(6-18),          REF, 1.
C
   60 CONTINUE
      REWIND  4
      DO 70 M=1,NNP
      READ(4) N,KODE,ULX,VLY
           IF(KODE    .GE.0.AND.KODE    .LE.3) GO TO 72
                ISTOP = ISTOP + 1
           GO TO 70
   72      IF(KODE    .EQ.0) GO TO 70
           IF(KODE    .EQ.2) GO TO 71
           CALL GEOMBC(ULX    ,2*M-1)
           IF(KODE    .EQ.1) GO TO 70
   71      CALL GEOMBC(VLY    ,2*M)
```

```
   70     CONTINUE
          ENDFILE 1
          ENDFILE 2
          ENDFILE 3
          ENDFILE 4
          ENDFILE 8
              IF(ISTOP.EQ.0) GO TO 81
          WRITE(6,100) ISTOP
   20 FORMAT(/5X,17H AREA OF ELEMENT ,I5,14H  IS NEGATIVE /)
  100 FORMAT(////42H SOLUTION WILL NOT BE PERFORMED BECAUSE OF  ,I5,
         1 15H   DATA ERRORS     /)
   81 RETURN
          END

          SUBROUTINE   QUAD(M,TOTALA)
          IMPLICIT REAL*8 (A-H,O-Z)
          COMMON/CONS/ NNP,NEL,NMAT,NSLC,NOPT,NBODY,MTYP,NCKEL
          COMMON E(10),PR(10),RO(10),TH(10),X(300),Y(300)
          COMMON/ONE/ QK(10,10),Q(10),B(3,10),C(3,3),BT(3,6),XQ(5),YQ(5)
          COMMON/T1/ IE(250,5)
          COMMON/TWO/ IBAND,NEQ,R(600),AK(600,64)
C
                    I= IE(M,1)
                    J= IE(M,2)
                    K= IE(M,3)
                    L= IE(M,4)
                    MTYP = IE(M,5)
                    TOTALA = 0.0
C
C   CONSTRUCT STRESS-STRAIN MATRIX C,EQ.(3-16C).  FOR PLANE STRAIN
C   NOPT=1, AND FOR PLANE STRESS  NOPT=2,  PRESENT  CODE  IS FOR
C   ISOTROPIC MATERIALS
              IF(NMAT.EQ.1.AND.M.GT.1) GO TO 5
              IF(NOPT.EQ.2) GO TO 2
                   CF = E(MTYP)/((1.0+PR(MTYP))*(1.0-2.0*PR(MTYP)))
                   C(1,1)=  CF*(1.0-PR(MTYP))
                   C(1,2)=  CF* PR(MTYP)
                   C(2,1)= C(1,2)
                   C(2,2)= C(1,1)
                   C(3,3)= CF*(1.0-2.0*PR(MTYP))/2.0
              GO TO 5
    2             CF = E(MTYP)/(1.0-PR(MTYP)*PR(MTYP))
                  C(1,1)= CF
                  C(1,2)= PR(MTYP)*CF
                  C(2,1)= C(1,2)
                  C(2,2)= CF
                  C(3,3) = CF*(1.0-PR(MTYP))/2.0
    5             LIM = 4
              IF(K.EQ.L) LIM = 3
                   XQ(5) = 0.0
                   YQ(5) = 0.0
              DO 10 N=1,LIM
                   NN = IE(M,N)
                   XQ(N) = X(NN)
                   YQ(N) = Y(NN)
                   XQ(5) = XQ(5) + X(NN)/FLOAT(LIM)
   10              YQ(5) = YQ(5) + Y(NN)/FLOAT(LIM)
C
C  INITIALIZE QUAD. STIFFNESS, LOAD VECTOR AND STRAIN-DISPLACEMENT VECTOR
              DO 13 II =1,10
                   Q(II)=0.0
              DO 12 JJ = 1,10
   12              QK(II,JJ)=0.0
              DO 13 JJ=1,3
   13              B(JJ,II) = 0.0
              IF(K.NE.L) GO TO 15
          CALL CST(1,2,3,TOTALA)
              GO TO 999
   15     CALL CST(1,2,5,AREA)
                   TOTALA = TOTALA + AREA
          CALL CST(2,3,5,AREA)
                   TOTALA = TOTALA + AREA
          CALL CST(3,4,5,AREA)
                   TOTALA = TOTALA + AREA
          CALL CST(4,1,5,AREA)
                   TOTALA = TOTALA + AREA
  999 RETURN
          END
```

```
      SUBROUTINE   CST(I,J,K,AREA)
      IMPLICIT REAL*8 (A-H,O-Z)
      COMMON/CONS/ ANP,AEL,NMAT,NSLC,NOPT,NBODY,MTYP,NCKEL
      COMMON E(10),PR(10),RO(10),TH(10),X(300),Y(300)
      COMMON/ONE/ QK(10,10),Q(10),B(3,10),C(3,3),BT(3,6),XQ(5),YQ(5)
      COMMON/TWO/ IBAND,NEQ,R(600),AK(600,64)
      DIMENSION CB(3,6),LC(6),LT(3),TK(6,6)
C
               LT(1)= I
               LT(2)= J
               LT(3)= K
C
C     COMPUTE  STRAIN-DISPLACEMENT MATRIX B FOR TRIANGLE, EQ, (5-35A)
               BT(1,1)= YQ(J)-YQ(K)
               BT(1,2)= YQ(K)-YQ(I)
               BT(1,3) = YQ(I)-YQ(J)
               BT(2,4)=XQ(K)-XQ(J)
               BT(2,5) = XQ (I)-XQ(K)
               BT(2,6) = XQ(J) -XQ(I)
               BT(3,1)=BT(2,4)
               BT(3,2) = BT(2,5)
               BT(3,3) = BT(2,6)
               BT(3,4) = BT(1,1)
               BT(3,5)= BT(1,2)
               BT(3,6)= BT(1,3)
               AREA =(BT(2,4)*BT(1,3) - BT(2,6)*BT(1,1))/2.0
C
C  COMPUTE   C*B
          DO 10 II=1,3
          DO 10JJ = 1,6
               CB(II,JJ) = 0.0
          DO 10 KK = 1,3
   10          CB(II,JJ) = CB(II,JJ) + C (II,KK)*BT(KK,JJ)
C
C  COMPUTE (B**T)*C*B, EC,(5-45A)
          DO 12 II = 1,6
          DO 12 JJ = 1,6
               TK(II,JJ)=0.0
          DO 12 KK=1,3
   12          TK(II,JJ)=   TK(II,JJ)+BT(KK,II)*CB(KK,JJ)
C
C  ADD TRIANGLE STIFNESS TO QUADRILATERAL STIFFNESS, EX,(6-2),
C  ADD TRIANGLE STRAIN-DISPLACEMENT MATRIX TO QUADRILATERAL  STRAIN-
C  DISPLACEMENT MATRIX
          DO 15 II=1,3
               LC(II) = 2*LT(II) - 1
   15          LC(II+3) = 2*LT(II)
          DO 30 II=1,6
               LL = LC(II)
               FK = 1.0/(4.0*AREA)
               FB = 2.0*FK
          DO 20 JJ=1,6
               MM = LC(JJ)
   20          QK(LL,MM) = QK(LL,MM) + TK(II,JJ)*TH(MTYP)*FK
          DO 30 JJ = 1,3
   30          B(JJ,LL) = B(JJ,LL) + BT(JJ,II)*FB
C
C  DEVELOP  BODY  FORCE  VECTOR,  EQ,(5-61B)
          IF(NBODY.EQ.0) GO TO 999
               TBODYF =  AREA* RO(MTYP)*  TH(MTYP)
               BODYF  =  -TBODYF/3.0
          DO 35 II=1,3
               JJ= 2* LT(II)
   35          Q(JJ)= Q(JJ)+ BODYF
  999 RETURN
      END
```

```
      SUBROUTINE CRACK
      IMPLICIT REAL*8 (A-H,O-Z)
      COMMON/CONS/ ANP,AEL,NMAT,NSLC,NOPT,NBODY,MTYP,NCKEL
      COMMON E(10),PR(10),RO(10),TH(10),X(300),Y(300)
      COMMON/TWO/ IBAND,NEQ,R(600),AK(600,64)
      COMMON/T3/BCR(2,18),EK(171),XXY(19),KCRK(9),LP(18)
      READ(5,12) KEY,MATYP,XC,YC,NCONT
   12 FORMAT(2I5,2F10.0,I5)
      IF(KEY.EQ.1) GO TO 10
      NODE = 9
      NOE = 18
      GO TO 20
   10 NODE = 5
      NOE = 10
   20 READ(5,2) (KCRK(I),I=1,NODE),MAXDIF
    2  FORMAT(10I5)
      K = 2 * (MAXDIF+1)
      IF(K.LE.IBAND) GO TO 91
      L = IBAND + 1
      DO 100 I=1,NEQ
      DO 100 J=L,K
  100 AK(I,J) = 0.
      IBAND = MAXO(IBAND,K)
   91 CONTINUE
      DO 30 I=1,NODE
      XXY(2*I-1) = X(KCRK(I))
   30 XXY(2*I) = Y(KCRK(I))
        DO 31 I=1,NOE
   31 WRITE(6,32) I,XXY(I)
   32 FORMAT('0',5X,'XXY(',I3,')=',G20.6)
      SMU = E(MATYP)/(2.*(1.+PR(MATYP)) )
      IF(NOPT.EQ.1) GO TO 40
      ETA = (3. - PR(MATYP))/(1.+PR(MATYP))
      GO TO 50
   40 ETA = 3. - 4.*PR(MATYP)
   50 CONTINUE
      WRITE(6,35) SMU,ETA
   35 FORMAT('0',5X,'SMU ETA =',2G20.6)
      CALL HYBRID(KEY,SMU,ETA,XC,YC,NCONT)
      DO 60 I=1,NODE
      LP(2*I - 1) = 2*KCRK(I) - 1
   60 LP(2*I) = 2*KCRK(I)
      DO 36 I=1,NCE
   36 WRITE(6,33) I,LP(I)
   33 FORMAT('0',5X,'LP (',I3,')=',I5)
      DO 70 LL=1,NOE
      I = LP(LL)
      DO 70 MM = 1,NOE
      J = LP(MM) - I + 1
      IF(J.LE.0) GO TO 70
      CALL LOC(LL,MM,IJ,NOE,NOE,1)
      AK(I,J) = AK(I,J) + EK(IJ)
      WRITE(6,84) IJ,EK(IJ),I,J,AK(I,J)
   84 FORMAT('0',5X,'EK(',I4,')=',G20.6,'AK(',I3,',',I3,')=',G20.6)
   70 CONTINUE
      WRITE(6,34) NODE,NOE,MATYP,XC,YC
   34 FORMAT('0',5X,'NODE NOE MATYP XC,YC =',3I4,2G15.5)
      KK= (NCE+1)*NCE/2
      WRITE(2) KK,NODE,NOE,KEY,(LP(I),I=1,NOE),(EK(I),I=1,KK),
     1  ((BCR(I,J),I=1,KEY),J=1,NOE),XC,YC,MATYP,(KCRK(I),I=1,NODE)
      RETURN
      END


      SUBROUTINE LOC(I,J,IR,N,M,MS)
C           COMPUTE A VECTOR SUBSCRIPT FOR AN ELEMENT IN A MATRIX OF
C           SPECIFIED STORAGE MODE
C           I    - ROW NUMBER OF ELEMENT
C           J    - COLUMN NUMBER  OF ELEMENT
C           IR   - RESULTANT VECTOR SUBSCRIPT
C           N    - NUMBER OF ROWS IN MATRIX
C           M    - NUMBER OF COLUMNS IN MATRIX
C           MS   - ONE DIGIT NUMBER FOR STORAGE MODE OF MATRIX
C                    0 - GENERAL
C                    1 - SYMMETRIC
C                    2 - DIAGONAL
C
      IX=I
      JX=J
      IF(MS-1) 10,20,30
   10 IRX=N*(JX-1)+IX
      GO TO 36
   20 IF(IX-JX) 22,24,24
   22 IRX=IX+(JX*JX-JX)/2
      GO TO 36
   24 IRX=JX+(IX*IX-IX)/2
      GO TO 36
   30 IRX=0
      IF(IX-JX) 36,32,36
   32 IRX=IX
   36 IR=IRX
      RETURN
      END
```

```
      SUBROUTINE HYBRID(KEY,SMU,ETA,XC,YC,NCCNT)
      IMPLICIT REAL*8(A,B,D-H,O-Y) ,COMPLEX*16(Z,C)
      COMPLEX SINT,SJNT
      COMPLEX*16 ZET,Z,DCMPLX,DCONJG,F1,F2,F3,FF2(32),FF3(32),XY
      COMPLEX*16  ZETK,CZK,ZETT,CZZ,ZET4,ZE,ZD,ZC,ZA,ZB,CI,CDSQRT
      COMMON/T3/BCR(2,18),EK(171),XXY(18),KCRK(9),LP(18)
      DIMENSION  VG(32,34),X(5),Y(5),O(5)
     1  ,BK(32,34),VA(136),VI(32,34), V8(136),W(5)
      EQUIVALENCE (Z,ZETT), (UX,UXX)
      EQUIVALENCE(VI(1,1),VG(1,1) )
      DATA B/.2369269,.4786287,.5688889, .4786287,.2369269/
      DATA Y/-.9061799,-.5384693,0.,.5384693, .9061799/
      DATA ANT/5/
      CI = DCMPLX(0.D0,1.D0)
      IF (KEY .EQ. 1) NDPE = 10
      IF (KEY .EQ. 2) NDPE = 18
      E=1.
      NT=KEY*ANT
      NNPE=NDPE/2
      IF(NCCNT.EQ.0) GO TO 5
      DO 6 I=1,NNPE
      I2 = I * 2
    6 XXY(I2) = -XXY(I2)
    5 CONTINUE
      NNN=(NNPE-1)/2
      NTT=(NNT*NNT+NNT)/2
      DO     1 I=1,NTT
      VA(I  )=0.
    1 V8(I  )=0.
      DO 4  I=1,NT
      DO 4 J=1,NDPE
    4 VG(I,J)=0.
C     INTEGRATION COEFFICIENTS
      DO 11 I=1,5
      X(I)=(1.+Y(I))/2.
   11 O(I)=W(I)/2.
      ISIDE=NNPE/KEY+KEY/2
      ES=DSQRT( (XXY(1)-XC)**2+(XXY(2)-YC)**2)
      UXX=(XXY(2)-YC)/ES
      UY=(XXY(1)-XC)/ES
      DO 440 I=1,ISIDE
      II=I+I
      XXY(II-1)=(XXY(II-1)-XC)/ES
      XXY(II  )=(XXY(II)  -YC)/ES
      XT= XXY(II-1)*UY +XXY(II)*UXX
      XXY(II)=-XXY(II-1)*UXX+ XXY(II)*UY
  440 XXY(II-1)=XT
      ISIDE=NNPE/KEY-1/KEY
      DO 41 ISI=1,ISIDE
      IE=ISI+ISI
      UXX=XXY(IE+2)-XXY(IE)
      UY =XXY(IE-1) -XXY(IE+1)
      DO 41 II=1,5
      XX=XXY(IE-1)*(1.-X(II) ) +XXY(IE+1)*X(II)
      YY=XXY(IE  )*(1.-X(II) ) +XXY(IE+2)*X(II)
      Z = DCMPLX(XX ,YY)
      ZET =CDSQRT(ZETT)
      ZET4 = ZETT*ZETT
      CZZ = DCONJG(ZETT)
      ZETK = 1./ZET4
      KK = 1
      IF (KEY .EQ. 2) GO TO 1011
      DO 1010 K = 1,NNT
      FF2(K) = 0.
      ZETK = ZETK*ZET
      CZK = DCONJG(ZETK)
      KK = -KK
      IF (UY .EQ. 0.) GO TO 1009
      ZD = CZK*CZZ-KK*ZETK*ZETT
      ZC = ZETK*(CZZ-ZETT)
      FF2(K) = 0.5*K*(K-2)*ZC+K*ZD
      FF2(K) = FF2(K)*UY*.5
 1009 ZE = CZK*CZZ*(CZZ-ZETT)
      FF3(K) = ETA*ZETK*ZET4+KK*CZK*DCONJG(ZET4)+.5*K*ZE
      FF3(K) = FF3(K)*.25
      IF (UX .EQ. 0.) GO TO 1010
      IB = K+2+KK+KK
      ZA = (K-2)*ZETK-2.*CZK
      FF2(K) = -K*(CZZ*ZA-IB*ZETK*ZETT)*CI*.25*UX+FF2(K)
 1010 CONTINUE
      GO TO 2000
 1011 DO 1012 K = 1,NNT
      FF2(K) = 0.
      FF2(K+NNT) = 0.
      ZETK = ZETK*ZET
      CZK = DCONJG(ZETK)
      KK = -KK
      IF (UY .EQ. 0.) GO TO 1014
      ZD = CZK*CZZ-KK*ZETK*ZETT
      ZC = ZETK*(CZZ-ZETT)
      FF2(K) = .5*K*(K-2)*ZC+K*ZD
      FF2(K) = FF2(K)*UY*.5
      FF2(K+NNT) = (FF2(K)-K*ZD*UY)*CI
 1014 ZE = CZK*CZZ*(CZZ-ZETT)
      FF3(K) = ETA*ZETK*ZET4+KK*CZK*DCONJG(ZET4)+.5*K*ZE
      FF3(K) = FF3(K)*.25
```

```
      FF3(K+NNT) = (FF3(K)-.25*K*ZE)*CI
      IF (UX .EQ. 0.) GO TO 1012
      IB = K+2+KK+KK
      ZA = (K-2)*ZETK-2.*CZK
      FF2(K) = -K*(CZZ*ZA-IB*ZETK*ZETT)*CI*.25*UX+FF2(K)
      IB = K+2-KK-KK
      ZA = (K-2)*ZETK+2.*CZK
      FF2(K+NNT) = K*(CZZ*ZA-IB*ZETK*ZETT)*.25*UX+FF2(K+NNT)
 1012 CONTINUE
 2000 KJ=0
      DO 41 K=1,NNT
      L=2*ISI-1
      DO 40 J=1,KEY
      I=J*NNT-NNT+K
      SINT=FF2(I)*X(II)
      SJNT=FF2(I)-SINT
      VG(I,L) = VG(I,L) + O(II)*AIMAG(SJNT)
      VG(I,L+1) = VG(I,L+1) + O(II)*REAL(SJNT)
      VG(I,L+2) = VG(I,L+2) + O(II)*AIMAG(SINT)
   40 VG(I,L+3) = VG(I,L+3) + O(II)*REAL(SINT)
      DO 41 J=1,K
      SINT= FF2(K)*FF3(J)+FF2(J)*FF3(K)
      KJ=KJ+1
      VA(KJ) = VA(KJ) + O(II)*AIMAG(SINT)/SMU
      IF (KEY .EQ. 1) GO TO 41
      I=K+NNT
      L=J+NNT
      SINT= FF2(I)*FF3(L)+FF2(L)*FF3(I)
      VB(KJ) = VB(KJ) + O(II)*AIMAG(SINT)/SMU
   41 CONTINUE
      IF (KEY .EQ. 1) GO TO 64
      DO 500 III=1,NNT
      VG(III,2)=0.
      VG(III ,1)=2.*VG(III,1)
      II=III+NNT
      VG(II,  2)=2.*VG(II,2)
      VG(II ,1)=0.
      DO 455 J=1,NNN
      JU=J+1
      JL=NNPE+1-J
      VG(III,2*JL-1)=VG(III,2*JU-1)
      VG(III,2*JL  )=-VG(III,2*JU  )
      VG(II,2*JL-1)=-VG(II,2*JU-1)
  455 VG(II,2*JL  )= VG(II,2*JU  )
  500 CONTINUE
      DO 501 I=1,NDPE
  501 VG(NNT+2,I)=0.
      DO 63 I=1,NTT
      VA(I  )=VA(I  )*2.
   63 VB(I  )=VB(I  )*2.
      VB(2)=0.
      VB(3)=1.
      DO 62 I=3,NNT
   62 VB( (I*I-I)/2+2)=0.
   64 CONTINUE
      CALL SINV (VA,NNT, .1D-05,IER)
      IF (KEY .EQ. 2) CALL SINV (VB,NNT,.1D-05,IEE)
      DO 111 J=1,NDPE
      DO 110 I=1,NNT
      II= (I *I -I)/2
      BK(I,J)=0.
      DO 110 K=1,NNT
      IK=II+K
      IF ( K .GT. I  ) IK=(K*K-K)/2+I
  110 BK(I,J)=BK(I,J)+VA(IK )*VI(K,J)
       IF ( KEY .EQ. 1) GO TO 111
      II=NNT+1
      DO 121 I=II,NT
      IJ=I-NNT
      IJ=( IJ*IJ-IJ)/2
      BK(I,J)=0.
      DO 121 K=1,NNT
      IK=IJ+K
      IF ( K .GT. I-NNT) IK=(K*K-K)/2+I-NNT
  121 BK(I,J)=BK(I,J) + VB(IK      )*VI(K+NNT,J)
  111 CONTINUE
      IJ=0
      DO 112 I=1,NDPE
      DO 112 J=1,I
      IJ=IJ+1
      EK(IJ )=0.
      DO 112 K=1,NT
  112  EK(IJ )=EK(IJ )+ BK(K,J)*VI(K,I)
      E =DSQRT(2./ES)
      DO 113 J = 1,NDPE
      BCR(2,J) = 0.
      IF (KEY .EQ. 2) BCR(2,J) = E*BK(10,J)
  113 BCR(1,J) = E*BK(1,J)
      RETURN
      END
```

```
      SUBROUTINE SIFAC(M,TOTAL)
      IMPLICIT REAL*8 (A-H,O-Z)
      COMMON/TWO/ IBAND,NEQ,R(600),AK(600,64)
      COMMON/T3/BCR(2,18),EK(171),XXY(18),KCRK(9),LP(18)
      REAL*8  K1,K2
      WRITE(6,35) M
   35 FORMAT('0',5X,'CKEL =',I5,/)
      READ (2) KK,NODE,NOE,KEY,(LP(I),I=1,NOE),(EK(I),I=1,KK),
     1  (((BCR(I,J),I=1,KEY),J=1,NOE),XC,YC,MATYP,(KCRK(I),I=1,NODE)
      TOTAL = 0.
      K1 = 0.
      K2 = 0.
      DO 20 I=1,NOE
      K1 = K1 + BCR(1,I) * R(LP(I))
      IF(KEY.EQ.1) GO TO 20
      K2 = K2 + BCR(2,I) * R(LP(I))
   20 CONTINUE
      PI = 3.1415926
      K1 = K1 * DSQRT(PI)
      K2 = K2 * DSQRT(PI)
      WRITE(6,1) M ,K1, K2
    1 FORMAT('-',5X,'*** STRESS INTENSITY FACTOR ***',I2,/,
     1  '0',5X,'OPENING  MODE K1 = ',G20.6,/,
     2  '0',5X,'SHEARING MODE K2 = ',G20.6)
      WRITE(6,100) XC,YC,MATYP
  100 FORMAT('0',5X,'CRACK TIP  XC =',G16.6,' YC =',G16.6,
     1  '  AT MATERIAL' ,I4)
      WRITE(6,200) NODE,(KCRK(I),I=1,NODE)
  200 FORMAT('0',5X,'THE',I4,'NODES =',10I4)
      W = 0.
      DO 30 I=1,NOE
      XXY(I) = 0.
      DO 30 J=1,NOE
      CALL LOC(I,J,IJ,NOE,NOE,1)
   30 XXY(I) = XXY(I) + R(LP(J)) * EK(IJ) * .5
         DO 40 I=1,NOE
   40 W = W + XXY(I)*R(LP(I))
      WRITE(6,2) W
    2 FORMAT('0',5X,'STRAIN ENERGY =' ,G16.6)
      TOTAL = TOTAL + W
      WRITE(6,300)
  300 FORMAT('0',10X,' * * * * * * * * * * * * * * * * * * * * *',//)
      RETURN
      END
```

```
      SUBROUTINE GECMBC(L,N)
      IMPLICIT REAL*8 (A-H,O-Z)
      COMMON/TWO/ IBAND,NEQ,R(600),AK(600,64)
C  THIS SUBROUTINE MODIFIES THE ASSEMBLAGE STIFFNESS AND LOADS FOR THE
C  PRESCRIBED DISPLACEMENT U AT DEGREE OF FREEDOM N, EQ.(6-18B). (REF.1)
         DO 100 M=2,IBAND
            K = N - M + 1
            IF(K.LE.0) GO TO 50
            R(K) = R(K) - AK(K,M)*U
            AK(K,M) = 0.0
   50       K = N + M - 1
            IF(K.GT.NEQ) GO TO 100
            R(K) = R(K) - AK(N,M)*U
            AK(N,M) = 0.0
  100    CONTINUE
            AK(N,1) = 1.0
            R(N) = U
      RETURN
      END
```

```
      SUBROUTINE STRESS(WORK)
      IMPLICIT REAL*8 (A-H,O-Z)
      COMMON/CONS/ NNP,NEL,NMAT,NSLC,NOPT,NBODY,MTYP,NCKEL
      COMMON E(10),PR(10),RO(10),TH(10),X(300),Y(300)
      COMMON/TL/ IE(250,5)
      COMMON/ONE/ QK(10,10),Q(10),B(3,10),C(3,3),BT(3,6),XQ(5),YQ(5)
      COMMON/TWO/ IBAND,NEQ,R(600),AK(600,64)
      DIMENSION SIG(6)
C
      REWIND 1
      REWIND 3
      WRITE(6,300)
      WORK = 0.
            NOLINE = 47
C
C  RETRIEVE MULTIPLIERS, PIVOTS, MATRICES B AND C, AND CENTROIDAL COORD.
C  FOR ELEMENT
         DO 5 M=1,NEL
      READ(1) ((QK(I,J),J=1,10),I=1,2),  Q(9), Q(10),
     1     ((B(I,J),J=1,10),I=1,3), ((C(I,J),J=1,3),I=1,3), XC,YC
C
C  SELECT NODAL DISPLACEMENTS FOR THE ELEMENT
            LIM = 4
         IF(IE(M,3).EQ.IE(M,4)) LIM = 3
         DO 10 I=1,LIM
            II = 2*I
            JJ = 2*IE(M,I)
            Q(II-1) = R(JJ-1)
   10       Q(II) = R(JJ)
C
C  RECOVER CONDENSED DISPLACEMENTS FOR THE QUADRILATERAL, EQ. (5-64G)
         IF(LIM.EQ.3) GO TO 16
         DO 15 K=1,2
            JK = K + 8
            IK = JK - 1
         DO 15 L=1,IK
   15       Q(JK) = Q(JK) - QK(K,L)*Q(L)
C
C  COMPUTE ELEMENT STRAINS, EQ,(5-35A)
            LIM = 10
            FAC=0.25
         GO TO 17
   16       LIM = 6
            FAC=1.0
   17    DO 20 I=1,3
            E(I) = 0.0
         DO 20 J=1, LIM
   20       E(I) = E(I) + B(I,J)*Q(J)*FAC
C
C  COMPUTE STRAIN ENERGY STORED IN EACH ELEMENT
      READ(3) KK, ((QK(I,J),J=1,KK),I=1,KK)
      DO 40 I=1,KK
      RO(I) = 0.
      DO 40 J=1,KK
   40 RO(I) = RO(I) + .5*Q(J)*QK(I,J)
      W = 0.
      DO 50 I=1,KK
   50 W = W + RO(I)*Q(I)
      WORK = WORK + W
C
C  COMPUTE ELEMENT STRESSES  , EQ.(5-35B)
         DO 30 I=1,3
            SIG(I) = 0.0
         DO 30 J=1,3
   30       SIG(I) = SIG(I) + C(I,J)*E(J)
C  COMPUTE PRINCIPAL STRESSES AND THE ANGLE WITH THE POSITIVE X AXIS
            SP = (SIG(1)+SIG(2))/2.0
            SM = (SIG(1)-SIG(2))/2.0
            DS =DSQRT(SM*SM+SIG(3)*SIG(3))
            SIG(4) = SP + DS
            SIG(5) = SP - DS
            SIG(6) = 0.0
         IF(SIG(3).NE.0.0.AND.SM.NE.0.0) SIG(6) = 28.648*DATAN2(SIG(3),
     1                                                          SM)
C  PRINT STRESSES, 50 LINES PER PAGE
         IF(NOLINE.GT.0) GO TO 54
      WRITE(6,1000)
            NOLINE = 49
   54    NOLINE = NOLINE - 1
    5 WRITE(6,1010) M,XC,YC,(SIG(I),I=1,6)
      WRITE(6,21) WORK
   21 FORMAT('-',5X,' . . . STRAIN ENERGY W/O CKEL =',G20.6,' . . .')
      ENDFILE 1
  300 FORMAT(47H1OUTPUT TABLE 2.. STRESSES AT ELEMENT CENTROIDS //
     11X,7HELEMENT,9X,1HX,9X,1HY,4X,8HSIGMA(X),4X,8HSIGMA(Y),4X,
     28HTAL(X,Y),4X,8HSIGMA(1),4X,8HSIGMA(2), 7X,5HANGLE )
 1000 FORMAT(1H1,    7HELEMENT,9X,1HX,9X,1HY,4X8HSIGMA(X),4X,8HSIGMA(Y),
     14X,8HTAL(X,Y),4X,8HSIGMA(1),4X,8HSIGMA(2), 7X,5HANGLE )
 1010 FORMAT(I8, 2F10.2,1P6E12.4)
      RETURN
      END
```

APPENDIX D

Calculation of Service Life by Numerical Integration

This program integrates the following equation

$$N_f = \int_{C_o}^{C_f} \frac{dc}{A(\Delta K)^n}$$

The function $\Delta K = \Delta K(c)$ is approximated using the polynominal curve fit by least square method. The integration is performed by Simpson's rule. The program is limited to the polynominal curve fit and also computes the correlation coefficient of the estimated curve fitting.

Following are the main program and subroutines in the program:

MAIN Reads and prints data. Calls the subroutine

FUNC Calculates the value of an assumed polynominal equation (function subroutine)

INGRT Provides numerical integrations by Simpson's rule

LSCF Performs least square curve fitting

STATIC Computes the correlation coefficient

CHOLES Solves the simultaneous equation by Cholesky's method

Guides for Data Input

Card 1 (2I5)

cc 1-5	N	Number of data points
cc 6-10	M	The degree of the polynominal

Card 2 (4F10.0)

cc 1-10	XI	Initial value of crack length within overlay
cc 11-20	XF	Final value of crack length within overlay

cc 21-30 CA Fatigue experiment constant

cc 31-40 CN Fatigue experiment constant

Card 3 (2F10.0) A set of N cards

cc 1-10 X(I) crack length within overlay

cc 11-20 Y(I) calculated stress intensity factor

Card 4 (I5, 5X, F10.0)

cc 1-10 NSTEP Number of integration steps

cc 11-20 SKC Critical stress intensity factor

```
      IMPLICIT REAL*8(A-H,O-Z)
      DIMENSION X(12),Y(12),A(12)
      DIMENSION RK(200)
      DIMENSION F(200)
      WRITE(6,3)
    3 FORMAT('1',2X,'CURVE FITTING BY LEAST SQUARE METHOD')
    1 READ(5,11) N, M
   11 FORMAT(2I5)
      IF(N.EQ.0)GO TO 99
      DO 21 I=1,N
   21 READ(5,12) X(I),Y(I)
   12 FORMAT(2F10.0)
  100 WRITE(6,111) M
  111 FORMAT ('0',14X,'THE DEGREE OF THE POLYNOMIALS IS M =',I3)
      CALL LSCF(X,Y,N,M,A)
  200 CONTINUE
      READ(5,50) XI,XF,CA,CN
C     XI-- INITIAL VALUE
C     XF-- FINAL VALUE
C     CA CN -- FATIGUE EXPERIMENT CONSTANTS
   50 FORMAT(4F10.0)
      WRITE(6,70) XI,XF,CA,CN
   70 FORMAT('0',14X,'THE INITIAL VALUE OF CRACK LENGTH',T75,G15.5,
     1 /,14X,'THE FINAL VALUE OF CRACK LENGTH',T75,G15.5,
     2 /,14X,'THE FATIGUE CONSTANT CA',T75,G15.5,
     3 /,14X,'THE FATIGUE CONSTANT CN',T75,G15.5)
      M1 = M+1
   10 CONTINUE
      READ(5,60) NSTEP,SKC
   60 FORMAT(I5,5X,F10.0)
      IF(NSTEP.EQ.0) GO TO 90
      H = (XF-XI)/(NSTEP-1.)
      DO 5 I=1,NSTEP
      XX=XI + (I-1)*H
      XX = XI + H*(I-1)
      RK(I) = FUNC(M1,XX,A)
      IF(RK(I).GE.SKC) GO TO 501
    5 CONTINUE
  501 CONTINUE
      NSTEP= I
      SKC = RK(I)
      XF = XX
      DO 502 K=1,6
      CN = DFLOAT(K)
      WRITE(6,601) CN, XF
  601 FORMAT('1',10X,'CN=',G15.4,5X,'XF =',G15.4)
      DO 503 I=1,NSTEP
  503 F(I) = 1.00/(RK(I)**CN)
      CALL INTGRT(NSTEP,F,H,AREA)
      WRITE(6,602)
  602 FORMAT('0',8X,'CA ',15X,'CYCLE ')
      SR = 1.D-15
      DO 504 II=1,5
      SINC = SR*10.D0** II
      DO 504 J=1,10
      CA=SINC * J
      S = 1.DC/CA*AREA
      WRITE(6,603) CA, S
  603 FORMAT('0',15X,2G15.5)
  504 CONTINUE
  502 CONTINUE
      GO TO 10
   90 CONTINUE
      GO TO 1
   99 WRITE(6,20)
      WRITE(6,30)
   20 FORMAT('0',6X,'END OF PROBLEM')
   30 FORMAT('1')
      STOP
      END
```

```
      FUNCTION FUNC(M1,XX,A)
      IMPLICIT REAL*8(A-H,O-Z)
      DIMENSION A(12)
      SUM = 0.
      DO 20 I=2,M1
   20 SUM = SUM + A(I)*XX**(I-1)
      FUNC = SUM + A(1)
      RETURN
      END
```

```
      SUBROUTINE LSCF(X,Y,N,M,A)
      IMPLICIT REAL*8(A-H,O-Z)
      DIMENSION X(12),Y(12),A(12),C(11,12),D(11),FX(12),ERROR(12)
      DIMENSION ERR(12)
      M1=M+1
      DO 1 J=1,M1
      SUM=0.0
      IF(J.GT.1)GO TO 6
      DO 5 K=1,N
      SUM=SUM+Y(K)
    5 CONTINUE
      GO TO 1
    6 DO 2 K=1,N
      SUM=SUM+Y(K)*X(K)**(J-1)
    2 CONTINUE
    1 D(J)=SUM
      DO 10 I=1,M1
      DO 10 J=1,M1
      SUM=0.0
      IF(I.GT.1)GO TO 16
      IF(J.GT.1)GO TO 16
      SUM=N
      GO TO 10
   16 DO 12 K=1,N
      SUM=SUM+X(K)**(I+J-2)
   12 CONTINUE
   10 C(I,J)=SUM
      IP=0
      CALL CHOLES(M1,C,D,A,IND)
      IF(IND.EQ.0)GO TO 29
      WRITE(6,22)
   22 FORMAT('0',2X,'NO CURVE FITTING')
      GO TO 99
   29 WRITE(6,28) A(1)
   28 FORMAT('0',15X,E11.4)
      DO 24 I=2,M1
      L=I-1
      WRITE(6,25) A(I),L
   25 FORMAT(' ',15X,E11.4,2X,'*X** ',I2)
   24 CONTINUE
      WRITE(6,31)
   31 FORMAT('0',25X,'X',15X,'Y',15X,'FX',15X,'ERROR',15X,'R**2')
      DO 50 K=1,N
      SUM=0.0
      DO 37 J=2,M1
      SUM=SUM+A(J)*X(K)**(J-1)
   37 CONTINUE
      FX(K) = A(1) + SUM
      ERROR(K)=Y(K)-FX(K)
      ERR(K)=ERROR(K)**2
   50 CONTINUE
      SUM = 0.
      DO 41 K=1,N
      WRITE(6,42) X(K),Y(K),FX(K),ERROR(K),ERR(K)
      SUM = SUM+ERR(K)
   42 FORMAT(' ',15X,5(5X,E11.4))
   41 CONTINUE
      RSME = DSQRT(SUM/N)
      WRITE(6,46) RSME
   46 FORMAT('-',10X,'** RSME ** =',G20.6)
      CALL STATIC(N,Y,FX,R2)
   99 RETURN
      END
```

```
      SUBROUTINE CHOLES(N,A,C,X,IND)
      IMPLICIT REAL*8(A-H,O-Z)
      REAL*8 A(11,12),C(11),X(11),L(11,12),K(11),SAVE(12),T(11,12)
      INTEGER TEMP
      IND = 0
      DO 82 I=1,N
      A(I,(N+1))=C(I)
   82 CONTINUE
      I=1
      IF(N.EQ.1)GO TO 81
    5 IF(A(I,I).NE.0.)GO TO 4
      IF(I.EQ.N)GO TO 103
      I=I+1
      GO TO 5
  103 CONTINUE
      IND = 1
      WRITE(6,100)
      GO TO 200
  100 FORMAT('-',10X,'THIS PROB. CAN NOT BE SOLVED BECAUSE NON-ZERO
     1A(I,I) CAN NOT BE FIND')
    4 IF(I.EQ.1)GO TO 10
      J=1
   20 SAVEA=A(I,J)
      A(I,J)=A(I,J)
       A(I,J)=SAVEA
      IF(J.EQ.(N+1))GO TO 6
      J=J+1
      GO TO 20
    6 I=1
   10 CONTINUE
   11 L(I,I)=A(I,I)
      T(I,I)=1
      IF(I.EQ.N)GO TO 30
      I=I+1
      GO TO 11
   30 I=2
      J=2
   12 T(I,J)=A(I,J)/A(I,I)
      IF(J.EQ.(N+1))GO TO 40
      J=J+1
      GO TO 12
   40 IK=2
  500 J=2
   14 M=1
      SUML=0
   13 SUML=SUML+L(I,M)*T(M,J)
      IF(M.EQ.(J-1))GO TO 50
      M=M+1
```

```
      GO TO 13
   50 L(I,J)=A(I,J)-SUML
      IF(J.EQ.I)GO TO 70
      J=J+1
      GO TO 14
   70 IF(L(I,J).EQ.0.)GO TO 80
   18 J=J+1
      KK=1
      SUMT=0
   15 SUMT=SUMT+L(I,KK)*T(KK,J)
      IF(KK.NE.(I-1))GO TO 90
      T(I,J)=(A(I,J)-SUMT)/L(I,I)
      GO TO 60
   90 KK=KK+1
      GO TO 15
   60 IF(J.EQ.(N+1))GO TO 17
      GO TO 18
   17 IF(I.EQ.N)GO TO 200
      I=I+1
      IK=I
      GO TO 500
  200 I=1
   21 K(I)=T(I,(N+1))
      IF(I.EQ.N)GO TO 300
      I=I+1
      GO TO 21
  300 X(N)=K(N)
      I=N-1
   24 SUM=0
      J=I+1
   23 SUM=SUM+T(I,J)*X(J)
      IF(J.EQ.N)GO TO 22
      J=J+1
      GO TO 23
   22 X(I)=K(I)-SUM
      IF(I.EQ.1)GO TO 1000
      I=I-1
      GO TO 24
 1000 WRITE(6,71)
   71 FORMAT('-',15X,'ANSWER')
      WRITE(6,72) (I,X(I),I=1,N)
   72 FORMAT('0',15X,'X(',I2,')=',E14.7)
      GO TO 2000
   80 TEMP=I
      IF(IK.EQ.N)GO TO 150
      J=1
   32 SAVE(J)=A(I,J)
      IF(J.EQ.(N+1))GO TO 31
      J=J+1
      GO TO 32
   31 SAVEL=L(I,I)
   34 J=1
   33 A(I,J)=A((I+1),J)
      IF(J.EQ.(N+1))GO TO 440
      J=J+1
      GO TO 33
  440 L(I,I)=L((I+1),I)
      IF(I.EQ.(N-1))GO TO 550
      I=I+1
      GO TO 34
  550 J=1
   51 A(N,J)=SAVE(J)
      IF(J.EQ.(N+1))GO TO 660
      J=J+1
      GO TO 51
  660 L(N,I)=SAVEL
      IK=IK+1
      I=TEMP
      GO TO 500
 1500 WRITE(6,1510)
 1510 FORMAT('-', 2X,'PROB. MUST BE STOPPED BECAUSE NO ARRANGEMENT OF
     1ROWS CAN BE ACCOMPLISHED')
      IND = 1
      GO TO 2000
   81 X(I)=C(I)/A(I,I)
      WRITE(6,72) I,X(I)
 2000 RETURN
      END
```

```
C     ***************************************************************
C     TO INTEGRATE ANY ARBITRARY FUNCTION BETWEEN CERTAIN LIMITS.
C     THE FUNCTION TO INTEGRATED IS DEFINED BY A FUNCTION SUBPROGRAM.
C     ***************************************************************
      SUBROUTINE INTGRT(N,F,H,AREA)
      IMPLICIT REAL*8(A-H,O-Z)
      DIMENSION F(200)
      IF(N/2*2.EQ.N)GO TO 8
      IF(N.GT.3)GO TO 1
      AREA=H/3.*(F(1)+4.*F(2)+F(3))
      RETURN
    1 SUM1=0.0
      SUM3=0.0
      N1=N-1
      N2=N-2
      DO 2 I=2,N1,2
      SUM1=SUM1+F(I)
    2 CONTINUE
      SUM1=4.*H/3.*SUM1
      DO 3 I=3,N2,2
    3 SUM3=SUM3+F(I)
      SUM3=2.*H/3.*SUM3
      AREA=H/3.*(F(1)+F(N))+SUM1+SUM3
      RETURN
    8 IF(N.GT.4)GO TO 17
      AREA=H/2.*(F(1)+F(2))+H/3.*(F(2)+4.*F(3)+F(4))
      RETURN
   17 N1=N-1
      N2=N-2
      SUM1=.0
      SUM3=.0
      DO 18 I=3,N1,2
   18 SUM1=SUM1+F(I)
      SUM1=4.*H/3.*SUM1
      DO 19 I=4,N2,2
   19 SUM3=SUM3+F(I)
      SUM3=2.*H/3.*SUM3
      AREA=H/2.*(F(1)+F(2))+H/3.*(F(2)+F(N))+SUM1+SUM3
      RETURN
      END
```

```
C     ***************************************************************
C     TO COMPUTE THE CORELATION COEFFICIENT AND R SQUARE
C     ***************************************************************
      SUBROUTINE STATIC(N,X,Y,R2)
      IMPLICIT REAL*8(A-H,O-Z)
      DIMENSION X(N),Y(N)
C     X-- OBSERVED VALUE
C     Y-- ESTIMATED VALUE
      SX = 0.
      SY = 0.
      SXY = 0.
      SX2 = 0.
      SY2 = 0.
      DO 1 I=1,N
      SX = SX + X(I)
      SY = SY + Y(I)
      SXY = SXY + X(I)*Y(I)
      SX2 = SX2 + X(I)**2
      SY2 = SY2 + Y(I)**2
    1 CONTINUE
      XMEAN = SX/N
      YMEAN = SY/ N
      DE = DSQRT(DABS((SX2-XMEAN**2*N)*(SY2-YMEAN**2*N)))
      CORELA = (SXY - XMEAN*YMEAN*N)/DE
      R2 = CORELA**2
      WRITE(6,40) CORELA,R2
   40 FORMAT('-',5X,'THE CORELATION COEEF. =',G20.6,/,'0',
     1 5X,' R**2 = ',G20.6)
      RETURN
      END
```

CURVE FITTING BY LEAST SQUARE METHOD

THE DEGREE OF THE POLYNOMIALS IS M = 2

ANSWER

X(1)= 0.21493610 02

X(2)= 0.15750160 02

X(3)= 0.18329300 03

0.2149D 02
0.1575D 02 **x** 1
0.1833D 03 **x** 2

X	Y	FX	ERROR	R**2
0.1000D 00	0.2400D 02	0.2490D 02	-0.9018D 00	0.8128D 00
0.5500D 00	0.8900D 02	0.8856D 02	0.3398D 01	0.1154D 02
0.1050D 01	0.2300D 03	0.2401D 03	-0.1011D 02	0.1022D 03
0.1250D 01	0.3423D 03	0.3276D 03	0.1442D 02	0.2040D 03
0.1350D 01	0.3700D 03	0.3768D 03	-0.6808D 01	0.4635D 02

** RSME ** = 8.59053

THE CORELATION COEEF. = 0.998007

R**2 = 0.996018

THE INITIAL VALUE OF CRACK LENGTH 0.0
THE FINAL VALUE OF CRACK LENGTH 1.5000
THE FATIGUE CONSTANT CA 0.0
THE FATIGUE CONSTANT CN 4.0000

CN= 4.040 KF = 1.447

CA	CYCLE
0.1000D-13	0.6225D 08
0.2000D-13	0.3112D 08
0.3000D-13	0.2075D 08
0.4000D-13	0.1554D 08
0.5000D-13	0.1245D 08
0.6000D-13	0.1037D 08
0.7000D-13	0.8893D 07
0.8000D-13	0.7781D 07
0.9000D-13	0.6917D 07
0.1000D-12	0.6225D 07
0.1000D-12	0.6225D 07
0.2000D-12	0.3112D 07
0.3000D-12	0.2075D 07
0.4000D-12	0.1556D 07
0.5000D-12	0.1245D 07
0.6000D-12	0.1037D 07
0.7000D-12	0.8893D 06
0.8000D-12	0.7781D 06
0.9000D-12	0.6917D 06
0.1000D-11	0.6225D 06
0.1000D-11	0.6225D 06
0.2000D-11	0.3112D 06
0.3000D-11	0.2075D 06
0.4000D-11	0.1556D 06
0.5000D-11	0.1245D 06
0.6000D-11	0.1037D 06
0.7000D-11	88936.
0.8000D-11	77819.
0.9000D-11	69172.